

1. Report number

VK 2206.301

2. ISSN-number

LVV-Report 0920-0592

3. Title

Car-following under Non-congested and Congested Conditions

4. Theme

Traffic Engineering

5. Authors

Thomas Dijker
Piet H.L. Bovy
Raymond G.M.M. Vermijs

6. Research project

Traffic flow under congested conditions

7. Research institute

Delft University of Technology
Faculty of Civil Engineering and Geo Sciences
Transportation Research Laboratory
Postbus 5048, 2600 GA Delft

8. Report category

Research report

9. Principal

Delft University of Technology

10. Publication date

October, 1997

11. Abstract

In traffic flow analysis several regimes are distinguished, such as congested and non-congested flow conditions. Indications exist that driving behavior differs by regime, and that it may change discontinuously between regimes. In contrast, most traffic flow models used today basically assume the same car-following behavior irrespective of the traffic flow regime. It is hypothesized that because of this deficiency, these models do not always perform satisfactorily. To clarify this issue, differences in car-following between congested and non-congested flow are analyzed with data from two sites on Dutch freeways.

It is shown that, at the same speeds, passenger car drivers follow with smaller headways in non-congested flow than in congested flow. Car-following of truck drivers does not show differences between regimes.

Microscopic distance gap - speed models are established for several road user classes, valid for each of the two flow regimes. To show the improvements resulting from these new microscopic relationships, the latter are implemented in a micro simulation model (FOSIM) with which macroscopic patterns in traffic flow are modeled. The macroscopic findings produced with the regime specific car-following rules show a considerable improvement in modeling performance.

12. External Contacts

Transportation Engineering
Section

13. Number of pages

107

14. Price

f50,- (Dutch Guilders)
(all cost included)

CAR-FOLLOWING UNDER NON-CONGESTED AND CONGESTED CONDITIONS

Thomas Dijker
Piet H.L. Bovy
Raymond G.M.M. Vermijs

Delft University of Technology
Faculty of Civil Engineering and Geo Sciences
Transportation Research Laboratory

October, 1997

Preface

Congestion has become an important phenomenon in road traffic systems. Therefore, research on congested traffic flow becomes ever more relevant. This is acknowledged in the research program at the Laboratory of Transportation of the Delft University of Technology.

One of subjects of interest is car-following on freeways under non-congested and congested conditions. Characteristics of individual driving behavior (car-following, measured at two Dutch freeway sites) are studied separately for the two flow regimes. They are compared, and interesting differences are found. When this insight (different driving behavior for each regime) is applied in a simulation model, significant consequences are found.

The report is mainly written for traffic engineers. However, it may also be interesting for those somewhat less familiar with traffic flow theory. As an aid, some fundamentals of traffic flow are briefly described in chapter 2.

The report is divided into four main parts:

- Introduction, problem background, and research formulation: *Chapters 1, 2, and 3*;
- Description of the data collection (which freeway sites, characteristics), and of the operations performed on the data (calculation of variables, categorization of data): *Chapter 4*;
- Data analysis (individual driving behavior, traffic stream characteristics): *Chapter 5*;
- Modeling of the findings, and evaluation of the results: *Chapters 6, 7, and 8*.

We thank the Dutch Ministry of Transport, Public Works and Water Management (Henk Taale) for kindly providing some of the research data.

The authors
October 1997

Abstract

This report focuses on differences in individual car-following behavior, that is, distance gap keeping, for different flow regimes (congested, non-congested) on (Dutch) freeways. The main questions are whether differences between flow regimes exist, and whether they have a significant influence on traffic flow. If so, microscopic traffic flow models should incorporate these behavioral differences.

The questions are answered by analysis of data from two (6 lane and 4 lane) Dutch freeways. For the 6 lane freeway, the data originate from different cross sections, both upstream and downstream of a bottleneck (an on ramp), and at the bottleneck itself. For the 4 lane freeway, the data are collected at a cross section upstream of the bottleneck.

Using these data, both microscopic and macroscopic variables are analyzed. As a microscopic characteristic, the distance gap of followers as a function of speed is studied separately for non-congested and congested flow. Important aspects of the analysis are the identification of followers (using a critical distance gap), and determination of the traffic state (congested or non-congested, based on the fundamental diagram and a speed criterion). Further, vehicles are separated according to vehicle type (passenger cars, light trucks, and heavy trucks) and lane. Macroscopic data (speed, flow, and density) are calculated by aggregation of the microscopic data for 5 minute intervals, both by lane and carriageway as a whole.

On both freeways and at all cross sections, it is found that, on average, passenger cars in non-congested flow follow with shorter gaps than in congested flow for the same speed. For trucks, no differences are found. At the 4 lane freeway site, the differences are smaller than at the 6 lane freeway site.

Macroscopic variables are studied by plotting fundamental diagrams, which relate speed, flow, and density. It appears that in the median and middle lanes the densities on the congested branches of the fundamental diagrams are lower than expected according to conventional (continuous) fundamental diagrams. This confirms the microscopic findings, as longer distance gaps should macroscopically result in lower densities.

The (microscopic) distance gap - speed data are used to establish regime specific distance gap - speed functions. These functions are established for each vehicle type and lane. They can be used in microscopic traffic flow models.

To evaluate the performance of the regime specific distance gap - speed functions, the existing microscopic model FOSIM is modified to simulate car-following for non-congested and congested regimes. The resulting fundamental diagrams are compared by lane with both conventional FOSIM and real-life data. By using regime specific car-following models, the performance of the simulation model, in terms of replicating observed traffic stream data, improves significantly for congested flow.

Table of Contents

PREFACE	i
ABSTRACT	iii
1 INTRODUCTION	1
2 THEORY ON TRAFFIC FLOW BY FLOW STATE	3
2.1 Characteristics of traffic for different flow states	3
2.1.1 Macroscopic flow characteristics	3
2.1.2 Mesoscopic flow characteristics	5
2.1.3 Microscopic flow characteristics	6
2.2 Description of Traffic flow models	7
2.2.1 Macroscopic models	7
2.2.2 Mesoscopic models	7
2.2.3 Microscopic models	8
2.2.4 Relation between macroscopic and microscopic flow models	9
2.3 Research Questions	9
3 RESEARCH GOALS AND METHODOLOGY	11
4 OBSERVATIONS ON TRAFFIC CHARACTERISTICS IN NON-CONGESTED AND CONGESTED CONDITIONS	13
4.1 Data collection	13
4.1.1 Choice of suitable sites	13
4.1.2 Description of the sites	14
4.1.3 Influences of facility design, traffic regulations, traffic composition and external conditions on flow characteristics	14
4.2. Calculation and classification of data	16
4.2.1 Time aggregated data (macroscopic data)	16
4.2.2 Individual vehicle data (microscopic data)	16
5 CHARACTERISTICS OF THE NON-CONGESTED AND CONGESTED REGIMES AT DUTCH FREEWAY SITES	19
5.1 Analysis of the individual driving behavior at Dutch Freeway sites	19
5.1.1 Distance gap keeping at the A2 site	20
5.1.2 Distance gap keeping at the A9 site	26
5.1.3 Comparison of distance gap - speed relations at the A2 and A9 sites	27
5.2 Analysis of macroscopic characteristics at Dutch Freeway sites	30
5.2.1 Macroscopic flow characteristics at the A2 site	30
5.2.2 Macroscopic flow characteristics at the A9 site	36
5.2.3 Comparison of macroscopic measurements from the A2 and A9 sites	40
5.2.4 Summary of the macroscopic findings	42
5.3 Summary of the findings and the relation between macroscopic and microscopic findings	43
6 ESTABLISHMENT OF DISTANCE GAP - SPEED RELATIONSHIPS	45
6.1 Estimation of distance gap - speed relationships	45
6.1.1 Functional form	45
6.1.2 Parameter estimation	45
6.2 Estimated distance gap - speed models	46
7 IMPLEMENTATION OF REGIME DEPENDENT CAR-FOLLOWING IN THE MICROSCOPIC SIMULATION MODEL FOSIM51	
7.1 The microscopic traffic flow simulation model FOSIM	51
7.2 Implementation of regime dependent car-following behavior in FOSIM	52

8	APPLYING THE EXTENDED FOSIM MODEL TO SHOW THE CONSEQUENCES OF DIFFERENT CAR-FOLLOWING BEHAVIOR IN NON-CONGESTED AND CONGESTED CONDITIONS	55
8.1	Simulation of traffic at the A2 site, compared with real measurements and conventional FOSIM	55
8.1.1	Input for simulation of traffic at the A2 site	56
8.1.2	Comparison of simulation results of the A2 site with the conventional and extended FOSIM models and real measurements	57
8.2	Conclusions drawn from the simulations with the extended FOSIM model	61
9	CONCLUSIONS	63
9.1	Research summary	63
9.2	Summary of the findings	63
9.3	Conclusions	64
9.4	Recommendations	64
	REFERENCES	65
	APPENDIX A: CALCULATION OF MICROSCOPIC AND MACROSCOPIC DATA	69
	APPENDIX B: DETERMINATION OF THE CRITICAL GAP VALUE	71
	APPENDIX C: DISTANCE GAP DATA PER 5 KM/H SPEED INTERVAL	75
	APPENDIX D: STANDARD ERROR OF THE AVERAGE DISTANCE GAP - SPEED VALUES	87
	APPENDIX E: ESTIMATED PARAMETER VALUES FOR THE DISTANCE GAP - SPEED RELATIONSHIPS	91
	APPENDIX F: DESCRIPTION OF THE MICROSCOPIC TRAFFIC FLOW MODEL FOSIM	93

1 Introduction

In uninterrupted traffic flow operations on freeways usually several regimes of traffic flow are distinguished (see e.g. May (1)). In the literature these are denoted with terms such as free-flow conditions, congested-flow conditions, and transitional-flow conditions, and one could also add a capacity regime for the state in which maximum flows are produced in a facility. These various states can easily be associated with specific parts of the macroscopic fundamental diagram (relation between speed, flow, and density). At a microscopic level these states are characterized, among other things, by differences in the freedom of drivers with respect to speed choice, lane choice, distance headway, and maneuvering the vehicle.

There are many indications that driver behavior differs between regimes. These indications follow from theoretical inconsistencies, from poor goodness of fit of macroscopic flow models, and from observations of traffic flow under varying conditions. For example, May (1) shows that macroscopic flow models that use a single explanatory relationship for the whole range of flows, densities, and speeds (disturbingly called single-regime models) exhibit theoretical deficiencies such as implausible values for jam densities. These models also show a poor goodness of fit with data, and fail especially in faithfully matching observed data near capacity conditions. In contrast, macroscopic models that assume separate speed-density relationships for the various flow regimes with clearly identified breakpoints perform much better.

Therefore it may be hypothesized that the car-following behavior of drivers differs between various flow regimes. The frequently observed discontinuity in the speed-flow relationship in the vicinity of capacity conditions (see e.g. Hall et al (2), and Schuurman & Vermijs (3)) may be attributed to this regime-specific following behavior. However, this discontinuity in the fundamental diagram is often measured at a cross section upstream of the bottleneck. In such situations the flow is determined by the bottleneck, and the capacity of the *total* road section may be unaffected (Van Toorenburg (4)).

Consideration of regime-specific car-following is equally important for microscopic traffic simulation modeling. In most microscopic models, car-following rules do not differ with respect to the regime at hand. This is, for instance, the case with the so-called FOSIM model developed at the Delft University of Technology. In addition, the car-following rules have mostly been calibrated with non-congested flow data only. These models therefore have difficulties in satisfactorily reproducing traffic flow patterns over the whole range of flow conditions, including severe congestion.

It is therefore argued that there is an urgent need to empirically study car-following behavior of drivers under varying flow conditions in order to identify the hypothesized differences between regimes. Such an empirical analysis will lead to a better insight into microscopic traffic behavior, and consequently to a better understanding of macroscopic flow phenomena.

This report presents an empirical analysis into car-following behavior on basic freeway sections both downstream and upstream of a bottleneck, and at the bottleneck itself on Dutch freeways. Inter-vehicle distances as a function of speed and regime are analyzed and modeled separately for non-congested and congested conditions. The differences in car-following behavior are expressed in different minimum gap - speed models for different vehicle types and regimes. The quality of this description is assessed by implementing the new gap - speed models into the micro simulation model FOSIM with which the corresponding macroscopic patterns are reproduced.

The following chapter briefly summarizes current knowledge on differences in car-following behavior with respect to flow regimes. In the following chapter 3, the research objective is given, and a brief description of the research methodology is presented. A description of the observations used to test the hypothesis and establish individual following models is given in

chapter 4. The extent to which differences in car-following between the regimes are found, is presented in chapter 5. Attention is given to separate vehicle types and lane types of multi-lane freeways. Chapter 6 deals with modeling the findings of chapter 5, including the establishment of a set of microscopic desired distance gap - speed relationships which give insight into differences in behavior between user classes. In chapter 7 the integration of the new distance gap - speed models in the microscopic simulation mode FOSIM is described. In chapter 8 the new relationships are applied in a reproduction study to show the improvements in macroscopic flow description and in the performance of micro simulation modeling.

2 Theory on Traffic Flow by Flow State

This report analyzes individual behavior of drivers and traffic flow for different flow conditions. This chapter presents an introduction to existing theory.

This chapter first gives a short overview of traffic flow characteristics for different flow states (section 2.1). Then some modeling approaches of traffic flow are described (section 2.2). Combination of the two raises the questions which are to be answered in this report (section 2.3).

2.1 CHARACTERISTICS OF TRAFFIC FOR DIFFERENT FLOW STATES

Characteristics of traffic flow are described for three levels of aggregation: macroscopic, mesoscopic, and microscopic.

2.1.1 Macroscopic flow characteristics

Traffic flow can be described macroscopically. Then data are aggregated over time. Usually these data are obtained with measurements at cross sections.

The macroscopic quantities are flow rate (the number of cars passing a cross section per unit of time, q), density (the number of cars per unit of distance, k), and space mean speed (approximately the harmonic average speed of traffic on cross sections, u). Between these quantities the relation $q=k \cdot u$ exists.

The flow rate, density, and speed are usually shown in the fundamental diagrams (figure 1) which are based on measurement data.

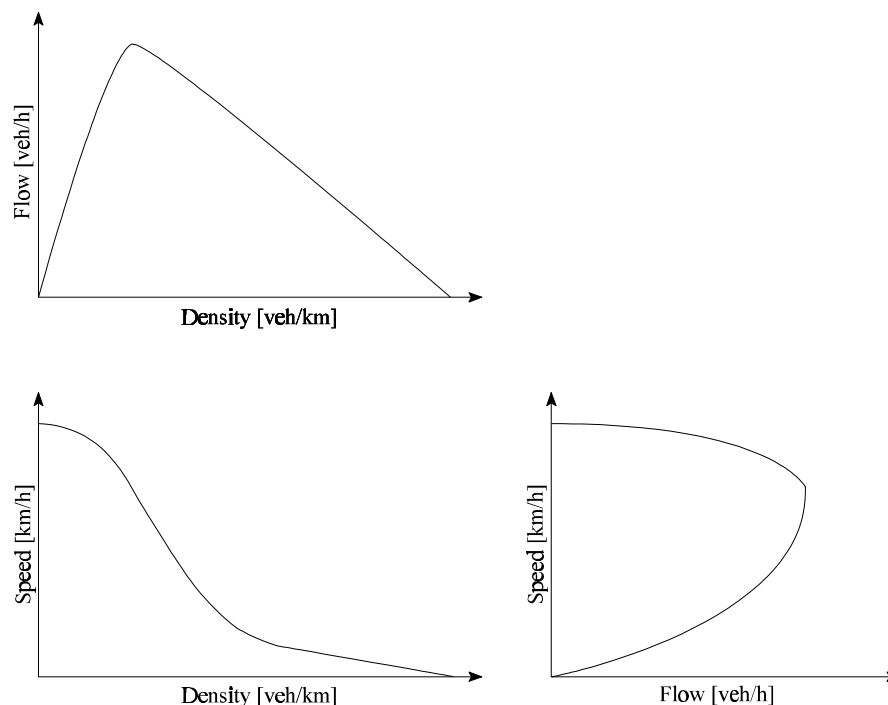


Figure 1: Fundamental diagram

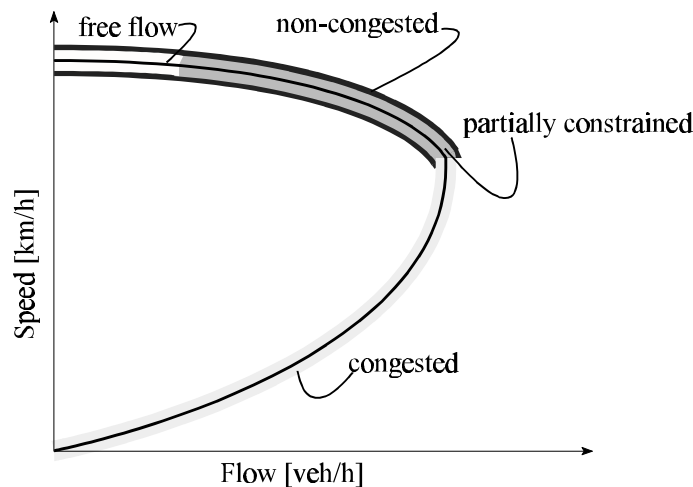


Figure 2: Regimes in the speed-flow diagram

In the diagrams several traffic flow states (regimes) can be distinguished: the non-congested regime, which consists of the free flow and partially constrained regime, and the congested regime (figure 2).

Applying the Level Of Service (LOS) definition of the Highway Capacity Manual (HCM (5)), free flow matches LOS A, congestion matches LOS F, and LOS B through E match the partially constrained state.

Free flow

In free flow the mutual influence of drivers is negligible. The measured macroscopic speed is called *free speed* (u_0).

In free flow, speed does not change with the density. Then the flow rate, which of course is equal to zero with zero density, increases linearly as density increases.

Partly constrained flow

As density increases further, drivers may influence each other. Then a driver has to adjust his speed to another driver for some period of time. Thus a part of the driver population is constrained in its driving behavior. Therefore, this flow state is called 'partially constrained'. With increasing density, drivers have to adapt their driving behavior to other vehicles more often and for longer periods of time. The average speed gradually goes down with increasing density.

The partially constrained regime can be divided further according to the HCM LOS-criteria:

- When densities are still small and speeds are only a little lower than free speed, LOS B applies. With this LOS drivers can still manoeuvre quite freely. The effects of minor incidents and breakdowns are limited.
- In LOS C speeds are still high but manoeuvrability has noticeably decreased. Increases in flow can cause substantial deterioration in service and minor incidents can locally have substantial effects.
- LOS D borders on unstable flow. Speeds are still considerable but freedom to manoeuvre is small. Even minor incidents can have major effects on the traffic stream.
- In LOS E traffic is extremely unstable. Traffic flow can break down with small disruptions.

Flow increases with density to a certain point. This point is called *capacity* (q_c): the maximum flow rate of the facility. The density at capacity is called *critical density* (k_c), the speed is called *critical speed* (u_c).

Congested flow

In congested flow, which matches LOS F, speeds are on average low. Higher speeds can only occur in stop and go waves. Densities are high. The maximum density (*jam density* k_{\max}) occurs at standstill.

Sometimes, empirical data suggest a drop in capacity for the congested flow: a considerably higher maximum flow rate for the non-congested regime than measured for the congested regime (figure 3). This can be an explanation for the sometimes noticed difficulty of recovering from a breakdown.

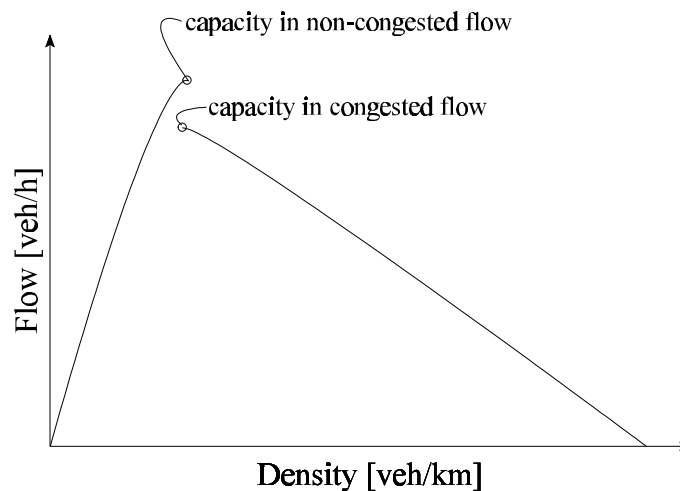


Figure 3: Capacity drop

Several LOS have been described. However, boundaries between the different LOS mostly are difficult to define. The non-congested and congested states are identified easier than the other LOS. Therefore often only these two states are discerned.

2.1.2 Mesoscopic flow characteristics

Instead of time-aggregated data, characteristics of individual vehicles can be obtained for cross sections. Then the characteristics of the distributions of the measured data can be examined (mesoscopic traffic flow characteristics) which also differ by flow condition.

The distributions of time headways are well studied because they can, for instance, be used to estimate capacity.

Random headway state

The random headway state matches the macroscopic free flow regime.

It is called random because cars drive independently (they do not have to adapt to other traffic) which means that vehicles arrive randomly.

Characteristic for the time headway distribution of this state is the rather uniform distribution form with a notable amount of large headways (figure 4, May (1)).

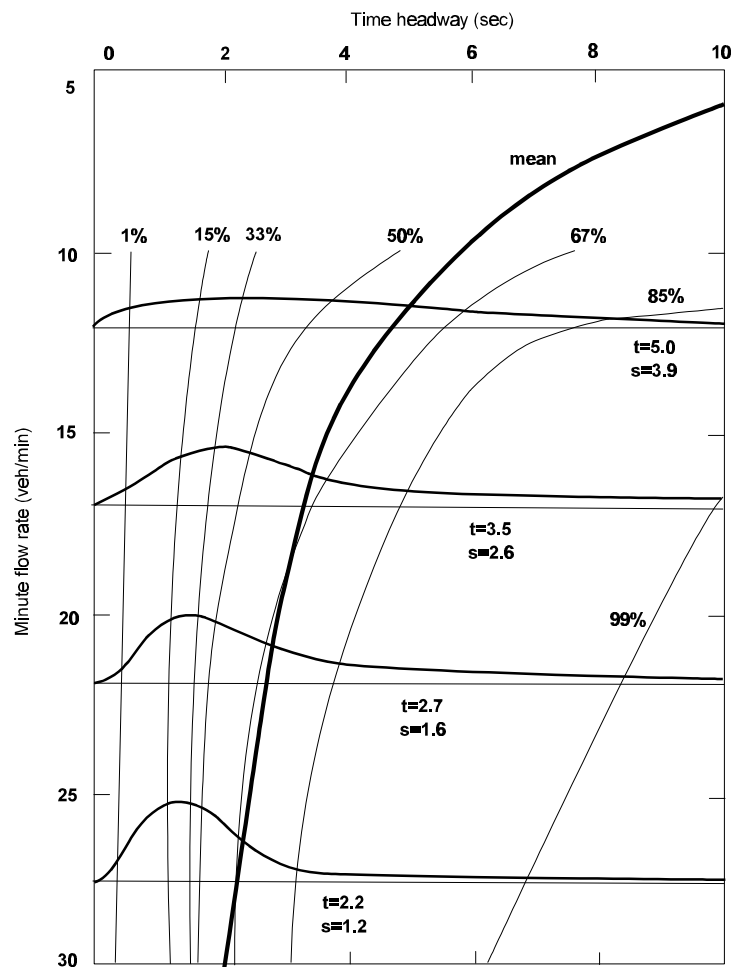


Figure 4: Mesoscopic data (May (1))

Intermediate headway state

The intermediate headway state matches the macroscopic partially constrained regime. Some drivers are free, others have to adjust their driving to other vehicles. Then not all arrivals are random anymore.

Because both free driving and constrained driving occurs, the distribution of time headways consists of both rather large headways and a peak of smaller headways (figure 4).

Constant Headway state

The constant headway state matches the macroscopic congested regime.

All driving is constrained by other traffic.

Then headways are concentrated around a small value (figure 4).

2.1.3 Microscopic flow characteristics

Microscopic traffic analysis means analyzing the behavior of the individual driver.

Characteristics of individual driving can be described with the following variables:

- speed;
- acceleration;
- time headway: time between the passage of two consecutive vehicles including the passage time of the first vehicle (from the front of the first vehicle to the front of the second vehicle);

- time gap: time between the passing moments of the back of the leading and the front of the following vehicle, thus excluding the passage time of the leading vehicle itself (=clearance time);
- distance headway: distance between two consecutive vehicles including the length of the first vehicle;
- distance gap: distance between two consecutive vehicles excluding the length of the first vehicle;
- relative speed: speed difference between two consecutive vehicles.

The individual driver is influenced by his environment. This environment consists of facility characteristics, surrounding traffic, and external conditions, like weather and light conditions. Drivers react, more or less consciously, to their environment which has results for speed, headway, et cetera. This research project analyzes the influence of the traffic flow state on driving characteristics. Therefore traffic should not be influenced by external conditions. Differences with respect to microscopic traffic characteristics can be found between regimes similar to macroscopic and mesoscopic flow characteristics.

Free flow

In free flow drivers can drive as they like. If they have to overtake they can do so immediately without changing their desired speed. Then knowledge on the desired speeds of the individual drivers is sufficient to describe this regime microscopically.

Partially constrained flow

In partially constrained flow individual drivers frequently have to adapt their driving to other vehicles before they can overtake to reach their desired speed again. Traffic flow in this state results from free driving and constrained driving characteristics.

Congested flow

In congested flow all drivers adapt their driving to other vehicles. Traffic flow in this state is completely determined by the way drivers react to other traffic.

2.2 DESCRIPTION OF TRAFFIC FLOW MODELS

In transportation planning, design of traffic facilities, and control of traffic operations often information is needed about non-existing traffic situations. To be able to make predictions about these situations traffic flow models are developed.

2.2.1 Macroscopic models

Macroscopic models try to describe traffic using only macroscopic quantities (flow rate, density, and speed). These macroscopic models are often based on best fit through measured data of the fundamental diagram, theory about driving behavior, or analogies with flow of other media (like gasses or water). Modeling efforts can be discerned which use only one model for all regimes, or which use more than one (May (1)).

Well known examples of the first category, as described by May (1), are models developed by Greenshields, Greenberg, and Underwood.

Because of reservations on the performance of these models, Edie proposed to use different models for the non-congested and congested part of the fundamental diagram. Later a research team at the Northwestern University used three models to cover all regimes (see again: May (1)).

2.2.2 Mesoscopic models

Mesoscopic models try establish mathematical distributions for the studied variables. Models of the time headway distribution are important because they can be used to estimate capacity.

In free flow all drivers are independent. In congested flow no driver is independent anymore. Then all drivers try to maintain a certain headway. In the intermediate headway state a part of the drivers is free, others adapt their driving to the surrounding traffic. Both Shuhl and Branston (Botma and Papendrecht (6)) propose composite models: a summation of a distribution for free and constrained drivers (figure 5).

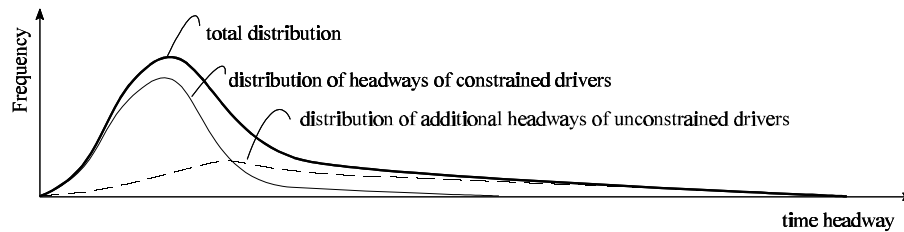


Figure 5: (Hypothetical) Composite time-headway distributions (Branston-type)

Several methods to estimate the parameter values of the composite models exist (e.g. Hoogendoorn, Botma & Bovy (7)).

2.2.3 Microscopic models

Microscopic models describe the driving behavior of the individual driver. In free flow drivers do not influence each other. This situation can be described using knowledge on the speeds that drivers maintain when they are free.

When densities increase, drivers have to adapt their driving to other traffic. When a free driver approaches another vehicle and cannot overtake this vehicle, he will have to adjust his speed to the vehicle in front. This process of adaption is determined by physiological abilities of the driver (what distance gap does he perceive, what speed difference), and on his psychological state (aggressive driving, defensive, et cetera). Wiedemann (8) found that the moment drivers start adjusting their speed to vehicles in front depends on the speed difference - distance gap ratio (figure 6).

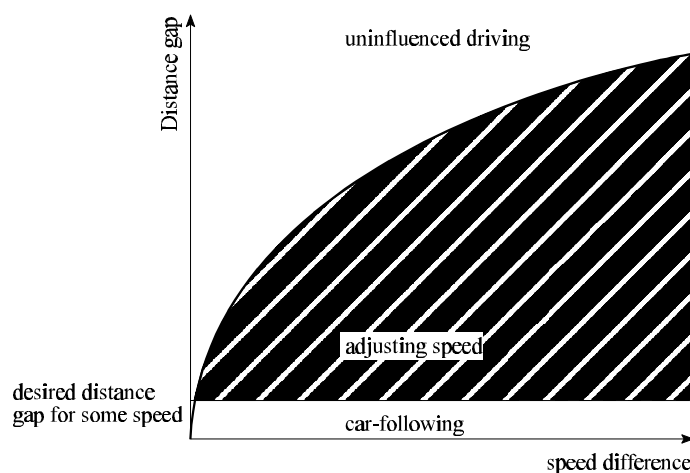


Figure 6: Speed adjustment model by Wiedemann (8)

When a driver has fully adjusted to the vehicle in front, he will try to maintain a certain distance gap, which depends on his speed. The speed of the following vehicle (the follower) will be about the same as the speed of the vehicle in front (the leader). When the leader changes his speed, the follower will change his speed to regain a small speed difference and a certain headway. This behavior is modeled with the general form:

$$\text{reaction}_{\text{follower}} = \text{sensitivity}_{\text{follower}} \cdot \text{stimulus}.$$

A research team of General Motors (Herman et al (9)) developed the 'general' car-following model of the form:

$$a_F(t+r) = \frac{c[v_F^{l-1}(t+r)]}{[x_L(t) - x_F(t)]^l} \cdot [v_L(t) - v_F(t)] \quad (1)$$

with:

F: follower, L: leader;

a: acceleration [m/s²];

v: speed [m/s];

x: vehicle location [m];

t: time [s], r: reaction time [s];

c, m, l: parameters.

The follower's reaction is an acceleration after some delay, instigated by the speed difference between him and the leader. He is more sensitive to speed differences (and thus will react stronger) when his speed is higher or the distance gap is smaller.

2.2.4 Relation between macroscopic and microscopic flow models

It was found that the general car-following model is related to macroscopic models. In the feasible region $0 \leq m < 1$, and $l > 1$, the generalized speed - density equation can be shown to be (May (1)):

$$u^{1-m} = u_f^{1-m} \cdot \left[1 - \left(\frac{k}{k_j} \right)^{l-1} \right] \quad (2)$$

with:

u_f = free flow speed;

k_j = jam density.

l, m = parameters

Thus when different macroscopic models are defined for different regimes, also differences of driving behavior will exist between the regimes (and vice versa).

2.3 RESEARCH QUESTIONS

In the previous two sections characteristics of traffic have been described as well as traffic flow modeling approaches. Different flow states can be discerned. These flow states mainly differ with respect to the influence of drivers on each other. In non-congested flow drivers are relatively free while in congested flow all driving is constrained.

Indications exist of essential differences between the non-congested, and congested flow states, such as a possible difference in capacity for the non-congested and congested state, and better results of fitting functions for the fundamental diagram when different functions for different flow states are used, compared to using one function for all states. Differences between the states are ultimately the result of different individual driving behavior for each flow state.

Because the microscopic simulation model FOSIM (Vermijs (10)) only uses a single model for car-following, and only achieves good results for the non-congested flow state, the Transportation Research Laboratory of the Delft University of Technology needs answers for the following questions:

- Does driving behavior differ per regime?
- If it does, what are the consequences for flow characteristics?
- What are the consequences of such differences for traffic flow modeling?

A better understanding of microscopic characteristics from answering these questions will also lead to improved understanding of macroscopic flow.

In the next chapter, the questions which result from this chapter are used to define the objectives of the research project. Also the research methodology is briefly described.

3 Research Goals and Methodology

Much theoretical work has been done on the car-following phenomenon. However, still the need exists to study different aspects of individual driving behavior with better empirical underpinning. There is an urgent need to look at the car-following phenomenon using observations collected in normal everyday traffic conditions. Such observations are needed to test the hypothesis of differences in car-following behavior with respect to different flow regimes.

It is expected that a deeper knowledge of these car-following relationships will dramatically improve our understanding of microscopic and macroscopic traffic patterns. In addition, if this knowledge is implemented in individual headway-speed relationships, it will strongly improve the performance of microscopic traffic models.

The first objective of this paper is to show empirically to what extent differences in car-following behavior with respect to traffic flow regimes on freeways exist. This analysis is done for specific user groups and specific lanes of a 4-lane and 6-lane Dutch freeway using individual vehicle data. To enable this analysis, the individual vehicle data are separated between followers and non-followers, whereas the prevailing traffic flow conditions are categorized into congested or non-congested regime. Measurements of cross sections downstream and upstream of the bottleneck, and at the bottleneck itself are all used because differences in flow characteristics are often attributed to the location of the measurement site relative to the bottleneck.

The second objective is to establish mathematical relationships relating desired distance gaps to the prevailing driving speeds for different user groups and flow regimes.

To show whether these efforts indeed lead to an improved description of traffic phenomena, the established headway-speed relationships are built into a microscopic simulation model (FOSIM). This model is used to reproduce macroscopic flow patterns. Using the extended FOSIM model the performance of reproducing observed flow patterns is assessed.

4 Observations on traffic characteristics in non-congested and congested conditions

Indications exist that traffic flow should be described differently for the non-congested and congested flow regimes. This proposition is to be evaluated with empirical traffic data. The choice of suitable sites, and the operations performed on the data are described in this chapter. In section 4.1 the choice of suitable measurement sites and their characteristics with possible consequences for traffic flow are described. In section 4.2 the operations which are performed on the data, consisting of calculation of relevant quantities and classification of the data, are presented.

4.1 DATA COLLECTION

4.1.1 Choice of suitable sites

The choice of the sites for measurements is based on three main criteria:

- If useful data already is available for an adequate site, this site is preferred;
- Because congestion should occur, sites on urban freeways with a large amount of commuter traffic are most suited;
- It is intended to measure flow at different locations:
 - on basic freeway sections (such as defined in the HCM (5)) which means that the sections should not be influenced by merging or diverging movements at nearby ramps or by weaving movements. The Highway Capacity Manual (HCM) suggests generally 500 ft (± 150 meters) *downstream* and 2,500 ft (± 750 meters) *upstream* of the off ramp as boundaries for the influenced area.
 - at the bottleneck itself.

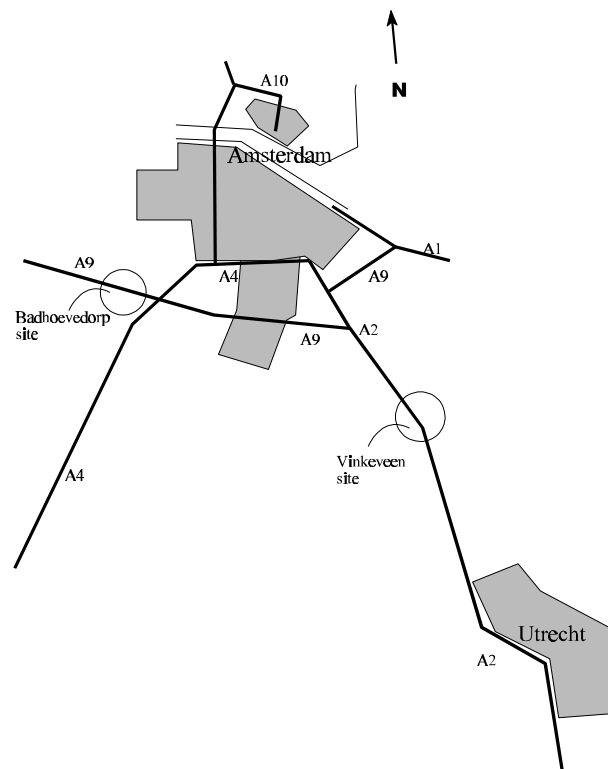


Figure 7: Location of the measurement sites

Useful microscopic data by lane, obtained with measurement systems of the Ministry of Transport, Public Works and Water Management, are available for two sites (figure 7):

- upstream and downstream of the ramp of Vinkeveen, and at the on and off ramp itself on the 6-lane 'A2' freeway in the direction of Amsterdam;
- upstream of the ramp of Badhoevedorp on the 4-lane 'A9' freeway in the direction of Amsterdam.

4.1.2 Description of the sites

An overview of the sites is presented in figure 8. The figure shows the lane configuration and detector locations relative to the ramps.

The road sections meet the Dutch freeway design standards, such as:

- Design speed of 120 km/h;
- minimal lane width of 3.5 meters;
- a lateral clearance large enough not to influence traffic flow;
- small grades which do not influence traffic flow;
- curves which enable high speeds and good view.

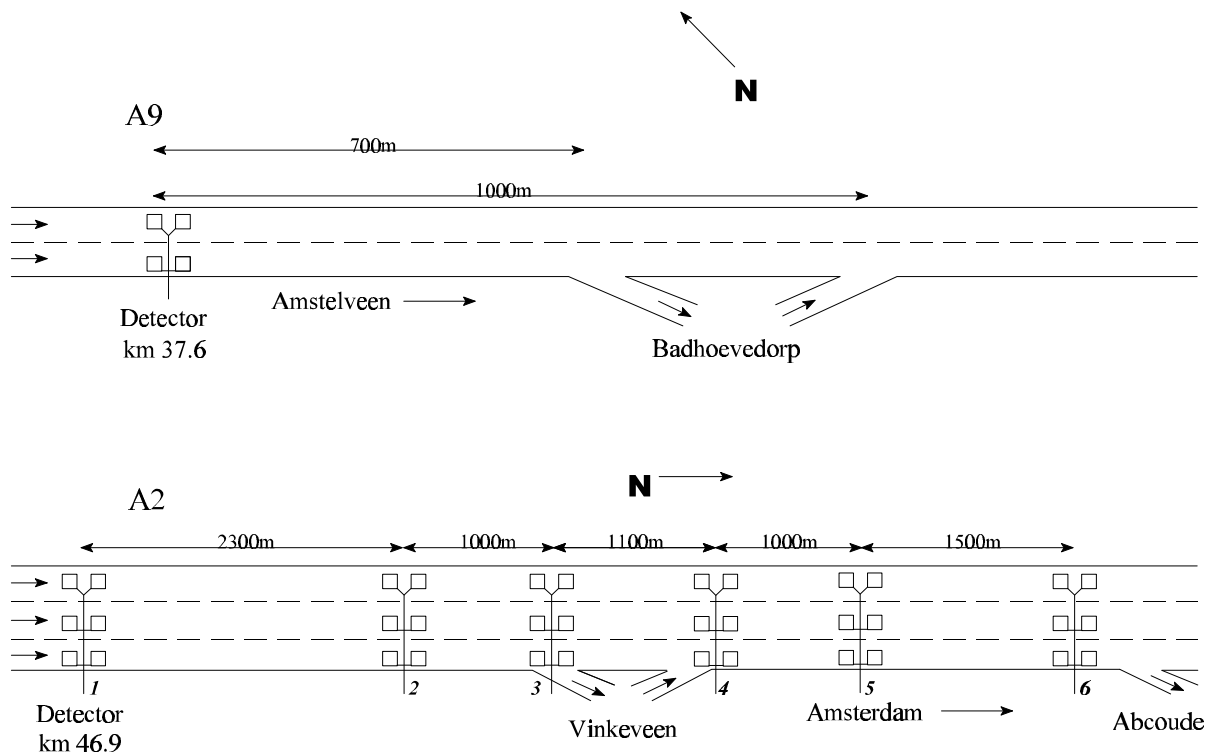


Figure 8: Overview of the measurement sites on the A2 and A9 respectively

Several detectors are available at the sites. At the A2 site, detectors both upstream, downstream, and at the ramps are used. A detector upstream of the bottleneck is used on the A9, mainly as a comparison for the A2 data.

For the A2 site, data are available from Tuesday May 26, 1992 during the morning peak (6.30 - 9.25 a.m.). For the A9 site, data are used from morning peak (7.00 - 9.30h a.m.) traffic for Friday October 14, 1994. About 110 minutes of data from congested flow is available from the A2 site, and about 60 minutes from the A9 site. Congestion is caused by traffic demand exceeding capacity at the on ramps Vinkeveen, respectively Badhoevedorp.

4.1.3 Influences of facility design, traffic regulations, traffic composition and external conditions on flow characteristics

Flow characteristics are influenced by:

- the design of the facility;

- traffic regulations;
- composition of the vehicle/driver population;
- external conditions (weather).

The design of the facility

The Highway Capacity Manual (5) distinguishes the following roadway factors influencing traffic flow:

- the type of facility, and its development environment;
- lane widths;
- shoulder widths, and/or lateral clearances;
- design speed;
- horizontal, and vertical alignments.

The design of Dutch freeways is standardized in '*Standards for Freeway Design*' (ROA (11)). The roadway factors at the A2 and A9 sites (designed according to the ROA-standards) are the following:

- *the type of facility and its development environment:*
The measurement sites are located on freeways. Thus flow is uninterrupted, and that the carriageways are separated by medians. The freeways are located in an urban environment.
- *lane width:*
The minimal lane width required by the ROA (11) is 3.5 meters. This lane width is sufficient not to influence flow negatively.
- *shoulder widths and/or lateral clearances:*
The shoulder widths and lateral clearances are large enough not to influence flow negatively.
- *design speed:*
The design speed is 120 km/h.
- *horizontal and vertical alignments:*
The horizontal alignment is adjusted to the design speed. The terrain of the Netherlands is generally very level which means that the vertical alignment is not an important factor.

In summary, the Dutch freeway system is suited for high speed travel. The freeway design does not influence flow negatively.

Traffic regulations

Some relevant traffic regulations which influence traffic flow on basic freeway sections are:

- Maximum speed on freeways: 120 km/h;
Maximum speed for trucks: 80 km/h;
In practice higher speeds than the official maximum occur. Especially the maximum speed for trucks is frequently ignored during the measurements;
- No trucks are allowed in the median lane of 6 lane freeways:
Indeed, trucks rarely drive in this lane;
- Drivers are supposed to drive in the shoulder lane when they are not overtaking:
This rule is often broken but it has no negative consequences for traffic flow;
- It is illegal to pass slower vehicles in a lane to the right, except in congested conditions, and at ramps and weaving areas:
A consequence of this rule, which is kept reasonably well, is that the lowest average speed is found for the shoulder lane, where most trucks drive, and the highest for the median lane.

Composition of the vehicle/driver population

The vehicle/driver population influences traffic flow. For instance the lower acceleration of trucks can influence flow negatively.

At the sites most traffic during the peak hour is commuter traffic. Thus most drivers are well experienced, are (very) familiar with the road, and feel a certain time pressure. Consequently, high flow rates can be reached.

During the measurement periods 10% of all traffic are trucks on the A2, and 5% on the A9. Because the terrain is level the influence of the trucks on flow is not too large.

External conditions

External conditions (e.g. weather conditions) on the A2 and A9 do not influence flow negatively during the measurements.

4.2. CALCULATION AND CLASSIFICATION OF DATA

From induction loop measurements for each lane microscopic and macroscopic variables are calculated (the calculation methods are described in Appendix A).

4.2.1 Time aggregated data (macroscopic data)

When traffic data is aggregated over time, the following variables can be calculated:

- flow rate (q);
- space mean speed (u);
- density (k).

The choice of an appropriate averaging interval is somewhat arbitrary (e.g. Minderhoud, Botma & Bovy (12)). Large intervals smooth fluctuations, while small intervals show a lot of variation. Aggregation intervals of five minutes are used as a compromise. The macroscopic data is calculated both by lane, and for the carriageway as a whole.

4.2.2 Individual vehicle data (microscopic data)

The calculated microscopic variables are:

- *vehicle speed*;
- *vehicle length*;
- *relative speed*: speed difference between follower and leader;
- *time headway*: time between the passage moments of the front of the leading and following vehicle;
- *time gap*: time between the passing moments of the back of the leading and the front of the following vehicle, thus excluding the passage time of the leading vehicle itself (=clearance time);
- *distance headway*: distance between the front of the leading and the following vehicle;
- *distance gap*: distance between the back of the leading and the front of the following vehicle, thus excluding the length of the leading vehicle.

It is expected that drivers of different vehicle types (passenger cars, light trucks, heavy trucks) show different car-following behavior. Also, probably differences in driving behavior between lanes exists. Therefore, the microscopic data are separated as follows:

- passenger cars in the median lane;
- passenger cars in the middle lane;
- passenger cars in the shoulder lane;
- light trucks in the shoulder lane;
- heavy trucks in the shoulder lane.

It is intended to find differences in car-following between flow regimes. Therefore the data are separated according to the regime. Only the non-congested and congested regimes are distinguished. The non-congested regime can be separated further but no main differences in car-following behavior are to be expected between these regimes, and development of sound separation criteria for these regimes is not straightforward.

The regimes are identified with **macroscopic** variables (see figure 9). The congested branch of the fundamental diagram generally shows larger densities and lower speeds. Figure 10 (above) shows the relation of flow rate and density for the median lane at detector 1 on the A2. Clearly one non-congested and one congested period can be distinguished. (Nevertheless, the congested data sometimes show densities smaller than the highest densities in non-congested flow.) Vehicles are identified as driving in congested or non-congested traffic based on these macroscopic data.

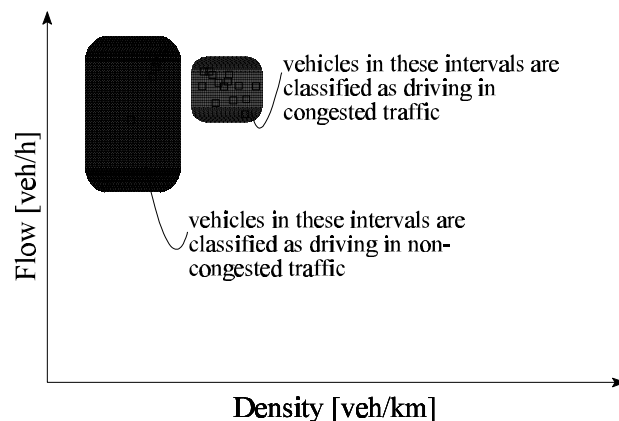


Figure 9: Classification of individual vehicles driving in congested or non-congested flow based on time-aggregated data

However, the first vehicles in congested traffic can still be in a time interval which is macroscopically non-congested. Therefore, a **complementary**, microscopic selection criterion. To select the first (and *only* to select the first) individual vehicle in congested traffic, individual speeds at cross sections are visually inspected. As can be seen in figure 10 (below), speeds go down abruptly at the beginning of congestion. Therefore, the identification of the flow state is only complicated for a small number of vehicles, and is therefore not critical. A speed criterion (e.g. 50 km/h in figure 10) may be used to define the exact breakpoint between non-congested and congested flow.

Flow *remains* classified as congested until the macroscopic variables are plotted on the non-congested branch of the fundamental diagrams again.

It is stressed that the identification of the flow state is not based on individual speeds but on the macroscopic relations. Individual speeds are only used to determine the *boundary* between the congested and non-congested states at the most detailed level.

To find differences in traffic flow between regimes, car-following behavior is analyzed. Then drivers who are following need to be distinguished from free drivers. Free and following drivers are discerned using a critical time gap: drivers with a smaller time gap than this critical gap are assumed to be following, others non-following. The (difficult) choice of the value for the critical time gap is described in Appendix B.

Eventually, for passenger cars a critical time gap value of 3.5 seconds is chosen, and for trucks a value of 5 seconds. Further, it is assumed that all drivers are following in congested flow.

In the next chapter the microscopic and macroscopic data from the two freeways are analyzed.

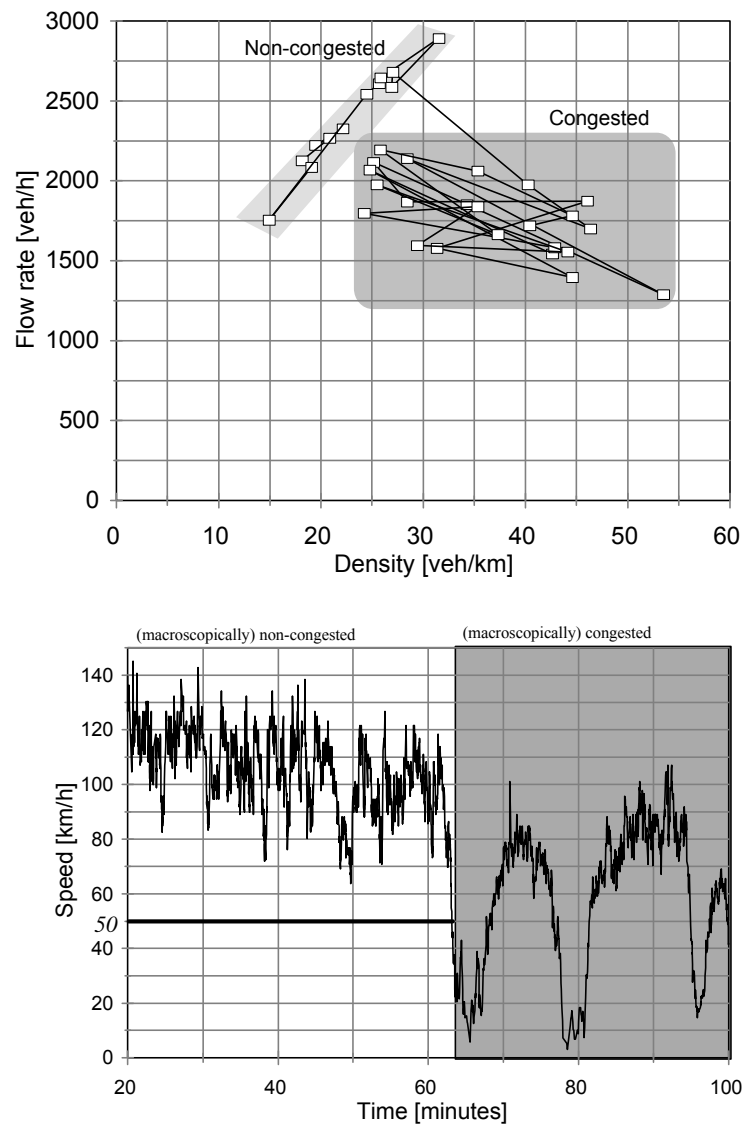


Figure 10: Macroscopic data (above, consecutive 5 minute aggregates connected by lines) to identify the traffic state and individual speeds of consecutive vehicles (below) to identify the first vehicle in congested traffic (median lane, detector 1 at the A2 site (20 minutes = 6.50 a.m.))

5 Characteristics of the Non-congested and Congested Regimes at Dutch Freeway sites

Traffic flow may differ by flow regime. Specifically, indications exist that car-following behavior differs for the non-congested and congested regimes. Differences between regimes can be determined by analysis of traffic data. In chapter 4 the measurement sites on two Dutch freeways and the available data have been described. Both macroscopic and microscopic data are available for cross sections upstream, downstream, and at the bottleneck.

Thus traffic can be studied both microscopically and macroscopically. If differences between regimes exist, this is ultimately caused by different behavior of individual drivers in different regimes. Therefore, individual distance gap keeping as a function of speed is analyzed in section 5.1 as an important aspect of car-following behavior. This is done by regime, separately for different lanes, for different vehicle types, for different locations relative to the bottleneck (overload at an on ramp), and for two freeway types (6 lane and 4 lane).

The sites used for microscopic analysis in section 5.1 are revisited in section 5.2 for macroscopic examination. The results from the microscopic and macroscopic analyses are combined in section 5.3 and some conclusions are drawn.

5.1 ANALYSIS OF THE INDIVIDUAL DRIVING BEHAVIOR AT DUTCH FREEWAY SITES

With cross section measurements speeds, headways, and car lengths of the passing vehicles are determined. They are used to study the distance gap keeping by regime, an important aspect of car-following behavior. Therefore, distance gaps as a function of speed are used for the microscopic analysis.

When drivers are following, they try to maintain a certain distance gap. This gap is larger for high speeds than for low speeds. This behavior is implicitly part of the car-following equation (equation 1). When differences in car-following between regimes exist, this can have consequences for the maintained distance gaps. In the analysis it is assumed that the average maintained distance gaps, which are measured for traffic with speeds changing in time, approximately equal the distance gaps which are maintained when speeds are constant.

These distance gap - speed data (of followers, separated from non-followers as described in section 4.2) are plotted with speeds on the horizontal axis and distance gaps on the vertical axis. Because of the very large amount of scatter these plots do not show a clear image of car-following characteristics (e.g. figure 11).

Therefore, the data are summarized by calculating the average distance gap per 5 km/h interval. These averages, together with standard deviations, are plotted. Average distance gaps, standard deviations, and sample sizes of all 5 km/h intervals at the cross section farthest upstream of the bottleneck (detector 1 on the A2 freeway) are presented in Appendix C.

It is expected that car-following differs by vehicle type and lane. Therefore, the data is analyzed separately for each vehicle type and lane, as described in section 4.2. The identification of data from the congested and non-congested regimes is also described in section 4.2.

Further, differences might be found between different freeway types. Both a 6 lane site on the A2 and a 4 lane site on the A9 freeway are studied. At the A2 site, 6 detectors at different locations relative to the bottleneck are available. A detector upstream of the bottleneck is studied on the A9 as a comparison for these results.

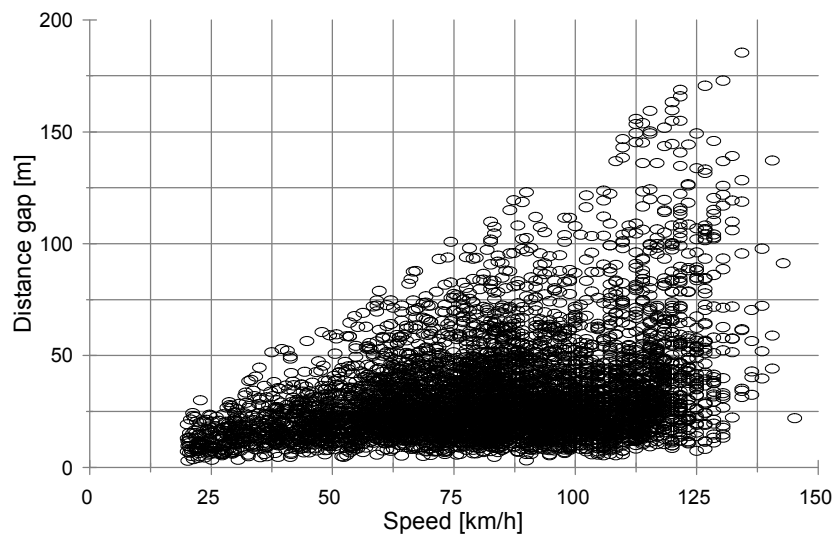


Figure 11: All distance gap - speed data from the median lane of the A2 site (detector 1), non-congested and congested

5.1.1 Distance gap keeping at the A2 site

Figures 13 until 17 show the average distance gap and the standard deviation per 5 km/h interval separated for non-congested (6.30-7.35h a.m.) and congested (7.35-9.25h a.m.) flow at detector 1 (the detector most upstream of the bottleneck) at the A2 site. Different lanes and vehicle types are distinguished as described in chapter 4. During the measurement period, when traffic has become congested it does not return to the non-congested state during the measurement session. Therefore, only a pre-congestion and a congestion period can be studied, and it cannot be studied whether measurements from periods before and after congestion resemble.

It appears that quite high speeds occur in congested flow. This is due to stop and go waves (figure 12). When these high speeds occur, densities are still high and the macroscopic measurements are plotted in the congested branch of the fundamental diagram.

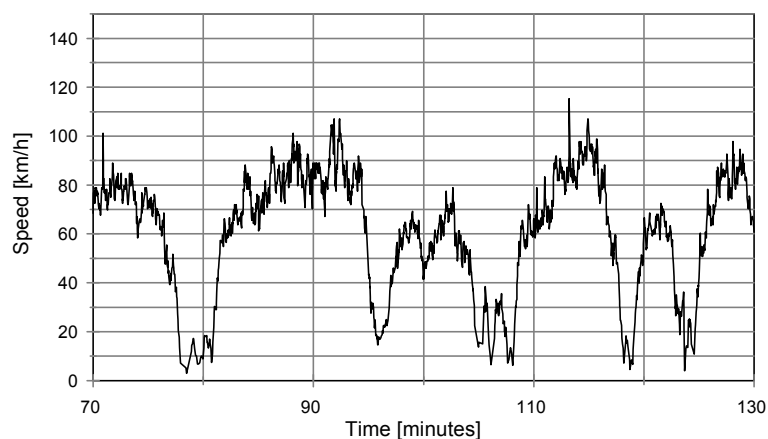


Figure 12: Stop and go waves in congested traffic in the median lane at detector 1 at the A2 site (70 minutes = 7.40 a.m.)

The figures show that on average, at detector 1 of the A2 site, passenger cars follow with larger distance gaps in congested than in non-congested flow. This difference is (relatively)

largest for the median lane. For distance gaps of trucks no differences are found. (Average distance gaps, standard deviations, and sample sizes of all 5-minute intervals of this detector are presented in Appendix C.)

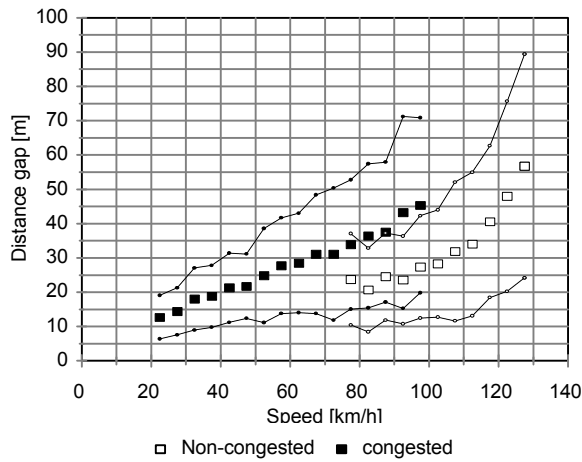


Figure 13: Average distance gap and standard deviation per speed interval, passenger cars in the median lane, detector 1 at the A2 site

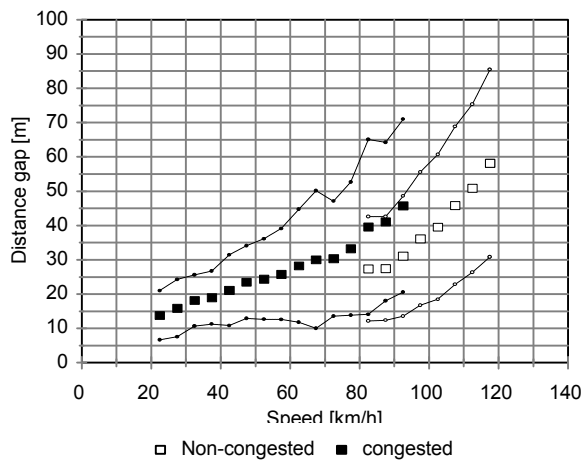


Figure 14: Average distance gap and standard deviation per speed interval, passenger cars in the middle lane, detector 1 at the A2 site

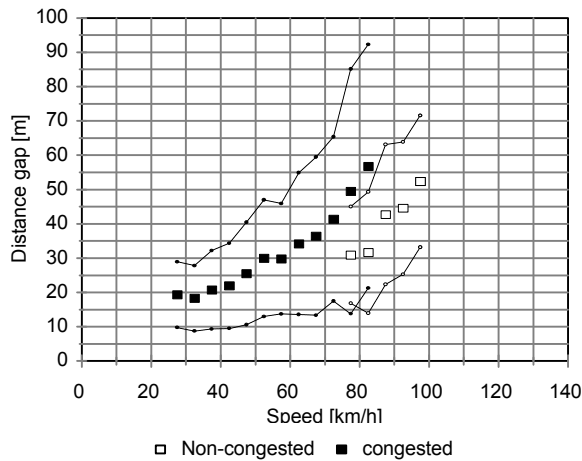


Figure 15: Average distance gap and standard deviation per speed interval, passenger cars in the shoulder lane, detector 1 at the A2 site

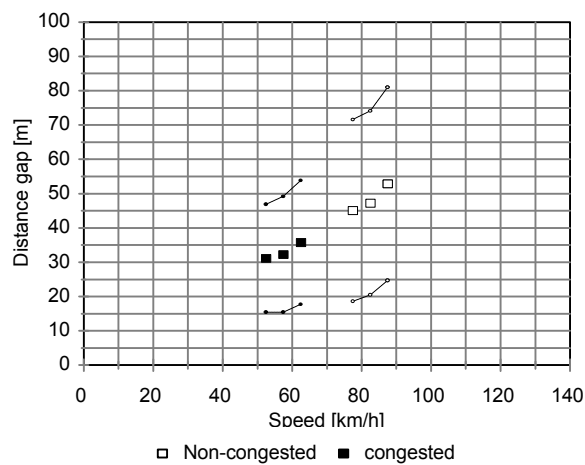


Figure 16: Average distance gap and standard deviation per speed interval, light trucks in the shoulder lane, detector 1 at the A2 site

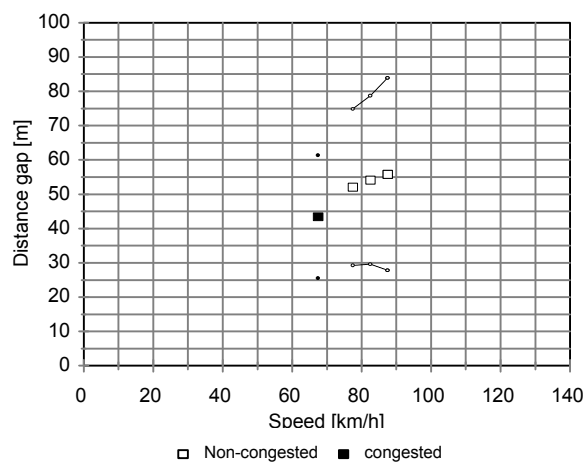


Figure 17: Average distance gap and standard deviation per speed interval, heavy trucks in the shoulder lane, detector 1 at the A2 site

In figures 18 and 19 the distance gap - speed results are compared by lane for the congested and non-congested states. It appears that the results for the *congested* state are somewhat similar for all lanes, especially for the lowest speeds. For higher speed the distance gaps in the shoulder lane increase faster than in the other two lanes. For the middle lane it appears to increase very similar to the median lane.

In non-congested flow, as expected, distance gaps of passenger cars are smallest for the median lane and largest for the shoulder lane.

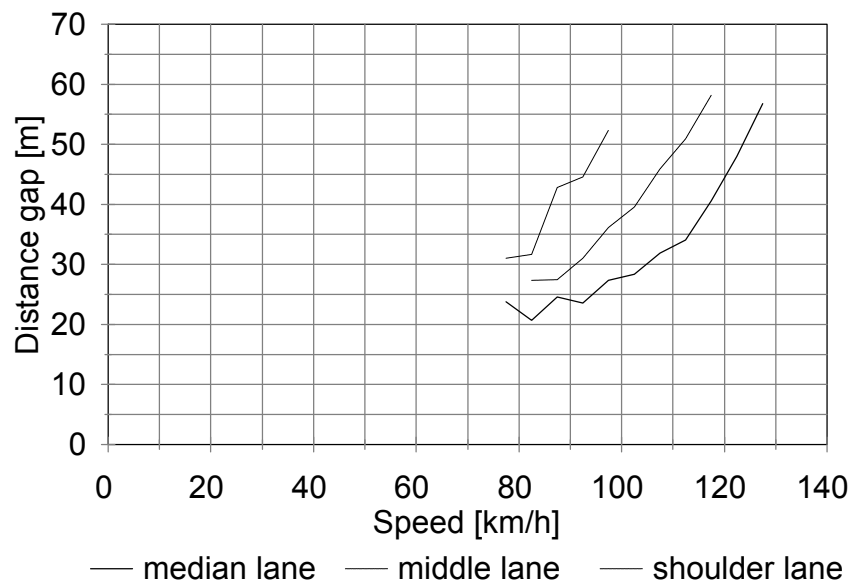


Figure 18: Distance gap - speed measurements of passenger cars for non-congested flow in the median, middle, and shoulder lane at detector 1 of the A2 site (detector 1)

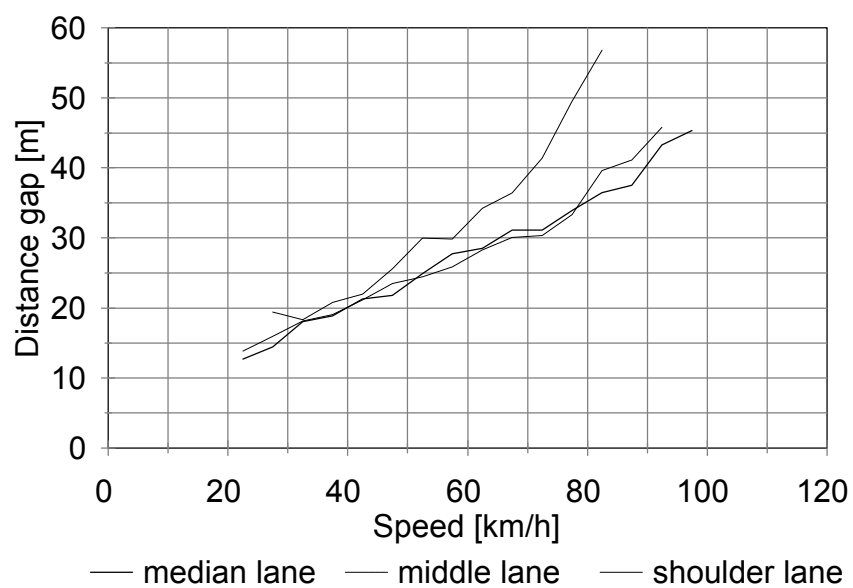


Figure 19: Distance gap - speed measurements of passenger cars for congested flow in the median, middle, and shoulder lane at detector 1 of the A2 site (detector 1)

The average distance gap - speed plots for the other five detectors of the A2 site are shown in figure 21. Only diagrams for passenger cars are shown because data on trucks in the shoulder lane are corrupted for the detectors 2 until 6.

The traffic characteristics at the different detectors are not the same. Far upstream of the bottleneck stop and go waves with large speed differences occur. Downstream of the bottleneck traffic is more stable (figure 20).

Cross sections upstream of the bottleneck where heavy congestion exists, at the bottleneck, and downstream of the bottleneck, where drivers can gain speed again, all show similar differences in the distance gap - speed relations for the two regimes. Especially at the off ramp some differences from other locations can be identified. These differences result from a different distribution of vehicles over the lanes, and lane changing movements. But always distance gaps in congested flow are larger than in non-congested flow.

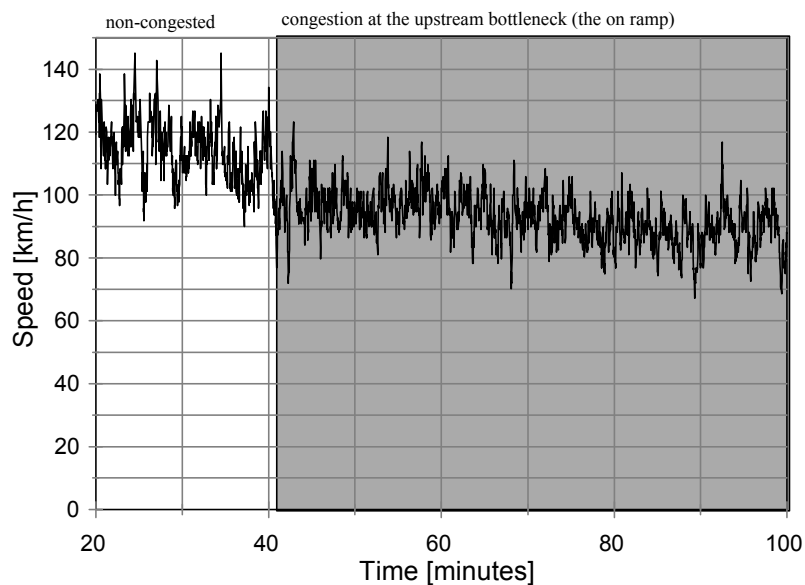


Figure 20: Speeds of consecutive vehicles in the median lane at detector 6 at the A2 site (20 minutes = 6.50 a.m.)

The fact that drivers still follow with these longer distance gaps *downstream* of the bottleneck, when the bottleneck causes upstream congestion, implies that drivers do not change back to shorter following immediately when congestion starts to dissolve again when the bottleneck is passed.

It can be argued that the measured difference in distance gap keeping for non-congested and congested part is caused by the traffic dynamics. In congestion stop and go waves occur. In other words large speed differences are common. Then the desired distance gaps are not measured but distance gaps influenced by accelerations and delayed reactions. All measured distance gaps per 5 km/h interval are averaged. It is assumed that the averaging cancels out the influence of accelerations and delays.

The influence of the dynamics can be examined by looking at different detectors. At the upstream detectors severe stop and go waves occur. At the downstream detectors, traffic flow is much less dynamic. Still at all cross sections quite similar results are found. Apparently, the influence of the traffic dynamics can reasonably be neglected when the *average* distance gap - speed relation is analyzed.

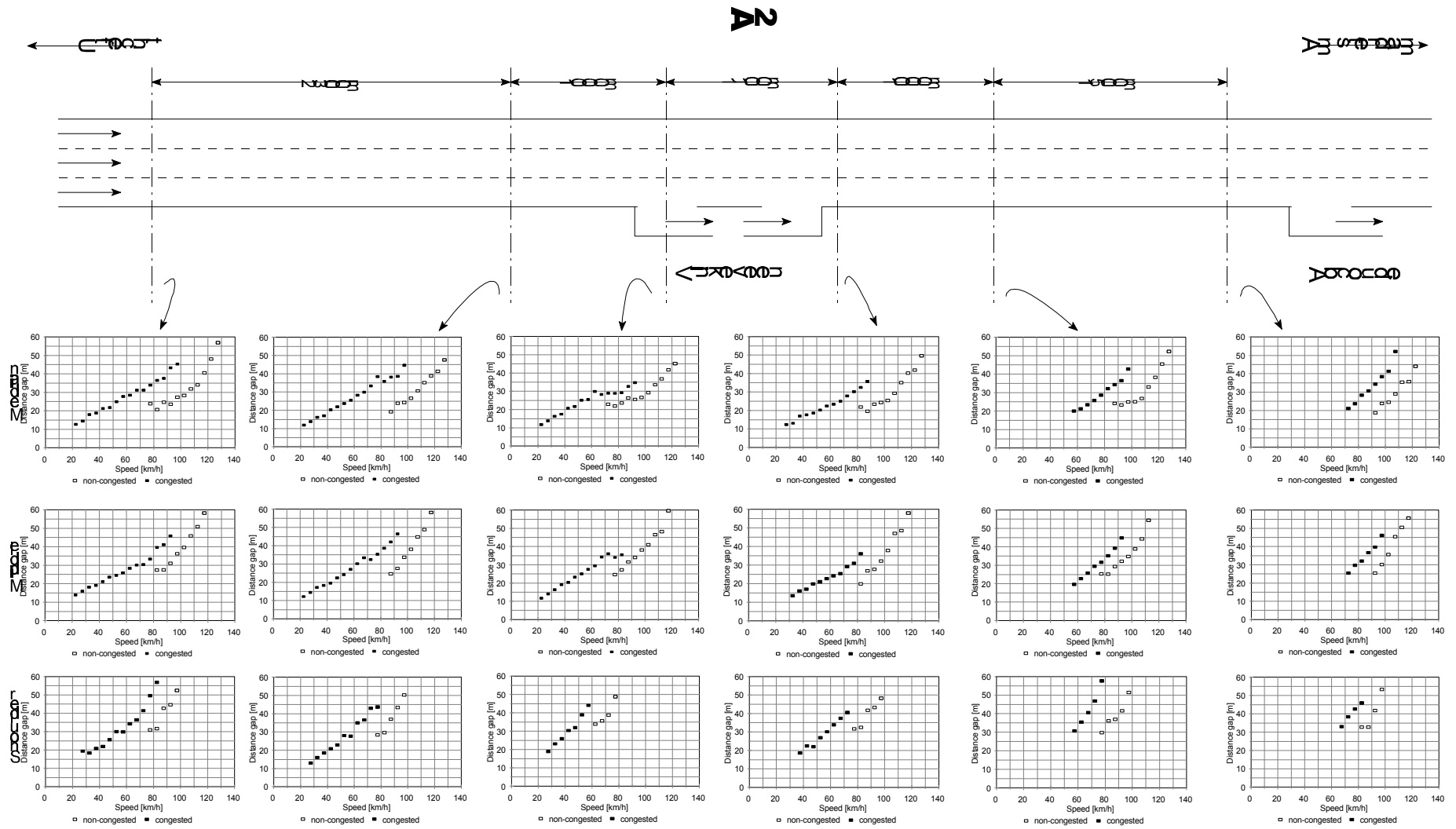


Figure 21: Distance gap - speed relationships of passenger cars by lane for all detectors at the A2 site

5.1.2 Distance gap keeping at the A9 site

Measurements at the A9 site are available for full days. Periods before congestion (7.00-7.55h a.m.), during congestion (7.55-8.55h a.m.), and after congestion (8.55-9.30h a.m.) are distinguished. Figures 22 and 23 show the average distance gaps and the standard deviations per 5 km/h interval, separated for the three periods for the detector at the A9 site, located upstream of the bottleneck. Different lanes and vehicle types are distinguished, as described in chapter 4. Distance gap - speed relations for trucks are not shown because of lack of data. Based on the available data the relations seem similar to the A2 results for trucks.

Similar to the A2, different distance gap - speed relations are found for passenger cars in non-congested and congested flow. Again, as expected, distance gaps are smallest in the median lane.

The results for the periods before and after congestion are similar. During both these periods drivers have not encountered congestion near the Badhoevedorp bottleneck. Therefore this measurement does not tell anything about changing back from congested following to non-congested following. This can only be studied using detectors downstream of the bottleneck (see section 5.1.1).

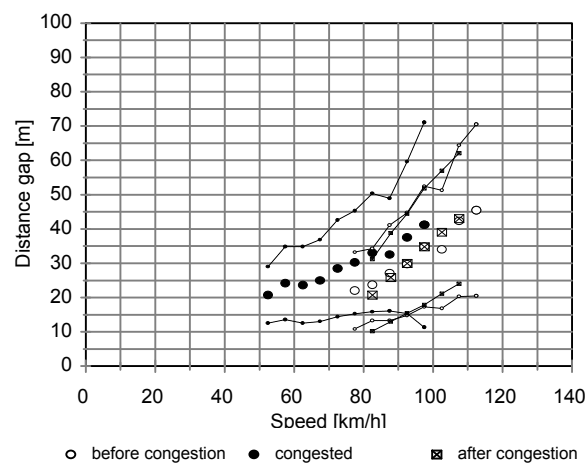


Figure 22: Average distance gap and standard deviation per speed interval, passenger cars in the median lane, detector at the A9 site

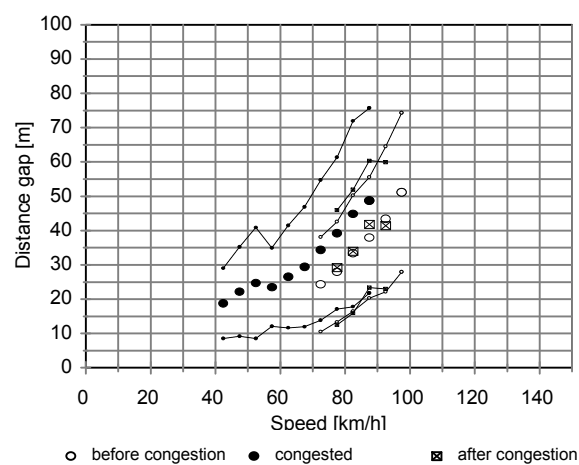


Figure 23: Average distance gap and standard deviation per speed interval, passenger cars in the shoulder lane, detector at the A9 site

In figures 24 and 25 the distance gap - speed results are compared by lane for the congested and non-congested states. It appears that the results for the *congested* state are similar for the two lanes for the lowest speeds. For higher speed the distance gaps in the shoulder lane increase faster than in the other lane.

In non-congested flow, as expected, distance gaps of passenger cars are always smallest for the median lane and largest for the shoulder lane.

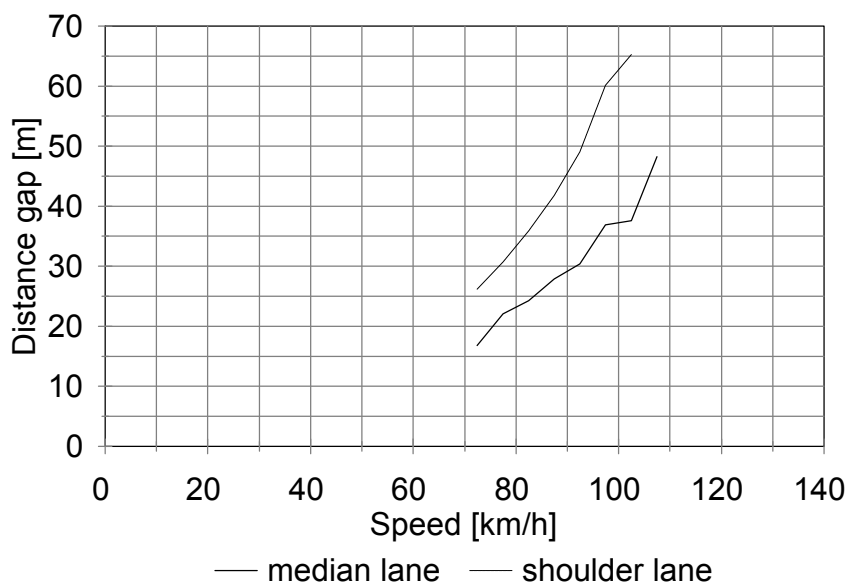


Figure 24: Distance gap - speed measurements of passenger cars for non-congested flow in the median and shoulder lane at the A9 site

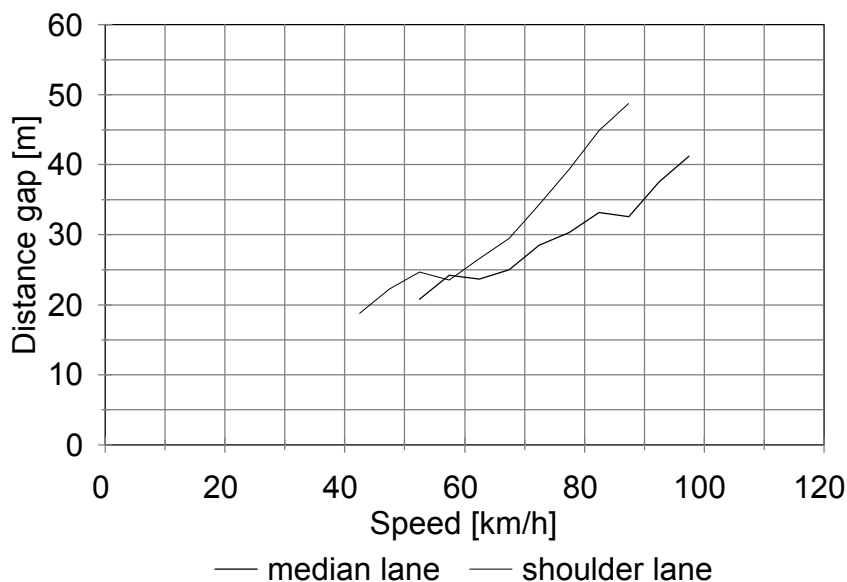


Figure 25: Distance gap - speed measurements of passenger cars for congested flow in the median and shoulder lane at the A9 site

5.1.3 Comparison of distance gap - speed relations at the A2 and A9 sites

There are 6 lanes on the analyzed freeway segment on the A2. At the A9 there are 4. Because of the difference of one lane per direction, some differences in the microscopic data are to be expected due to the difference in distribution of drivers and vehicle types over the lanes.

The following average distance gap - speed plots are compared:

- from the median lanes on the A2 (detector 1) and A9 for passenger cars (figure 26);
- from the middle lane on the A2 (detector 1) and the median lane on the A9 for passenger cars (figure 27);
- from the shoulder lanes on the A2 (detector 1) and A9 for passenger cars (figure 28).

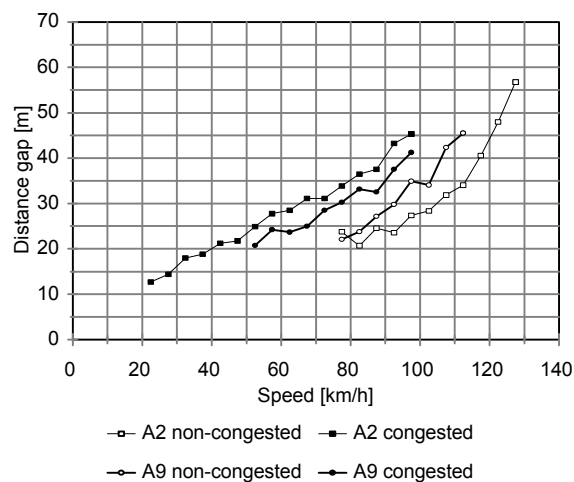


Figure 26: Average distance gap per speed interval, passenger cars in the median lanes at the A2 (detector 1) and the A9 sites respectively

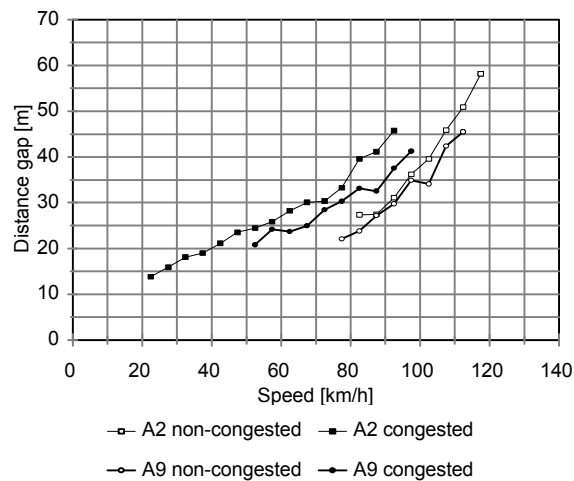


Figure 27: Average distance gap per speed interval, passenger cars in the middle lane at the A2 (detector 1) and in the median lane at the A9 site

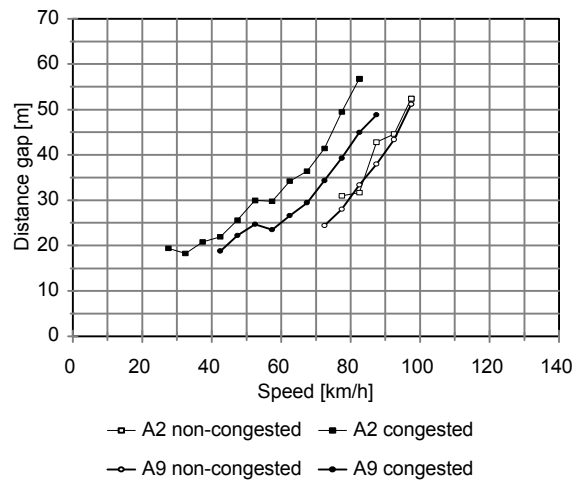


Figure 28: Average distance gap per speed interval, passenger cars in the shoulder lanes at the A2 (detector 1) and the A9 sites respectively

The distance gap - speed data from the median lane on the A9 are both different from the median and middle lane at the A2 site. The A9 median lane data look most like the data from the middle lane of the A2 shifted somewhat downward (smaller gaps on the A9). For the shoulder lane, the A2 and A9 data resemble well for the non-congested state. However, in congested flow, the distance gaps at the A9 site are smaller than at the A2 site.

These differences for non-congested flow might be explained by the difference in the number of lanes:

Suppose the distribution of drivers with different car-following behavior is similar on a 4 lane and 6 lane freeway. Then the distance gap - speed relationship for the carriageway should be on average similar for the 4 lane and 6 lane freeway.

The average distance gap for all passenger cars on the carriageway are shown in figure 29. The congested data still show a difference for the whole speed range. Apparently differences in car-following between the A2 and A9 for congested flow are not only a consequence of measuring at roads with a different number of lanes. The difference in distance gap between the two regimes for the 6 lane freeway A2 is larger than for the 4 lane freeway A9.

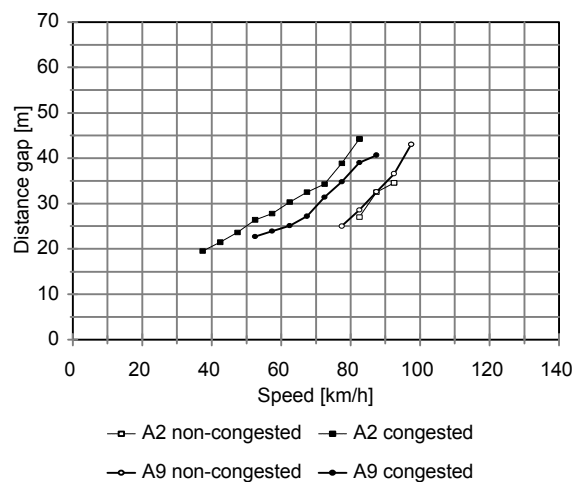


Figure 29: Average distance gap per speed interval, passenger cars on the carriageway at the A2 (detector 1) and the A9 sites respectively

Distance gap keeping by trucks on the A2 and A9 can only be compared roughly because of the small data sample from the A9. The distance gap - speed data from the A2 and A9 appear similar.

5.2 ANALYSIS OF MACROSCOPIC CHARACTERISTICS AT DUTCH FREEWAY SITES

In section 5.1 it is found that car-following behavior of passenger cars differs for non-congested and congested flow at sites on two Dutch freeways. In congested flow distance gaps are larger than in non-congested flow for the same speed.

The behavior of all individual drivers together eventually results in characteristics of the total flow. In this section macroscopic characteristics are presented for the sites that were used to study traffic microscopically in the previous section.

Macroscopically, traffic flow can be studied by analysis of the fundamental diagram. The fundamental diagram gives insight in the relation between flow rate q , density k , and speed u . The fundamental diagram can be used to determine characteristic values like the free flow speed, capacity, critical density, and such. Comparison of fundamental diagrams for different roads, cross sections, lanes, or for different moments in time can show differences in flow characteristics.

The fundamental diagrams are fully shown for the detector most upstream of the bottleneck on the A2 and for a detector on the A9, again upstream of the bottleneck. Only the flow density diagrams are shown for the other detectors on the A2. Of course, speeds can be calculated easily with these figures. Apart from the diagrams some characteristic values are summarized in tables. Diagrams and tables are given for each lane and for the carriageway.

The length of the time-interval for data aggregation partly determines the amount of variation in the measured data. In chapter 4 it was decided to use the 5-minute interval as a compromise between smoothing and showing variation. In the diagrams the consecutive 5-minute interval data points are connected with lines.

5.2.1 Macroscopic flow characteristics at the A2 site

In figures 30 until 32 the fundamental diagrams for each of the three lanes of detector 1 on the A2 freeway are presented. The related q - k , u - k , and u - q diagrams are shown in one figure. The dots in the diagrams represent 5-minute values which are connected with each other according to the chronological order. This way a clear distinction of the regimes can be visualized. Flow characteristics (summarized in table 1) are determined from these fundamental diagrams. Data from 6.30-9.25h a.m. of May 26, 1992 are shown. The fundamental diagrams show traffic to be congested during one continuous period of about 110 minutes (7.35-9.25h a.m.). Thus the data consist of only one shift from non-congested to congested flow. Because detector 1 is upstream of the bottleneck, capacity cannot be measured.

Median lane

The u - q relation indicates a free speed of above 120 km/h with a speed between 90 and 100 km/h when maximum volume is reached. The highest measured 5-minute flow rate value is approximately 2900 veh/h with a critical density of about 30 veh/km. However, most high flow rates are near 2700 veh/h with a density of about 27 veh/km.

The fundamental diagram shows a drop in maximum volume: the highest measured flow rate for congested traffic is about 2200 veh/h with a density of about 25 veh/km. Apparently both a different maximum volume and different critical density may exist for non-congested and congested flow. Because of lack of data for very high densities an estimation of jam density (at standstill) cannot be made.

Middle lane

The u-q relation indicates a free speed of above 110 km/h with a speed between 90 and 100 km/h when maximum volume is reached. The highest measured 5-minute flow rate value is approximately 2300 veh/h with a critical density of about 25 veh/km.

The fundamental diagram shows a drop in maximum volume: the highest measured flow rate for congested traffic is about 2100 veh/h with a density of about 26 veh/km. Because of lack of data for very high densities an estimation of jam density (at standstill) cannot be made.

Shoulder lane

The u-q relation indicates a free speed of about 100 km/h with a speed between 80 and 90 km/h when maximum volume is reached. The highest measured 5-minute flow rate value is approximately 1400 veh/h with a critical density of about 17 veh/km.

The fundamental diagram does not show a drop in maximum volume. Because of lack of data of very high densities an estimation of jam density (at standstill) cannot be made.

Comparison of the lanes

As expected, the highest free speed is found for the median lane, the lowest for the shoulder lane. The fundamental diagram also indicates that the highest maximum volume is reached in the median lane and the lowest in the shoulder lane. The median lane shows the clearest drop in maximum volume. For the shoulder lane a drop in maximum volume seems not to exist.

In figure 33 the u-k data by lane are shown in one figure. For the non-congested state parallel lines are found for the different lanes. The lines are only shifted somewhat toward lower speeds and lower critical densities. The congested data of the median and middle lanes are very similar. Densities at the shoulder lane are a little lower (assuming a person car equivalent (pce) of 1 for trucks).

The differences between the lanes are a result of differences in traffic composition (percentage of heavy vehicles) and of differences in driving behavior characteristics by lane (e.g. the desired speed of individual drivers).

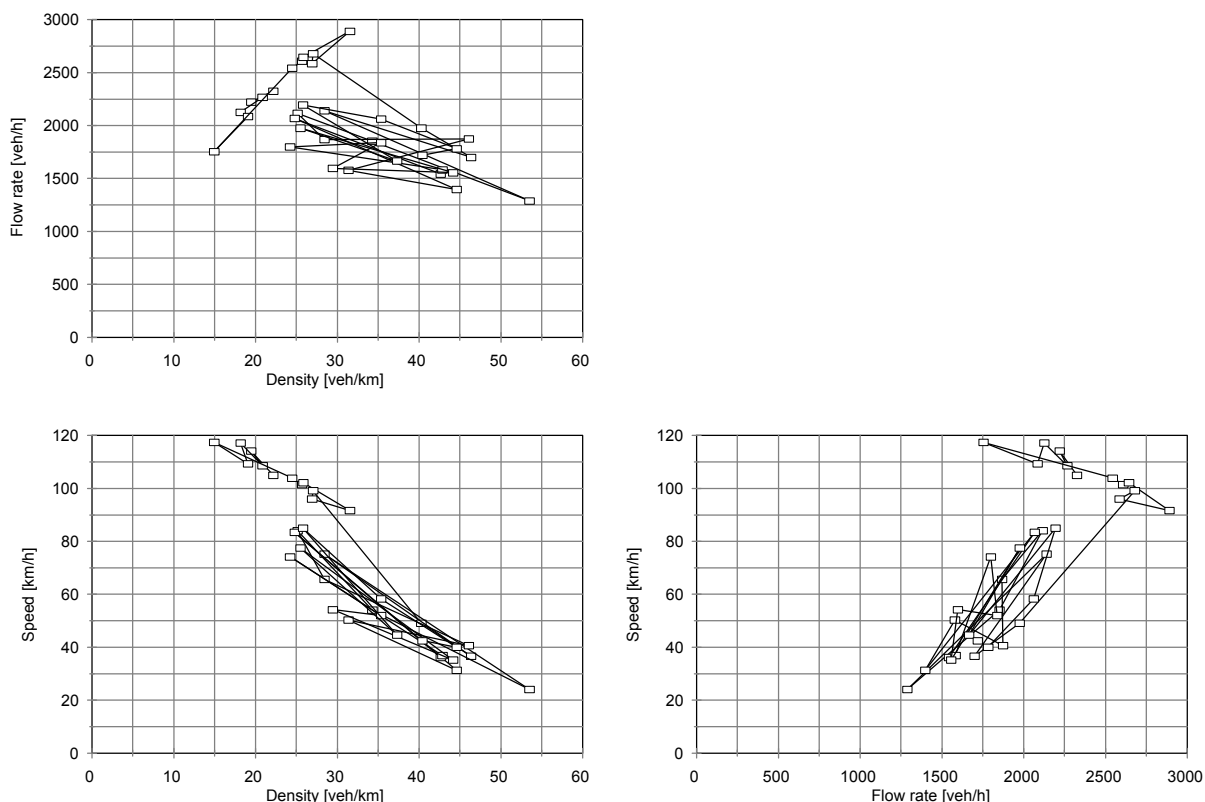


Figure 30: Fundamental diagram for the median lane at the A2 site (detector 1, 5 minute averages)

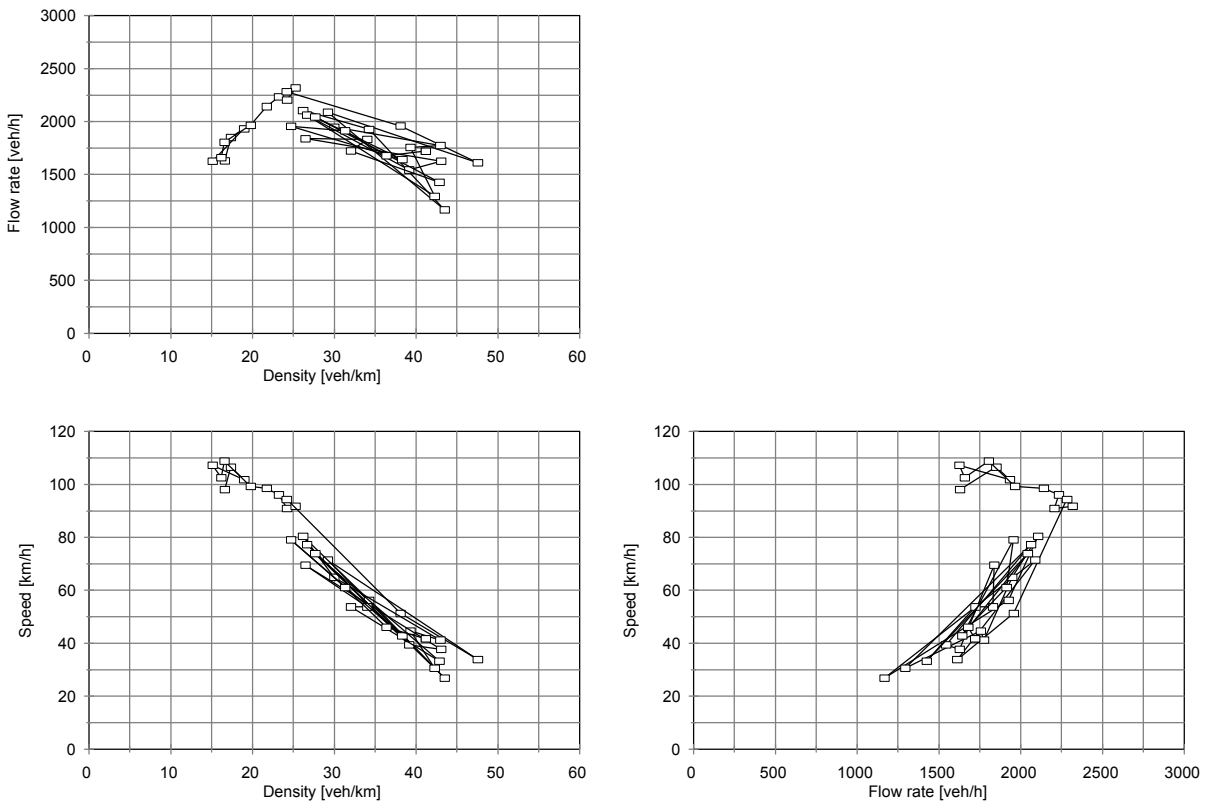


Figure 31: Fundamental diagram for the middle lane at the A2 site (detector 1, 5 minute averages)

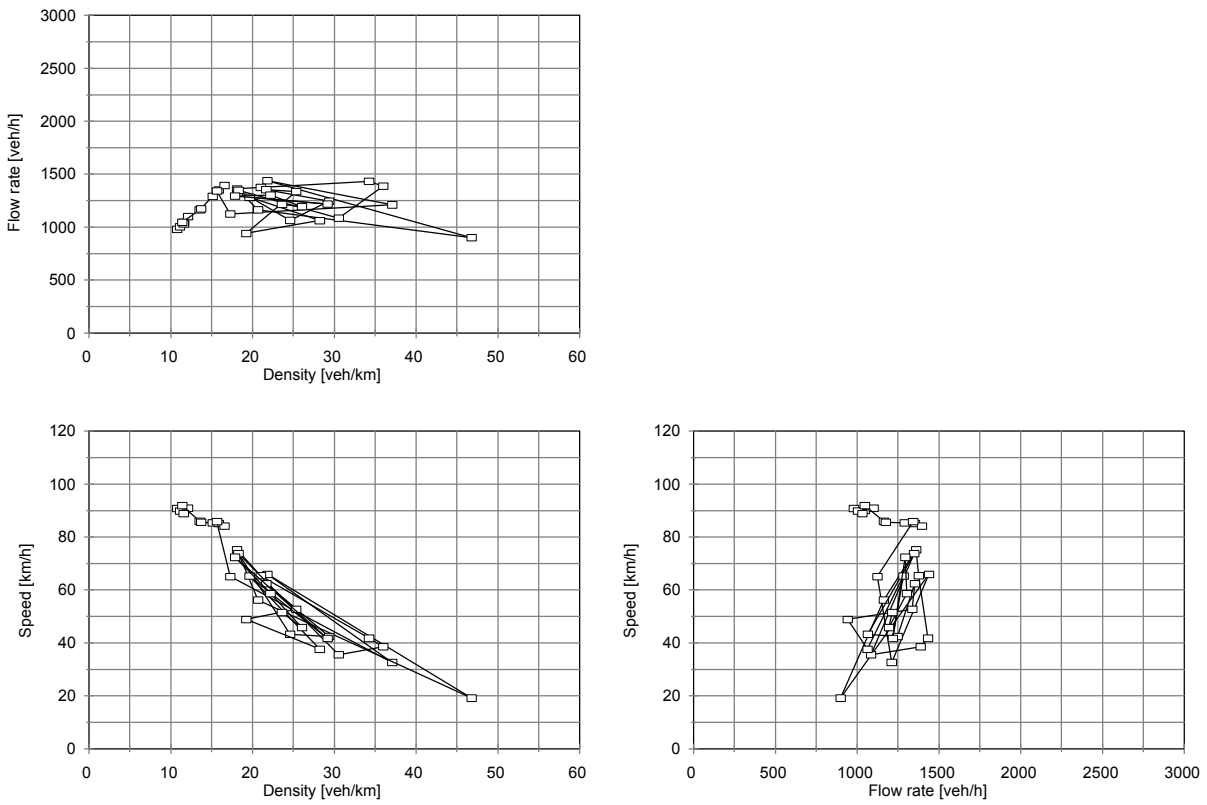


Figure 32: Fundamental diagram for the shoulder lane at the A2 site (detector 1, 5 minute averages)

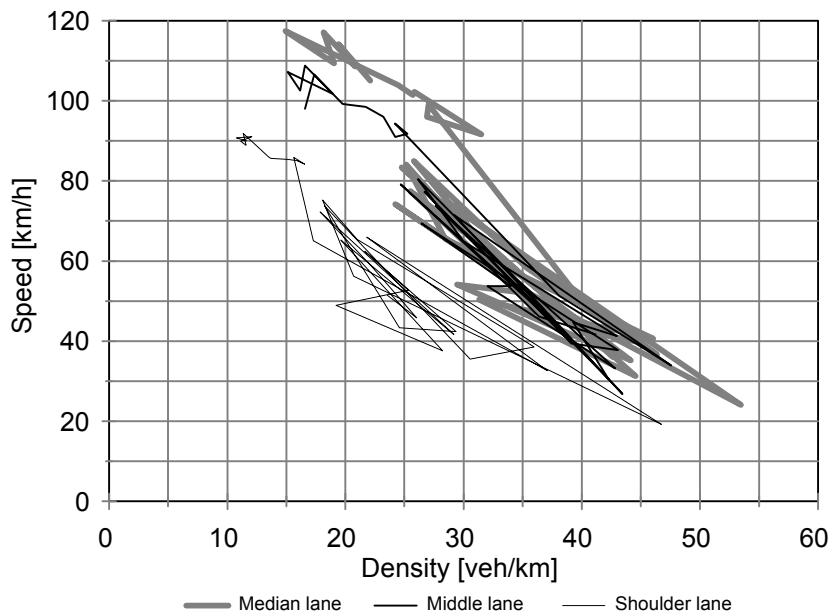


Figure 33: Speed-density diagram by lane for the A2 site (detector 1, 5 minute averages)

Fundamental diagram for the carriageway as a whole

In figure 34 the macroscopic data for the carriageway are shown. A free speed between 110 and 120 km/h is indicated. At maximum volume a speed of about 90 km/h is reached. The highest measured 5-minute flow rate value is approximately 6400 veh/h with a critical density of about 70 veh/km.

The fundamental diagram shows a drop in maximum volume: the highest measured flow rate in congested traffic is about 5500 veh/h with a density of about 69 veh/km.

Table 1 summarizes the key macroscopic findings for detector 1 site. The form of the diagrams clearly indicates that apart from a flow reducing impact at the location upstream of the bottleneck, also other factors must be at work. For the q-k points do not follow the conventional fundamental diagram: the densities in congested flow are lower than expected. This corresponds with the findings on individual car-following behavior of section 5.1. On average distance gaps are longer in congested than in non-congested flow for the same speed. Then smaller densities result.

A2 Detector 1	median lane	middle lane	shoulder lane	carriageway
non-congested maximum volume and critical density and speed	2700 veh/h 27 veh/km 95 km/h	2300 veh/h 25 veh/km 90 km/h	1400 veh/h 17 veh/km 85 km/h	6400 veh/h 70 veh/km 90km/h
congested maximum volume and critical density and speed	2200 veh/h 25 veh/km 85 km/h	2100 veh/h 26 veh/km 80 km/h	1400 veh/h 18 veh/km 75 km/h	5600 veh/h 70 veh/km 80 km/h
maximum volume drop	500 veh/h	200 veh/h	0 veh/h	800 veh/h
Free speed	+120 km/h	+110 km/h	100 km/h	between 110 and 120 km/h

Table 1: Summary of characteristics for the fundamental diagrams of the A2 site (detector 1, 5 minute averages)

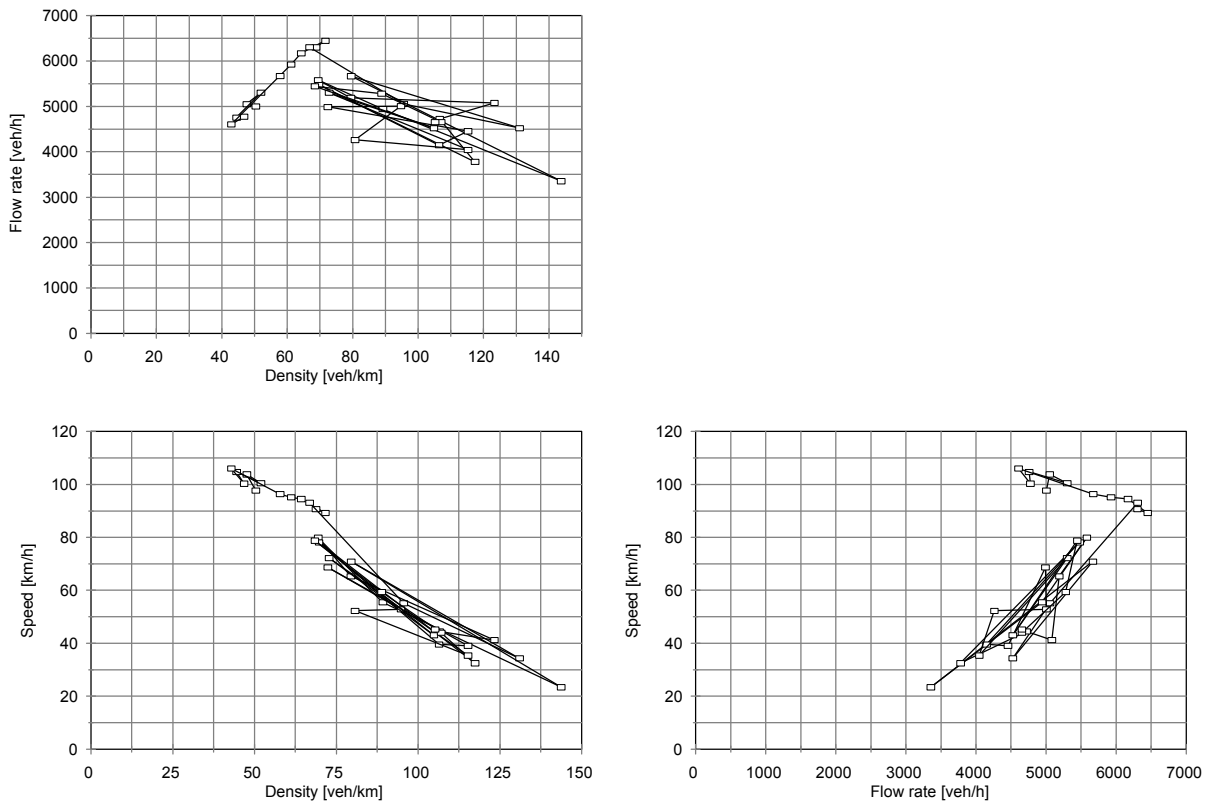


Figure 34: Fundamental diagram of the carriageway at the A2 site (detector 1, 5 minute averages)

Fundamental diagrams for the other detectors of the A2 site

The macroscopic measurements depend on the location of the measurement site (see e.g. May (1)). Upstream of a bottleneck, the flow rate in congested flow is determined by the traffic process at the bottleneck. Figure 35 shows the flow - density diagrams for the 6 detectors at the A2 site. The q-k diagram for the shoulder lane is only shown for detector 1, because the data files from the other detectors for this lane are not useable.

The q-k diagrams of detector 1, 2, and 3 belong to upstream cross sections, the q-k diagram of detector 4 to the bottleneck itself, and the q-k diagrams of detector 5 and 6 to downstream cross sections. The diagrams are consistent with these locations:

- Congestion is caused by the high demand at the bottleneck. Downstream of this bottleneck traffic speeds can increase again. The 5-minute values show only a limited amount of variation in speed.
- Upstream of the bottleneck the flow rates are always a bit smaller than at the on ramp location (the bottleneck) because at the bottleneck vehicles from the on ramp enter the freeway. Significant speed variations can be observed.

Some characteristic values for the detectors are summarized in table 2.

A2 Detector 2	median lane	middle lane
non-congested maximum volume and critical density and speed	2700 veh/h 25 veh/km 100 km/h	2300 veh/h 25 veh/km 90 km/h
congested maximum volume and critical density and speed	2200 veh/h 25 veh/km 85 km/h	2000 veh/h 26 veh/km 75 km/h
maximum volume drop	500 veh/h	300 veh/h
Free speed	+120 km/h	+110 km/h

A2 Detector 3	median lane	middle lane
non-congested maximum volume and critical density and speed	2600 veh/h 26 veh/km 100 km/h	2250 veh/h 25 veh/km 85 km/h
congested maximum volume and critical density and speed	2200 veh/h 41 veh/km 70 km/h	2100 veh/h 35 veh/km 60 km/h
maximum volume drop	400 veh/h	150 veh/h
Free speed	120 km/h	+110 km/h
A2 Detector 4	median lane	middle lane
non-congested maximum volume and critical density and speed	2950 veh/h 28 veh/km 100 km/h	2650 veh/h 30 veh/km 85 km/h
congested maximum volume and critical density and speed	2500 veh/h 34 veh/km 75 km/h	2500 veh/h 35 veh/km 70 km/h
maximum volume drop	450 veh/h	150 veh/h
Free speed	120 km/h	+110 km/h
A2 Detector 5	median lane	middle lane
non-congested maximum volume and critical density and speed	2950 veh/h 32 veh/km 90 km/h	2500 veh/h 30 veh/km 80 km/h
congested maximum volume and critical density and speed	2550 veh/h 31 veh/km 85 km/h	2400 veh/h 33 veh/km 70 km/h
maximum volume drop	450 veh/h	100 veh/h
Free speed	120 km/h	+110 km/h
A2 Detector 6	median lane	middle lane
non-congested maximum volume and critical density and speed	3050 veh/h 31 veh/km 95 km/h	2500 veh/h 30 veh/km 90 km/h
congested maximum volume and critical density and speed	2700 veh/h 30 veh/km 95 km/h	2400 veh/h 34 veh/km 90 km/h
maximum volume drop	350 veh/h	100 veh/h
Free speed	120 km/h	110 km/h

Table 2: Macroscopic characteristic values for the different detectors at the A2 site (5 minute averages)

All lanes show a difference in maximum volume for the non-congested and congested regime, also at the bottleneck. During congestion the density in the fundamental diagram is smaller than expected for a fundamental diagram of a continuous form. The smaller densities are consistent with the microscopic measurements.

5.2.2 Macroscopic flow characteristics at the A9 site

In figure 36 and 37 the fundamental diagram (again $q-k$, $u-k$, and $u-q$) for each of the two lanes at the A9 freeway site are presented. Data from October 14, 1994 are shown. The fundamental diagram shows traffic to be congested for one continuous period of about 60 minutes (7.55-8.55h a.m.)

Median lane

The u-q relation indicates a free speed of about 120 km/h with a speed between 80 and 90 km/h when maximum volume is reached. The amount of scatter for very low densities is the result of the passing of only one or two vehicles during night time intervals. The highest measured 5-minute flow rate value is approximately 2700 veh/h with a critical density of about 32 veh/km.

The fundamental diagram shows a drop in maximum volume: the maximum volume for congested traffic is about 2250 veh/h with a density of about 27.5 veh/h. Because of lack of data for very high densities an estimation of jam density (at standstill) cannot be made.

Shoulder lane

The u-q relation indicates a free speed between 110 and 100 km/h with a speed of about 80 km/h when maximum volume is reached. The highest measured 5-minute flow rate value is approximately 1800 veh/h with a critical density of about 22.5 veh/km.

The fundamental diagram does not show a drop in maximum volume. Because of lack of data for very high densities an estimation of jam density (at standstill) cannot be made.

Comparison of the two lanes

As expected, the highest free speed is achieved in the median lane, the lowest in the shoulder lane. Also, the fundamental diagram indicates that the highest maximum volume is reached in the median lane. The median lane shows a clear drop in maximum volume. The shoulder lane does not show a drop in maximum volume.

The q-k data by lane are shown in one figure (figure 38). For the non-congested state almost parallel lines are found for the different lanes which are only shifted somewhat with speed and critical density (with pce equal to one for trucks).

The differences between lanes are a result of differences in traffic composition (percentage of heavy vehicles) and of differences in driving behavior characteristics by lane (e.g. the desired speed of individual drivers).

Table 3 summarizes the key macroscopic findings for the A9 site.

A9	median lane	shoulder lane	carriageway
Approximate non-congested maximum volume and critical density	2700 veh/h 32 veh/km 85 km/h	1750 veh/h 22 veh/km 80 km/h	4500 veh/h 55 veh/km 85 km/h
Approximate congested maximum volume and critical density	2250 veh/h 27.5 veh/km 80 km/h	1750 veh/h 22.5 veh/km 80 km/h	4000 veh/h 50 veh/km 80 km/h
maximum volume drop	450 veh/h	0 veh/h	500 veh/h
Free speed	±120 km/h	+100 km/h	±110 km/h

Table 3: Summary of characteristics of the fundamental diagrams for the A9 site (5 minute averages)

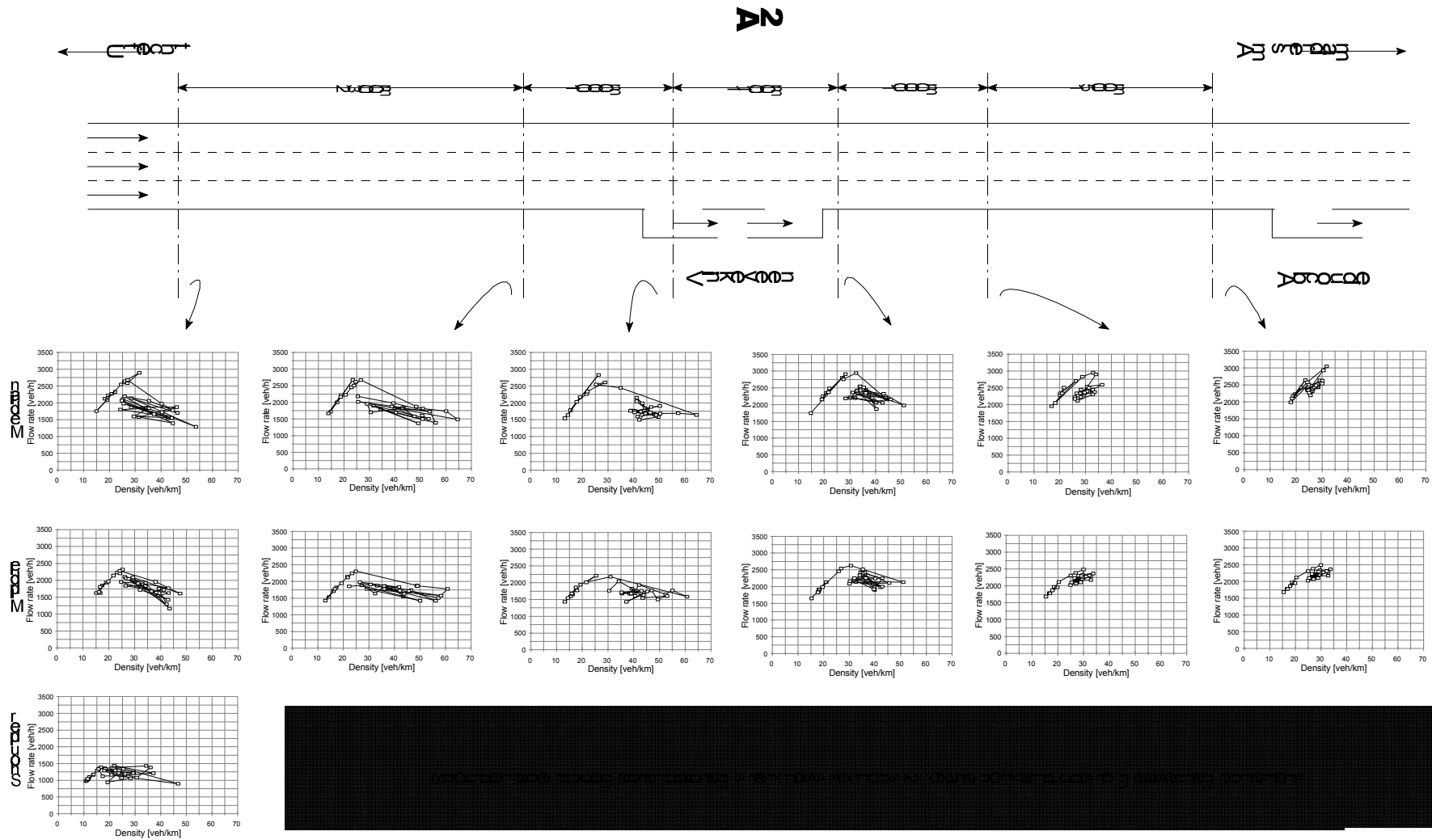


Figure 35: Q - k diagrams at the A2 site by lane for all cross sections; No q - k diagrams of the shoulder lane of all detectors except no. 1 because of corrupted data (5 minute values)

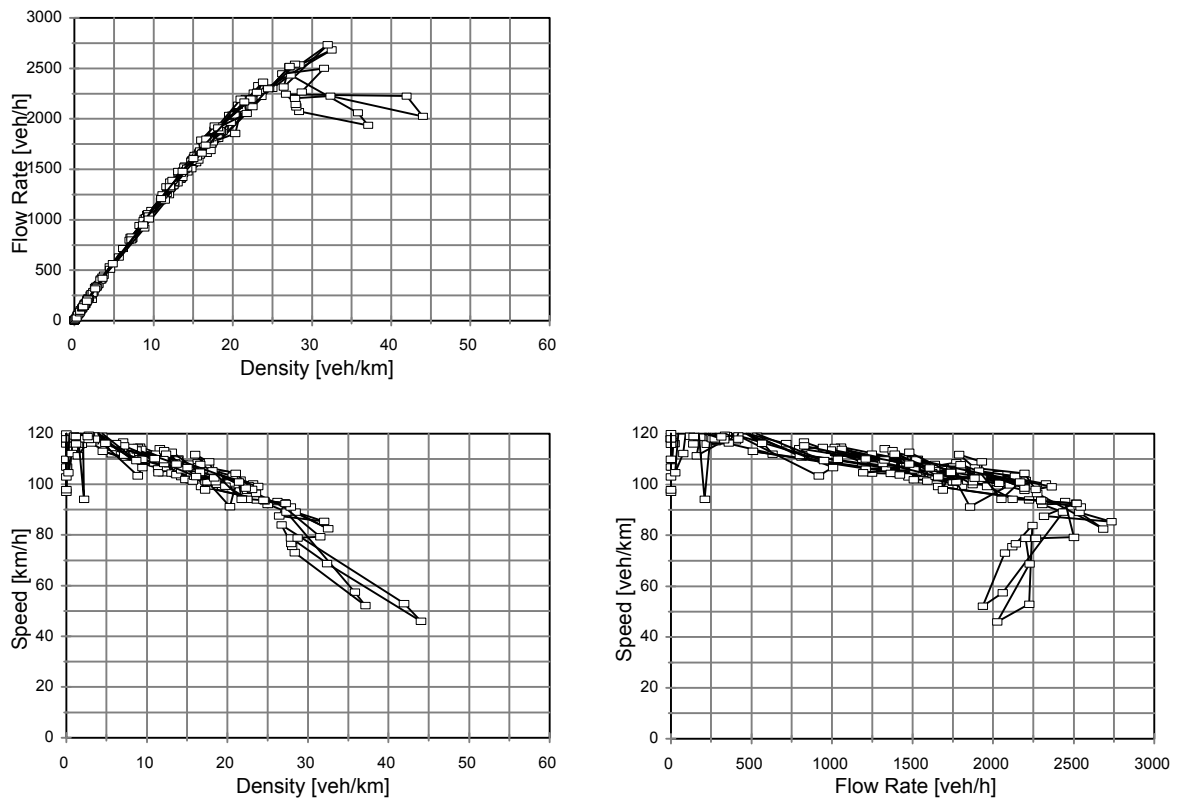


Figure 36: Fundamental diagram for the median lane at the A9 site (5 minute averages)

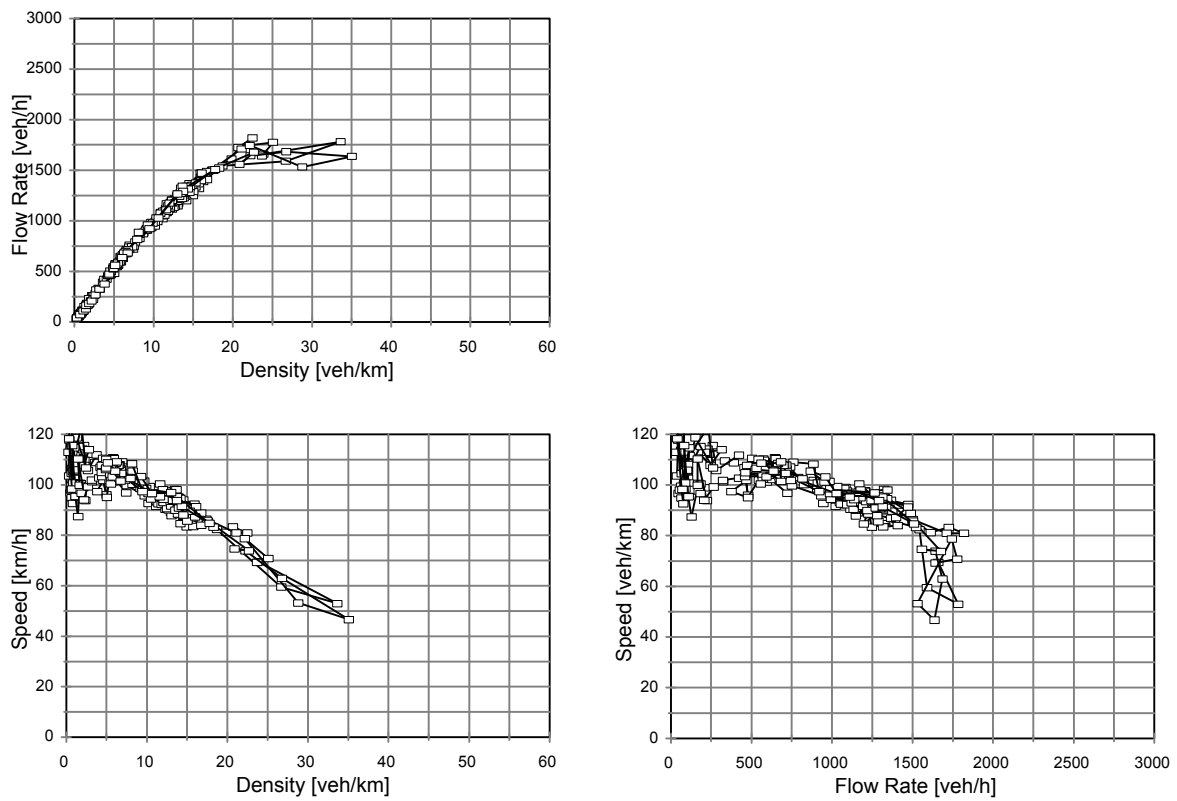


Figure 37: Fundamental diagram for the shoulder lane at the A9 site (5 minute averages)

Carriageway as a whole

In figure 39 the macroscopic data of all lanes together are shown. A free speed of about 110 km/h is indicated. At maximum volume a speed between 80 and 90 km/h is reached. The highest measured 5-minute flow rate value is approximately 4500 veh/h with a critical density of about 55 veh/km.

The fundamental diagram shows a drop in maximum volume: the highest measured flow rate in congested traffic is about 4000 veh/h with a density of about 50 veh/h.

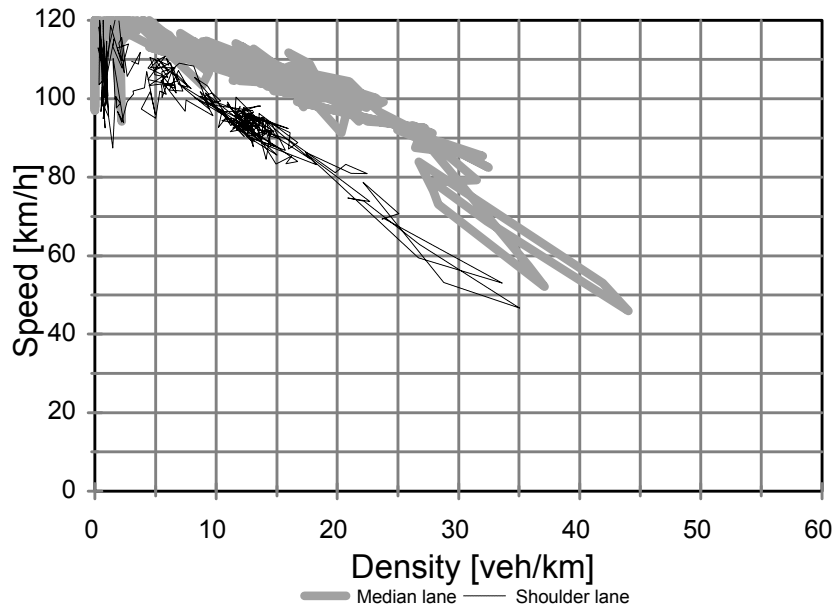


Figure 38: Speed-density diagram by lane at the A9 site (5 minute averages)

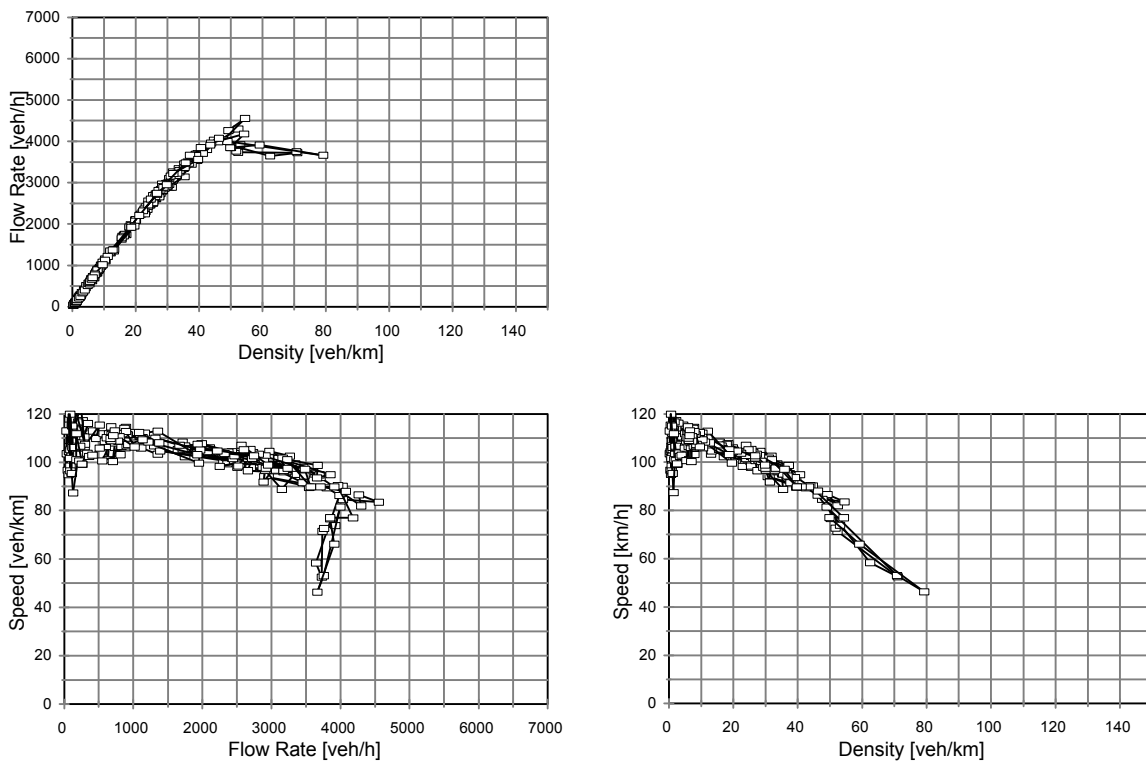


Figure 39: Fundamental diagram of the carriageway at the A9 site (5 minute averages)

5.2.3 COMPARISON OF MACROSCOPIC MEASUREMENTS FROM THE A2 AND A9 SITES

The total maximum volume for the A2 equals about 6400 veh/h, for the A9 about 4500 veh/h. The approximate maximum volumes for each lane on the A2 and A9 are shown in table 4.

	Median lane	Middle lane	Shoulder lane	Carriageway
A2 Detector 1	2700	2300	1400	6400
A9	2700	-	1750	4500

Table 4: Approximate maximum volume values [veh/h] (5 minute averages)

The percentages of trucks found by lane during the peak hour are shown in table 5.

	Median lane	Middle lane	Shoulder lane	Carriageway
A2 (6.30-8.30h)	0.27	3.9	36.8	10
A9 (7.00-9.00h)	0.37	-	12	5

Table 5: Percentage of trucks (=car length > 6 meters)

In table 6 maximum volume values are shown which are recalculated using the truck percentages of table 4 and a person car equivalent (pce) value of 1.75 for trucks.

	Median lane	Middle lane	Shoulder lane	Carriageway
A2 Detector 1	2705.5	2367.3	1786.4	6880.0
A9	2707.5	-	1962.0	4669.0

Table 6: Approximate lane maximum volume values with $pce_{trucks} = 1.75$ [pce/h] (5 minute averages)

Applying these pce-values, the differences in maximum volume for the A2 and A9 are smaller for the shoulder lane.

The measured differences in maximum volume values (measured upstream of the bottleneck) between 4 and 6 lane freeways are quite similar to differences of *capacity* values (measured downstream of the bottleneck, thus including the flow from the traffic entering the carriageway) as found in an overview study of measured capacity values ‘*Capacity values Infrastructure Freeways (CIA-I) - Phase 1 Literature Survey*’ (Minderhoud and Papendrecht (13)).

Both the A2 and A9 sites show a considerable drop in total maximum volume after the transition from non-congested to congested flow. The shoulder lanes do not show such a difference.

The free speed for all lanes combined is approximately the same for the A2 and A9 (± 110 km/h). The speed differences between the lanes are comparable for the A2 and A9 sites. Differences between the v-k plots for the A2 and A9 (figures 40, 41 and 42) are small with somewhat higher speeds for the A2.

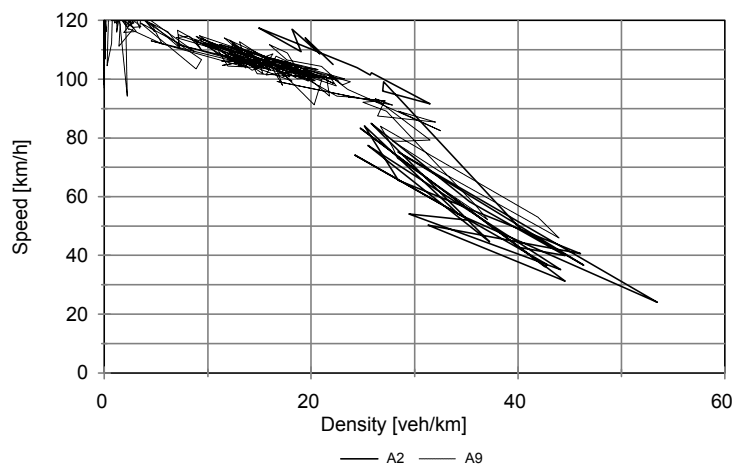


Figure 40: Comparison of the fundamental diagrams for the median lanes at the A2 (detector 1) and the A9 sites respectively (5 minute averages)

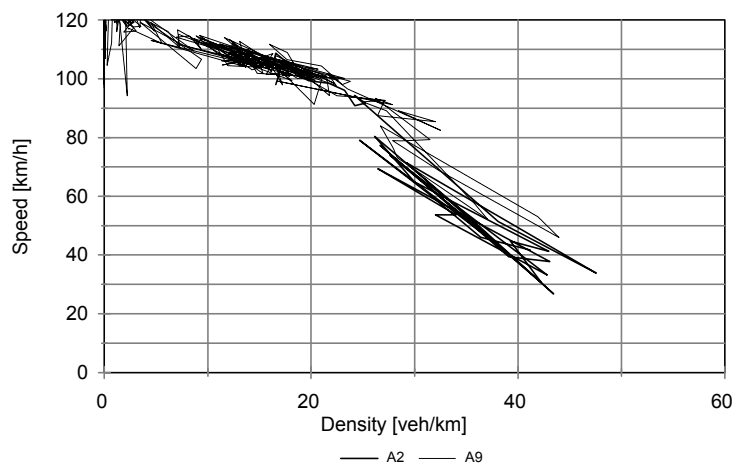


Figure 41: Comparison of the fundamental diagrams for the middle lane at the A2 site (detector 1) and the median lane at the A9 site (5 minute averages)

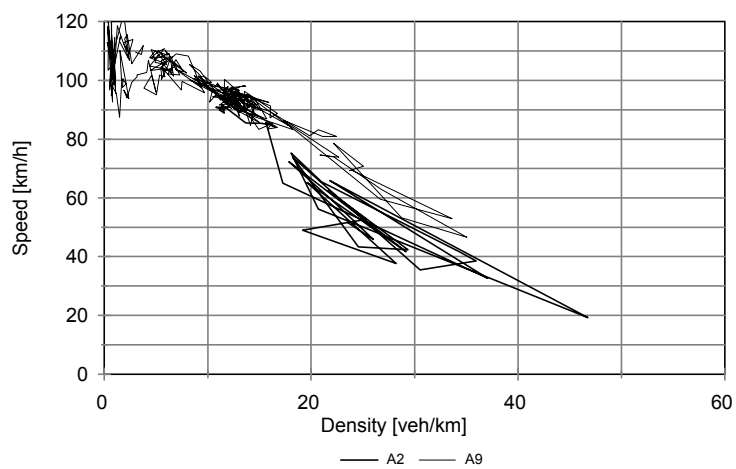


Figure 42: Comparison of the fundamental diagrams for the shoulder lanes at the A2 (detector 1) and the A9 sites respectively (5 minute averages)

5.2.4 SUMMARY OF THE MACROSCOPIC FINDINGS

To find traffic flow differences between the congested and non-congested regimes, macroscopic data for a 6 lane and 4 lane freeway have been presented in the form of fundamental diagrams. The data have been analyzed both by lane and for the carriageways for different detector locations relative to the bottleneck. Characteristic values and the form of the fundamental diagram have been compared for the different lanes and the two freeways. In table 7 some characteristic values on flow at upstream detectors are shown next to each other.

A2 Detector 1	median lane	middle lane	shoulder lane	carriageway
Approximate non-congested maximum volume and critical density and speed	2700 veh/h 27 veh/km 95 km/h	2300 veh/h 25 veh/km 90 km/h	1400 veh/h 17 veh/km 85 km/h	6400 veh/h 70 veh/km 90 km/h
Approximate congested maximum volume and critical density and speed	2200 veh/h 25 veh/km 85 km/h	2000 veh/h 26 veh/km 80 km/h	1400 veh/h 17 veh/km 75 km/h	5600 veh/h 69 veh/km 80 km/h
maximum volume drop	500 veh/h	300 veh/h	0 veh/h	800 veh/h
Free speed	+120 km/h	+110 km/h	100 km/h	between 110 and 120 km/h
A9	median lane		shoulder lane	carriageway
Approximate non-congested maximum volume and critical density and speed	2700 veh/h 32 veh/km 85 km/h		1750 veh/h 22 veh/km 80 km/h	4500 veh/h 55 veh/km 85 km/h
Approximate congested maximum volume and critical density and speed	2250 veh/h 27.5 veh/km 80 km/h		1750 veh/h 22 veh/km 80 km/h	4000 veh/h 50 veh/km 80 km/h
maximum volume drop	450 veh/h		0 veh/h	500 veh/h
Free speed	±120 km/h		+100 km/h	±110 km/h

Table 7: Summary of characteristics of the fundamental diagrams for the A2 and A9 sites (5 minute averages)

Expected differences between the different lanes are found: free speed is highest for the median lane, lowest for the shoulder lane, maximum volume is largest for the median lane, smallest for the shoulder lane, et cetera.

Comparison of the A2 and A9 shows differences that are to be expected because of the difference in the number of lanes. E.g. the free speed in the median lane of the A2 is somewhat higher than in the median lane of the A9.

Both at the A2 and A9 sites, a drop in maximum volume is found. This drop in maximum volume combined with the shape of the fundamental diagram indicates that traffic flow at the two sites differs between the congested and non-congested states. When simplifying between the congested and non-congested regimes the speeds at the critical densities slightly change with somewhat higher speeds at the non-congested maximum volumes. The macroscopic findings for the basic freeway sections upstream of the bottleneck are summarized by table 7 and the fundamental diagrams in figure 43.

For the A2 also other cross sections relative to the bottleneck have been studied. Again it is found that the macroscopic results for congestion differ from the traditional continuous fundamental diagram.

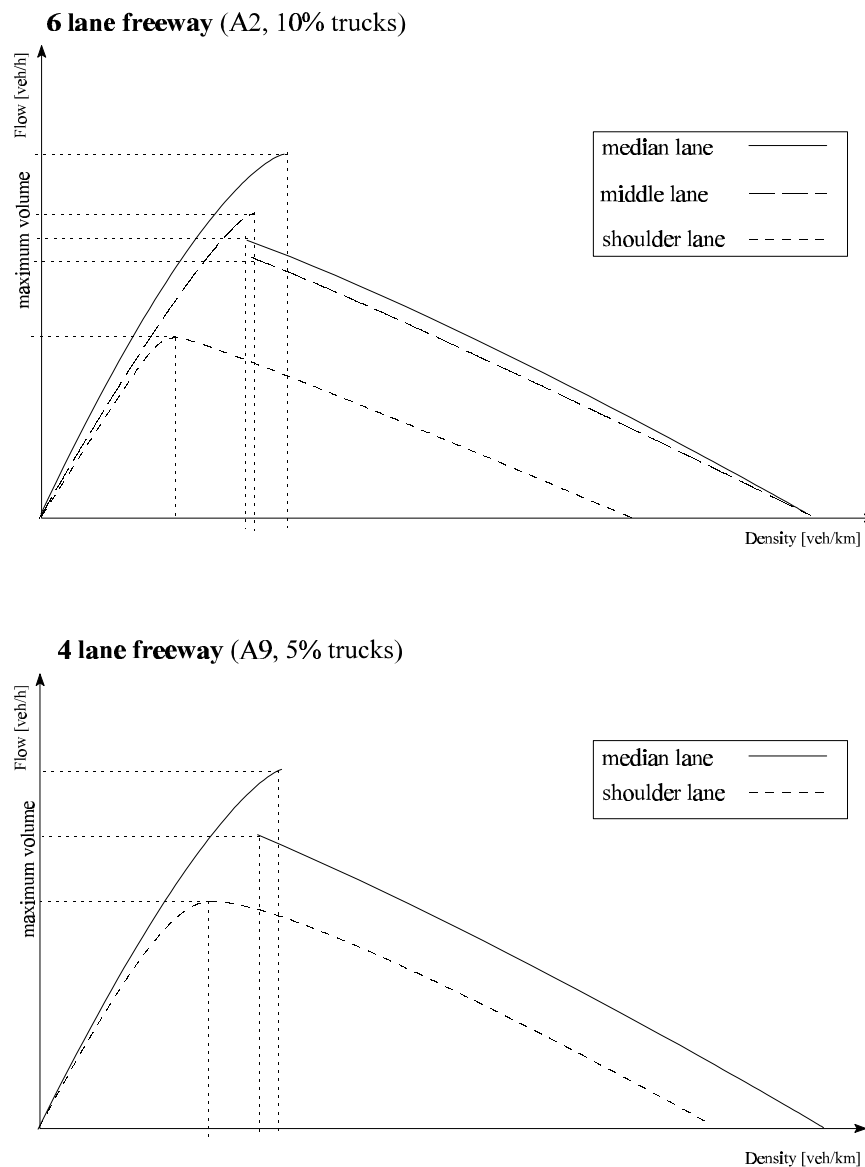


Figure 43: Graphical summary of the macroscopic findings of section 5.2

5.3 SUMMARY OF THE FINDINGS AND THE RELATION BETWEEN MACROSCOPIC AND MICROSCOPIC FINDINGS

Both macroscopic and microscopic measurement results of traffic flow have been presented. It is found in the microscopic analysis that the distance gap - speed relation of passenger cars differs for non-congested and congested flow. In congested flow passenger cars follow with larger distance gaps than in non-congested flow for the same speed. This result is found both at a 4 lane and 6 lane freeway site, at different cross sections relative to the bottleneck. The macroscopic analysis is performed for the same freeways and cross sections as the microscopic analysis. The constructed fundamental diagrams of the middle and median lanes show differences from the traditional continuous form. The density in congested flow turns out smaller compared with the conventional continuous fundamental diagram for the same speeds.

The microscopic and macroscopic results are related. The macroscopic flow characteristics are a result of behavior of all individual drivers together. The relation between the two is not straightforward. To adequately describe traffic flow based on individual driving behavior simulation models are necessary. However a tentative relation between the macroscopic and the microscopic findings can be made:

- Density is related to the distance headway (distance gap + length): high densities indicate small distance headways;
- Flow is related to time headway: high flow rates indicate small time headways.

When differences in density for equal speeds between non-congested and congested flow are measured, on average distance gap keeping will differ by regime. When differences in the distance gap - speed relations are found for the two flow states, different macroscopic findings are to be expected. And indeed, differences are found at the A2 and A9 sites.

The relation between microscopic and macroscopic measurements can be made more formal with some simplifications. When a road with one lane (no influence of lane changing), one single driver and vehicle type, and only following drivers is considered, the result of different car-following behavior for each regime on macroscopic flow can be roughly constructed as shown in figure 44.

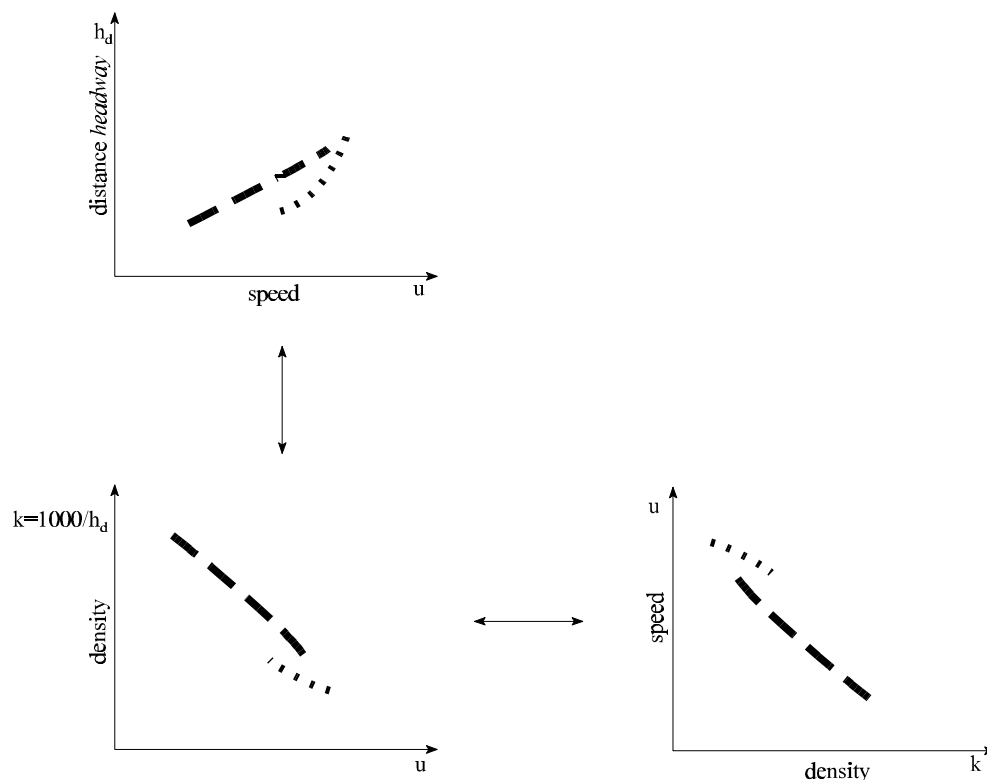


Figure 44: Relation between microscopic and macroscopic flow for a simplified situation

Car-following differences in non-congested and congested flow have important consequences for traffic at the analyzed sites. To adequately describe traffic at these sites, traffic models should incorporate the measurement results.

In the next chapter, microscopic equations of distance gap - speed are established which can be used in microscopic simulation models.

6 Establishment of distance gap - speed relationships

In chapter 5 it was found that car-following of passenger cars differs for non-congested and congested flow at two studied freeway sites. It is now challenging to investigate to what extent the modeling of traffic flow (in macroscopic terms) will improve when flow models take these differences in car-following in consideration. The microscopic simulation model FOSIM (Vermijs (10)) is used to show the resulting improvements. As the first step of implementation the microscopic findings from chapter 5 are used in this chapter to establish distance gap - speed functions. In section 6.1 the method for estimation of the functions is described. In section 6.2 the functions are presented.

6.1 ESTIMATION OF DISTANCE GAP - SPEED RELATIONSHIPS

Most microscopic traffic models distinguish different driver classes. These driver classes differ in driving behavior because of individual differences in driving style (different desired speed, different acceleration, et cetera) and because of differences of vehicle characteristics (passenger car, trucks). The microscopic measurements are classified according to lane and vehicle type and are used in the establishment of distance gap - speed functions:

- for 6 lane roads:
 - driver class 1 ↔ passenger cars in the median lane of the A2 site (desired speed: 125 km/h);
 - driver class 2 ↔ passenger cars in the middle lane of the A2 site (115 km/h);
 - driver class 3 ↔ passenger cars in the shoulder lane of the A2 site (100 km/h);
 - driver class 4 ↔ light trucks in the shoulder lane of the A2 site (95 km/h);
 - driver class 5 ↔ heavy trucks in the shoulder lane of the A2 site (85 km/h);
- for 4 lane roads:
 - driver class 1 ↔ passenger cars in the median lane of the A9 site (115 km/h);
 - driver class 2 ↔ passenger cars in the shoulder lane of the A9 site (100 km/h);
 - driver class 3 ↔ light trucks in the shoulder lane of the A2 site (95 km/h; not enough data for the A9);
 - driver class 4 ↔ heavy trucks in the shoulder lane of the A2 site (85 km/h; not enough data for the A9).

6.1.1 FUNCTIONAL FORM

Distance gap - speed functions are established using the microscopic data of chapter 5. It is hypothesized based on kinematic reasoning that the relationship between following distance and speed has both a linear and quadratic term:

$$g_d = a + b \cdot v + c \cdot v^2 \quad [m] \quad (3)$$

Safe braking distance increases quadratically with speed. It may be assumed that drivers are somewhat aware of this, and that therefore the distance gap when following also increases quadratically (like the current distance gap - speed in FOSIM). The Road Research Laboratory (14) gives a similar equation with a small value for the c parameter of equation 3.

Because small values for the parameter of the quadratic term have been found, results of regression with quadratic functions are compared to regression with linear functions.

6.1.2 PARAMETER ESTIMATION

The parameters of the distance gap - speed functions are estimated with regression analysis. Data from the *cross sections* farthest upstream from the bottleneck are used for the estimation because far enough from the ramps the influence of lane changing because of these ramps is minimal.

Regression can be performed using all single distance gap - speed data points or using only the averages. The resulting parameters only show very small differences. Somewhat arbitrarily, regression is applied on the averages per speed interval.

It also possible to perform weighed regression. Then the average values are weighed (e.g. with the standard errors) according to the variance of their estimates. In other words, averages based on large samples have a larger influence on the parameters than other averages. However, as can be seen in Appendix D, the estimated standard error of the estimates is approximately equal for most intervals, which means that results from non-weighed regression and weighed regression do not differ (much). Eventually, for practical reasons, non-weighed (i.e. all weights equal) regression is used.

Finally, the parameter estimation is performed with and without the following constraints:

- the parameters b and c are equal to or larger than zero;
- the distance gap at zero speed, c, is assumed equal to 3 meters.

6.2 ESTIMATED DISTANCE GAP - SPEED MODELS

The parameters of the functions:

$$g_d = a + b \cdot v \quad [m] \quad (4)$$

$$g_d = a + b \cdot v + c \cdot v^2 \quad [m] \quad (3)$$

with: g_d = the distance gap,

v = speed [km/h]

and a, b, c = parameters,

using the average measured distance gap values per 5 km/h interval, all equally weighed, have been estimated and are presented in Appendix E.

The resulting distance gap - speed equations are (shown in figures 45 until 51):

- 6 lane freeways, passenger cars:

$$\begin{aligned} g_{d_6 \text{ lane freeways, median lane, non-congested}} &= 3 + 0.22 \cdot v & , v < 91 \text{ km/h} \\ g_{d_6 \text{ lane freeways, median lane, non-congested}} &= 155.4 - 3.12 \cdot v + 0.0183 \cdot v^2 & , v \geq 91 \text{ km/h} \end{aligned} \quad (5)$$

$$g_{d_6 \text{ lane freeways, median lane, congested}} = 3 + 0.415 \cdot v \quad (6)$$

$$\begin{aligned} g_{d_6 \text{ lane freeways, middle lane, non-congested}} &= 3 + 0.29 \cdot v & , v < 81 \text{ km/h} \\ g_{d_6 \text{ lane freeways, middle lane, non-congested}} &= 108 - 2.31 \cdot v + 0.0161 \cdot v^2 & , v \geq 81 \text{ km/h} \end{aligned} \quad (7)$$

$$g_{d_6 \text{ lane freeways, middle lane, congested}} = 3 + 0.399 \cdot v + 0.00034 \cdot v^2 \quad (8)$$

$$\begin{aligned} g_{d_6 \text{ lane freeways, shoulder lane, non-congested}} &= 3 + 0.28 \cdot v & , v < 58 \text{ km/h} \\ g_{d_6 \text{ lane freeways, shoulder lane, non-congested}} &= 49.5 - 1.34 \cdot v + 0.014 \cdot v^2 & , v \geq 58 \text{ km/h} \end{aligned} \quad (9)$$

$$g_{d_6 \text{ lane freeways, shoulder lane, congested}} = 3 + 0.321 \cdot v + 0.00336 \cdot v^2 \quad (10)$$

- 4 lanes, passenger cars:

$$\begin{aligned}
 g_{d_4 \text{ lane freeways, median lane, non-congested}} &= 3 + 0.24 \cdot v & , v < 66 \text{ km/h} \\
 g_{d_4 \text{ lane freeways, median lane, non-congested}} &= 36.3 - 0.77 \cdot v + 0.0076 \cdot v^2 & , v \geq 66 \text{ km/h}
 \end{aligned} \tag{11}$$

$$g_{d_4 \text{ lane freeways, median lane, congested}} = 3 + 277 \cdot v + 0.00102 \cdot v^2 \tag{12}$$

$$\begin{aligned}
 g_{d_4 \text{ lane freeways, shoulder lane, non-congested}} &= 3 + 0.26 \cdot v & , v < 58 \text{ km/h} \\
 g_{d_4 \text{ lane freeways, shoulder lane, non-congested}} &= 53.9 - 1.49 \cdot v + 0.015 \cdot v^2 & , v \geq 58 \text{ km/h}
 \end{aligned} \tag{13}$$

$$g_{d_4 \text{ lane freeways, shoulder lane, congested}} = 3 + 0.172 \cdot v + 0.00383 \cdot v^2 \tag{14}$$

- Both 4 lane and 6 lane freeways, trucks:

$$g_{d_{\text{light trucks}}} = 3 + 0.454 \cdot v + 0.00117 \cdot v^2 \tag{15}$$

$$g_{d_{\text{heavy trucks}}} = 3 + 0.615 \cdot v \tag{16}$$

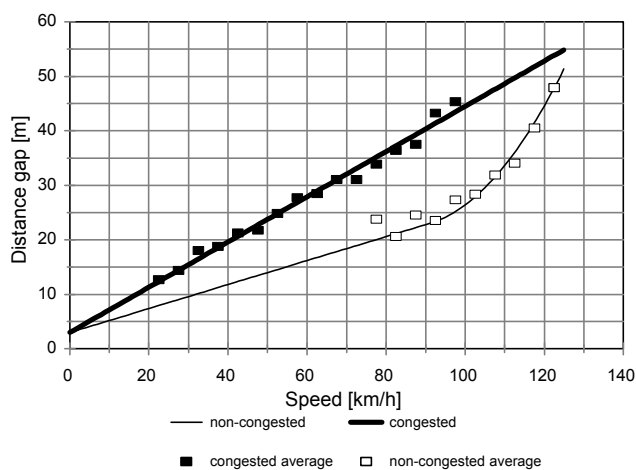


Figure 45: Distance gap - speed functions for driver class 1 (passenger cars), 6 lane freeways

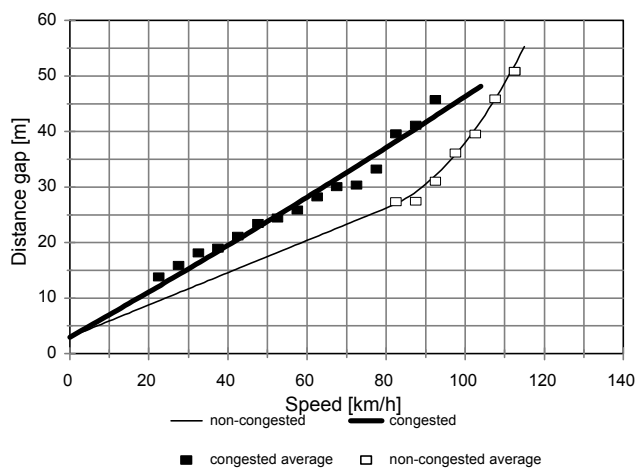


Figure 46: Distance gap - speed functions for driver class 2 (passenger cars), 6 lane freeways

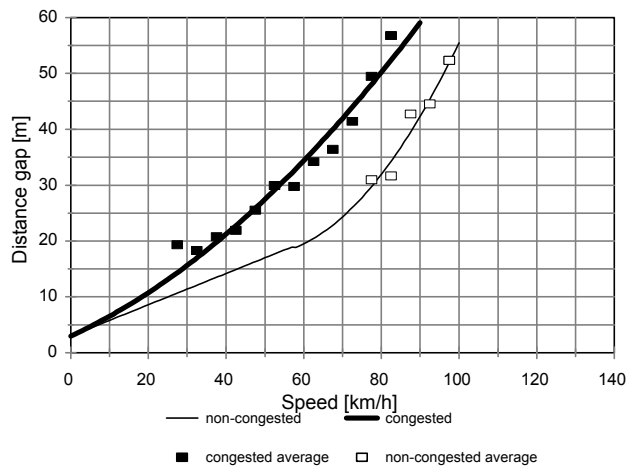


Figure 47: Distance gap - speed functions for driver class 3 (passenger cars), 6 lane freeways

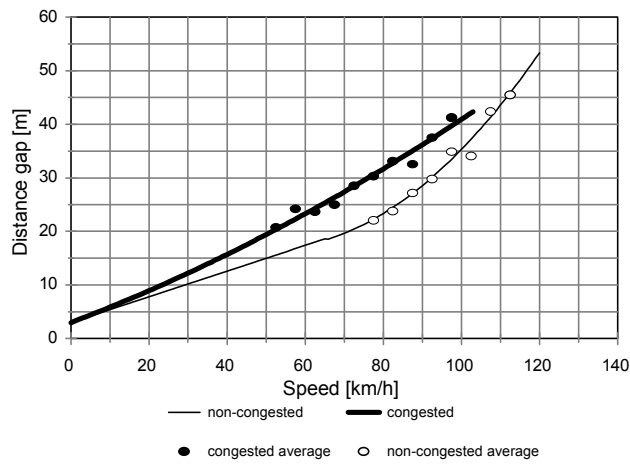


Figure 48: Distance gap - speed functions for driver class 1 (passenger cars), 4 lane freeways

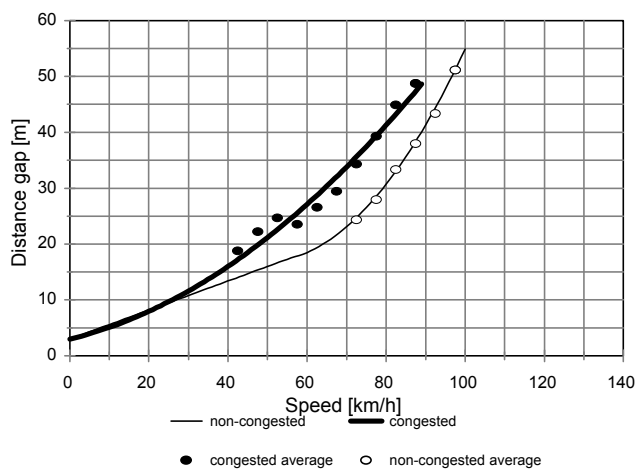


Figure 49: Distance gap - speed functions for driver class 2 (passenger cars), 4 lane freeways

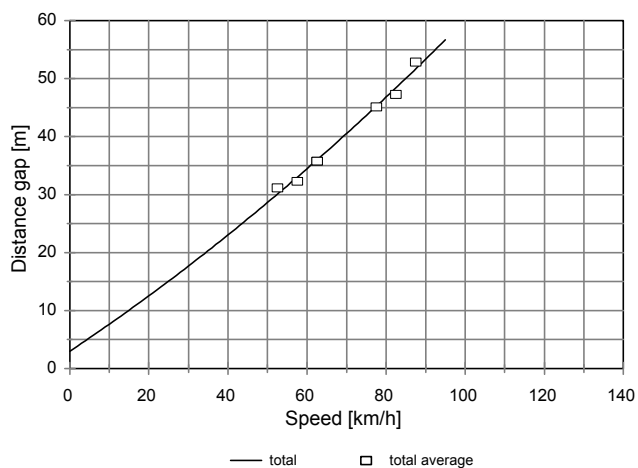


Figure 50: Distance gap - speed function for driver class 4 (light trucks)

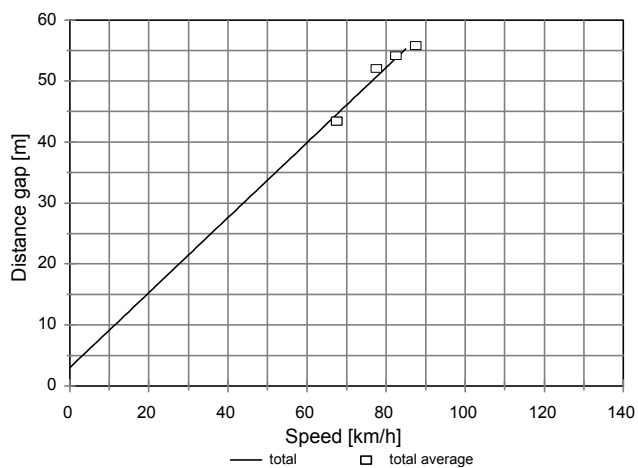


Figure 51: Distance gap - speed function for driver class 5 (heavy trucks)

The estimated distance gap - speed functions, which differ for drivers in non-congested and congested traffic, can be used in traffic flow simulation models. The implementation of these following functions for the microscopic traffic simulation model FOSIM is described in the next chapter. This implementation enables comparison of the model with reality, and shows the consequences of distinguishing different car-following behavior for different regimes compared to using only one model for all regimes.

7 Implementation of regime dependent car-following in the microscopic simulation model FOSIM

It was found that car-following of passenger cars differs between non-congested and congested flow at sites on a 4 lane and 6 lane freeway. In the previous chapter, functions were estimated which describe the relation between individual distance gap keeping and speed for the non-congested and congested regimes separately. Such functions play a key role in microscopic simulation models which simulate the total traffic flow process.

In existing microscopic simulation models car-following does not differ by regime. This is not consistent with the measurement results on the two Dutch freeways. Therefore it is questionable whether these simulation models are suitable for these freeway sites. Different car-following per regime probably improves simulation results. To assess the consequences of defining different car-following per regime, the existing simulation model FOSIM is adapted. Then, in the next chapter, macroscopic modeling results achieved with different car-following models for each regime are compared with results of a simulation using only a single model for all regimes.

In this chapter the implementation of the regime dependent car-following models in the existing microscopic simulation model FOSIM is described. First, in section 7.1 the FOSIM simulation model is summarized. In section 7.2 the integration of the regime dependent car-following model with FOSIM is presented.

7.1 THE MICROSCOPIC TRAFFIC FLOW SIMULATION MODEL FOSIM

Microscopic simulation models can be used to describe the traffic flow process. Ordinarily, these consist of a model for longitudinal and lateral movement of the individual vehicles.

The model for longitudinal driving consists of a description of uninfluenced driving, and of car-following. Lateral movement (lane changing), which in fact also depends on the longitudinal movement model, is modeled by defining when and how drivers change lanes. This model can be different for different situations (overtaking, merging).

The microscopic traffic simulation model FOSIM (Vermijs (10)) is developed at the Delft University of Technology. This model is used to implement different car-following for the non-congested and congested flow condition. FOSIM consists of:

- a schematization of traffic facilities;
- models for longitudinal movement (free driving, car-following);
- models for lateral movement (lane changing).

Here, only the longitudinal movement model is described. In Appendix F the FOSIM model is described more elaborately.

When a driver is uninfluenced by other traffic, he drives with a constant 'desired speed'. When a driver approaches another vehicle and does not overtake, he adjusts his speed to the vehicle in front. The moment he starts adjusting his speed depends on the ratio distance gap - speed difference according to the Wiedemann (8) model (figure 52). When a vehicle in front moves away from the follower, the follower accelerates with his leader after a small time lag unless he has already reached his desired speed.

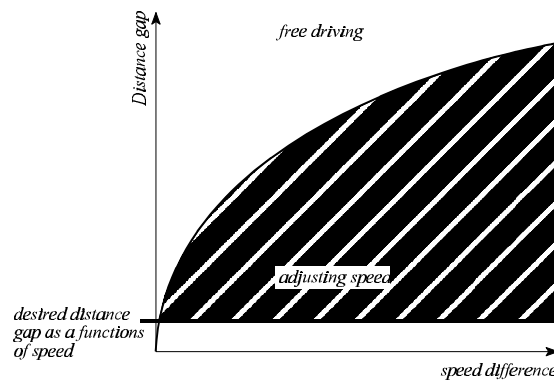


Figure 52: Speed adjustment model (Wiedemann (8))

The distance gap which followers try to maintain is a function of speed:

$$g_{d,i+1} = a_{i+1} + b_{i+1}v_{i+1} + c_{i+1}v_{i+1}^2 \quad [m] \quad (17)$$

with: i : leader;
 $i+1$: follower;
 g_d = distance gap [m];
 v = speed [m/s];
 a = parameter: distance gap at zero speed [m];
 b = parameter [1/s];
 c = parameter [s²/m].

(In FOSIM in fact distance *headway* (thus including the vehicle length of the leader) - speed functions are used but this makes no essential difference in modeling).

These parameters are defined for each driver class, just like other vehicle dependent parameters such as desired speed, vehicle length, et cetera.

In the current FOSIM version, the car-following parameters do not change with the flow conditions. However, it was found in chapter 5 that the distance gap keeping of passenger cars is different for non-congested and congested flow at two Dutch freeway sites. In chapter 6 distance gap - speed functions were estimated separately for the two regimes. A simple implementation of these models in FOSIM is described in the next section.

7.2 IMPLEMENTATION OF REGIME DEPENDENT CAR-FOLLOWING BEHAVIOR IN FOSIM

In the current FOSIM version the driver class specific distance headway - speed functions are the same for all flow conditions. However, analysis of measurements have revealed differences between non-congested and congested flow for passenger cars. Therefore, different distance headway - speed functions for non-congested and congested flow are assigned to each of the passenger car classes defined in FOSIM. The extension of FOSIM thus consists of:

- defining when passenger cars change from non-congested following to congested car-following;
- defining when passenger cars change from congested following to non-congested following;
- establishing new distance headway - speed functions resembling the measurements of section 5 (see chapter 6).

Three different passenger car driver classes and two truck driver classes for 6 lane freeways and two different passenger car driver classes and two truck driver classes for 4 lane freeways are currently defined in FOSIM. This remains the same for the new FOSIM version.

Unfortunately, so far no data is available about the way drivers change their following behavior. Therefore the modeling of the change of following mode is based on reasoning.

It is assumed that passenger car drivers gradually change from non-congested following to congested following when they experience traffic flow as being congested. In reality drivers then perceive low speeds and high densities. However, drivers in FOSIM are not aware of traffic density. Therefore the drivers' notion of congestion in FOSIM can only be based on speed. It is assumed that for a driver traffic has become congested when his speed has been less than 50 km/h. This speed value is suitable, because speeds this low will normally only occur when traffic flow really breaks down.

When a driver changes his distance gap as soon as his speed has been less than 50 km/h he ordinarily will have to break. This does not correspond with reality. It is more realistic when the longer gaps are a result of delaying acceleration when the speed of the leader is higher than the follower's speed. This way of changing from non-congested to congested following is used.

Drivers will perceive traffic as non-congested again when densities are smaller and speeds high. Again, because drivers in FOSIM are not aware of the density, the drivers notion of traffic conditions is based on their individual speed. It is, somewhat arbitrarily, assumed that drivers in the model perceive traffic as non-congested again when they can reach 90% of their desired speed.

The presented model is simple and probably not very realistic but useful for a first evaluation of the consequences of a change of distance keeping for the congested and non-congested regimes. The implementation of following mode changing in FOSIM is shown schematically in figure 53.

In the next chapter the simulation results of the extended FOSIM model, with different car-following rules for the non-congested and congested regimes, are evaluated.

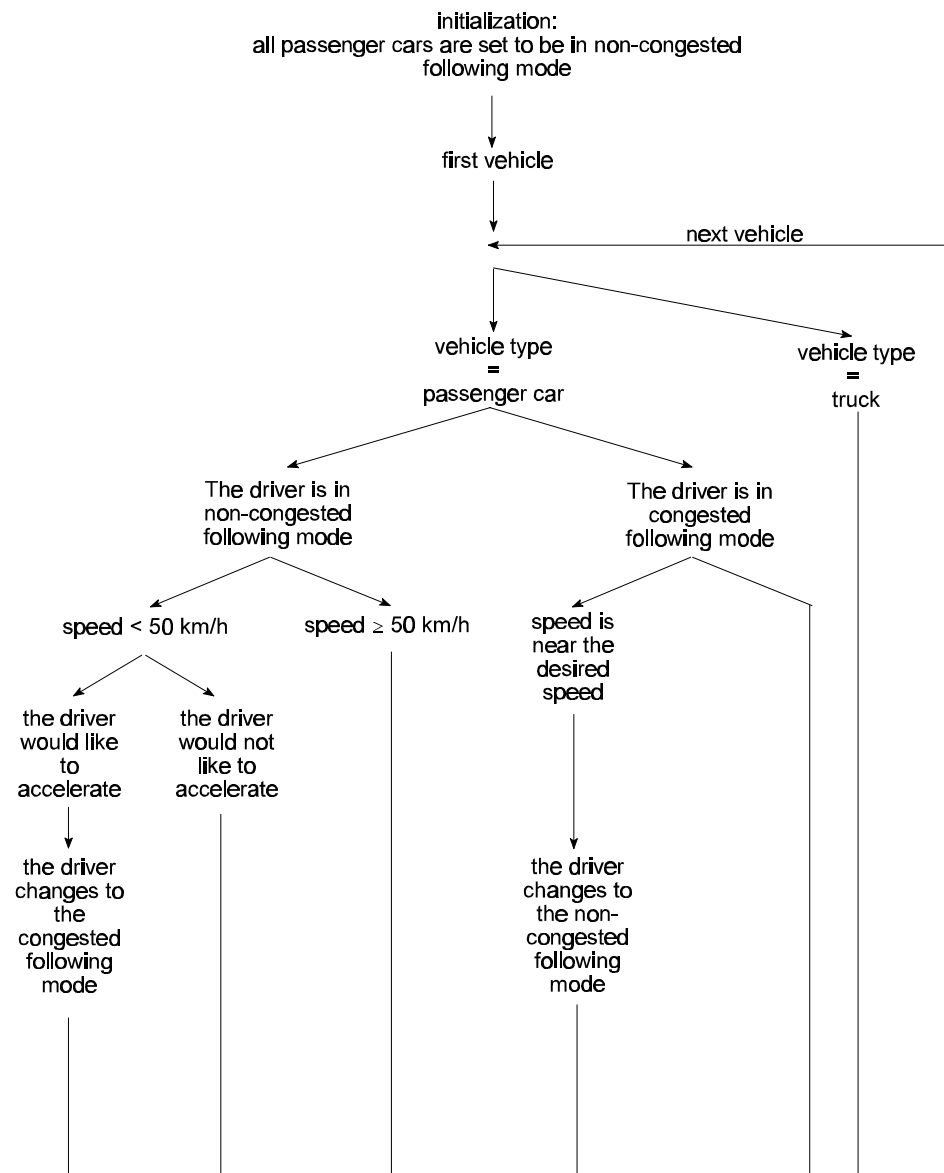


Figure 53: Following mode change model

8 Applying the extended FOSIM model to show the consequences of different car-following behavior in non-congested and congested conditions

The analyzed measurements on two Dutch freeways show different car-following behavior for congested and non-congested flow. On average drivers follow with shorter headways in non-congested than in congested flow, for the same speed. These findings were formalized in mathematical relationships between the distance gap and speed for each driver class.

Such relationships, different for non-congested and congested flow, can be used in microscopic traffic simulation models. Chapter 7 describes a method to quickly implement different car-following for the two regimes, e.g. for the simulation model FOSIM. The current FOSIM version uses one distance gap - speed function for every driver class for all situations. In an extended, experimental FOSIM version the new car-following model is implemented. Then impact of such a change compared to using only one function for all situations can be evaluated. Also, a first comparison of this experimental FOSIM version with reality is performed.

In section 8.1 the results of simulation of traffic at the A2 Vinkeveen site, which was also used in the previous chapters, are shown. These are compared with the real measurements and the simulation results of the one-following mode FOSIM version. In section 8.2 conclusions are drawn from the findings of section 8.1.

8.1 SIMULATION OF TRAFFIC AT THE A2 SITE, COMPARED WITH REAL MEASUREMENTS AND CONVENTIONAL FOSIM

In chapter 5 it was shown that in congested flow passenger cars follow with considerably longer distance gaps than in non-congested flow for the same speeds at two Dutch freeway sites. Macroscopic data (fundamental diagrams) show corresponding results: in congested flow smaller densities are found in the median and middle lanes than expected according to the conventional fundamental diagrams.

The change of distance gap keeping is implemented in the microscopic model FOSIM. Because the implemented model is only a simple (first) attempt and because other parts of the FOSIM model are not changed, the new FOSIM model does not correctly represent all traffic flow processes. The new model can therefore only be used to evaluate a simple traffic situation.

Only results from the simulation of the A2 site are presented. The studied A9 site can also be simulated. But although some differences between the A2 and A9 site exist, no principal simulation differences are expected. Also, no details are studied in this chapter, only the main results.

The macroscopic simulation results from the new (extended) model are compared with simulation results from the conventional FOSIM model which does not distinguish different car-following models for different regimes. This way the impact of modeling different car-following behavior by regime can be tentatively analyzed.

Further, a comparison with empirical data from the A2 site is performed. This gives a first indication of the correspondence of the simulation results with reality and, more importantly, shows whether the new modeling approach can be better than the results of the conventional model. The extended model is mainly developed to show the perspectives of the new model, and not as a direct operational tool.

8.1.1 INPUT FOR SIMULATION OF TRAFFIC AT THE A2 SITE

The schematization of the A2 freeway section is shown in figure 54.

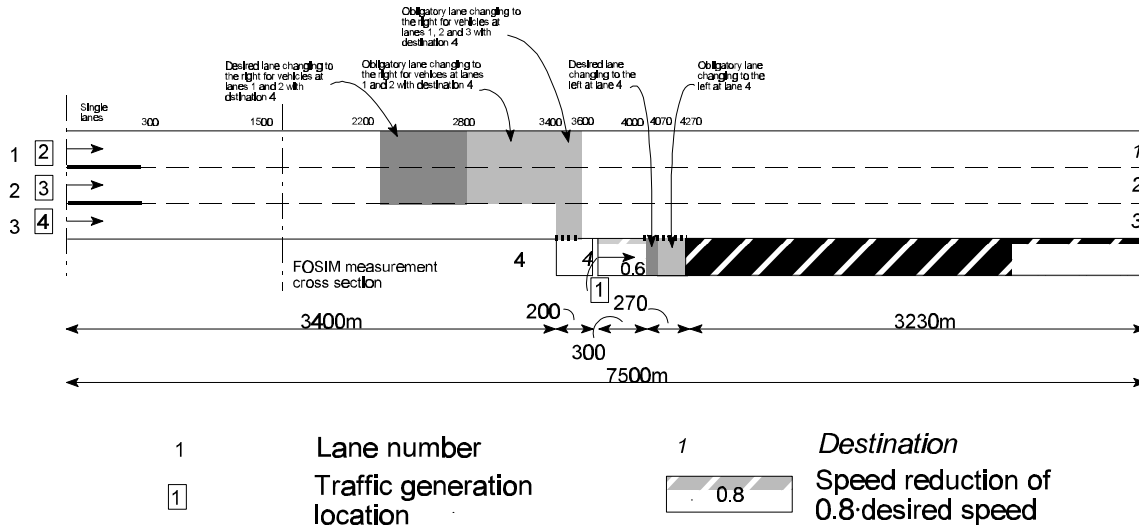


Figure 54: A2 freeway site schematization

The figure shows the lane configuration, origins (traffic generation locations) and destinations. Sections where drivers with certain destinations need to change lanes are defined, and the cross section used to collect data is shown. A detector far *upstream* of the bottleneck is chosen to collect data of congested traffic to prevent influence from desired or obligatory lane changes.

Two hours of traffic are simulated. The amount of traffic generated differs for simulations to gather data on congested, respectively non-congested flow (which of course could also be combined). The generation of traffic in time is shown in figure 55.

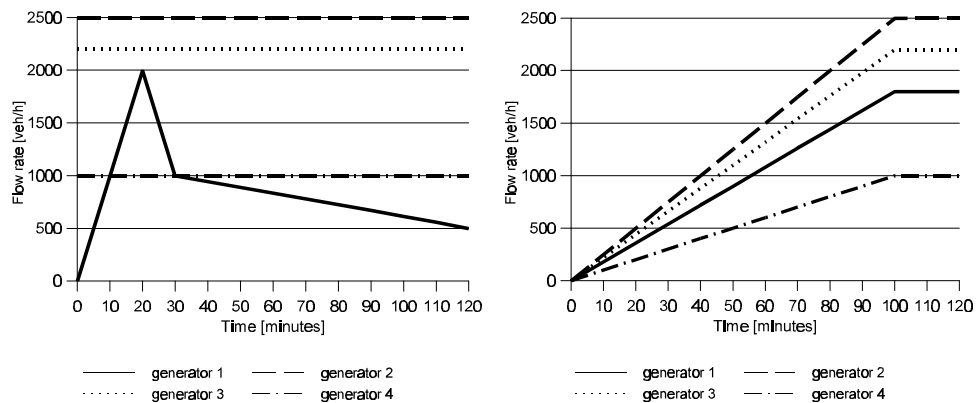


Figure 55: Traffic generation in time for the A2 simulation to collect data on congested flow (left) and non-congested flow (right)

Five vehicle types are defined, with distance gap - speed functions as determined in chapter 6. These vehicle types are distributed over the traffic generation locations as shown in table 8. In table 9 the origin-destination matrix is shown.

Several simulation runs, with different settings for the random generator, are performed. Simulations are run both with the conventional and extended FOSIM versions. The macroscopic results (fundamental diagrams by lane) for the detector upstream of the bottleneck are presented in the next section.

Driver class → Traffic generator ↓	1	2	3	4	5
1	35	35	24	4	2
2	95	5	0	0	0
3	0	90	2	6	2
4	0	5	38	35	22

Table 8: Driver class percentage for each traffic generation location for the A2 simulation with FOSIM

Destination → Origin ↓	1	2	3	4
1	0	0	100	0
2	0	0	97	3
3	0	0	96	4
4	0	0	90	10

Table 9: Origin-destination matrix for the A2 simulation with FOSIM

8.1.2 Comparison of simulation results of the A2 site with the conventional and extended FOSIM models and real measurements

In figures 56 until 58, for each lane at the A2 site, the fundamental diagrams are shown for the simulations with the conventional and extended (different distance gap-speed relations for passenger cars in congested and non-congested traffic) FOSIM versions and for real-life data.

The figures show a generally lower speed for congested traffic for the simulations than measured in reality. Still, the results can be used to compare the macroscopic results.

The results of the simulations with the conventional FOSIM version show a good correspondence with reality for non-congested traffic. Because FOSIM is mainly used for capacity estimation, this has always been most important. The congested part of the fundamental diagram, however, shows too high densities for the median and shoulder lanes.

The new FOSIM version still shows good results for the non-congested part of the fundamental diagram. However, it should be noted that capacity estimation cannot be done as reliably as with the (extensively validated) conventional version, because the new distance gap functions also have consequences on other parts of the model, which are not (yet) adjusted for the new car-following model.

The new version does show much better results for congested flow. Apparently the longer distance gap keeping of passenger cars in the new version has important consequences for the macroscopic characteristics.

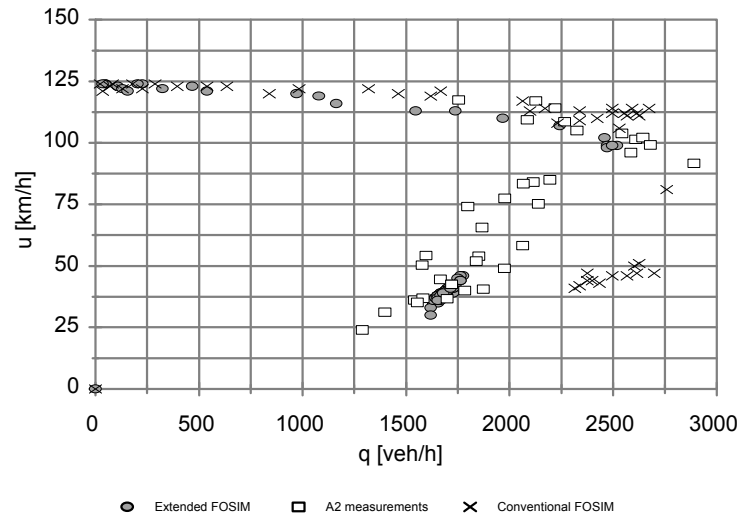
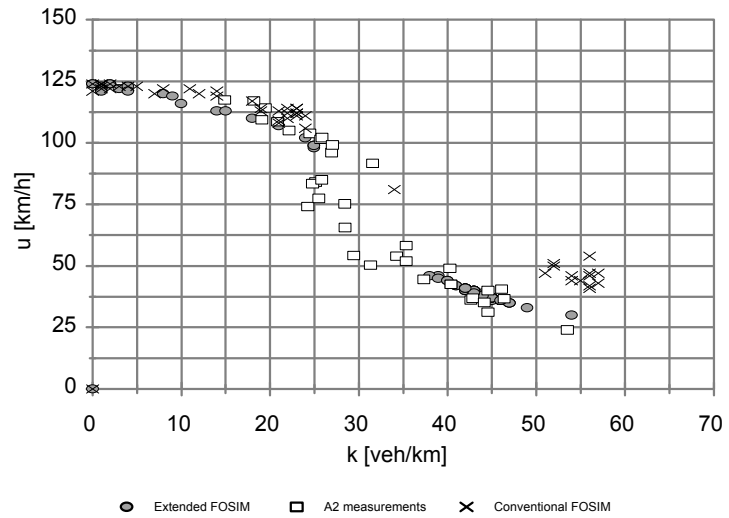
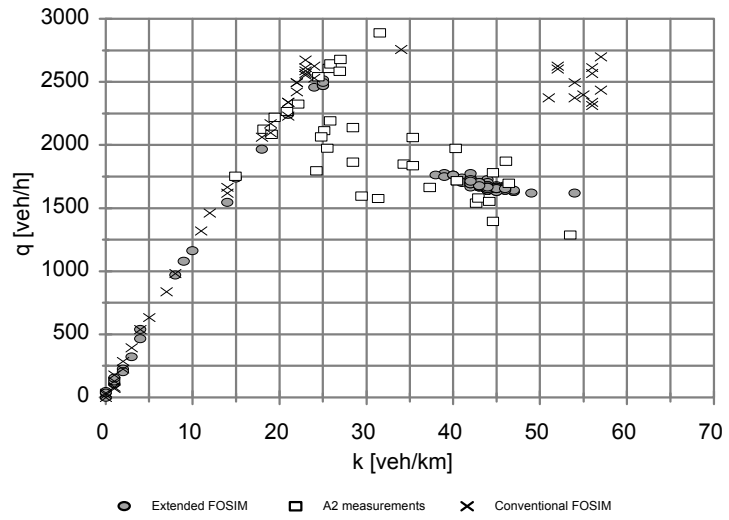


Figure 56: Comparison of the fundamental diagrams (5-minute values) from simulations of the A2 site with the extended and the conventional FOSIM models and from real-life values (A2 detector 1) for the median lane

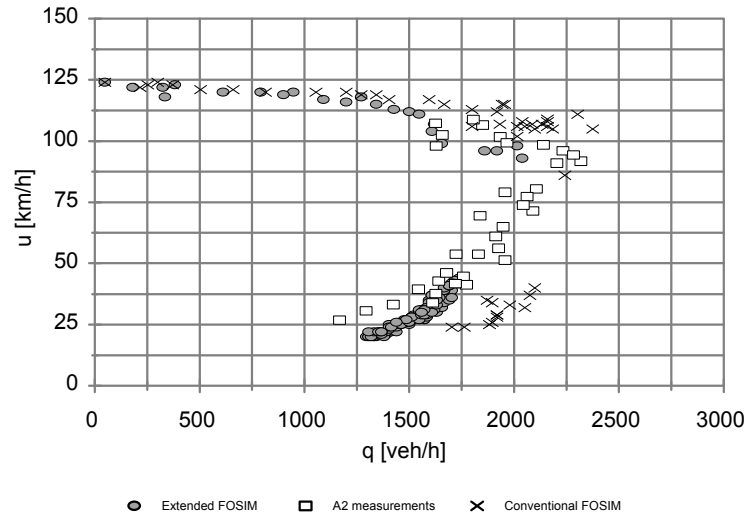
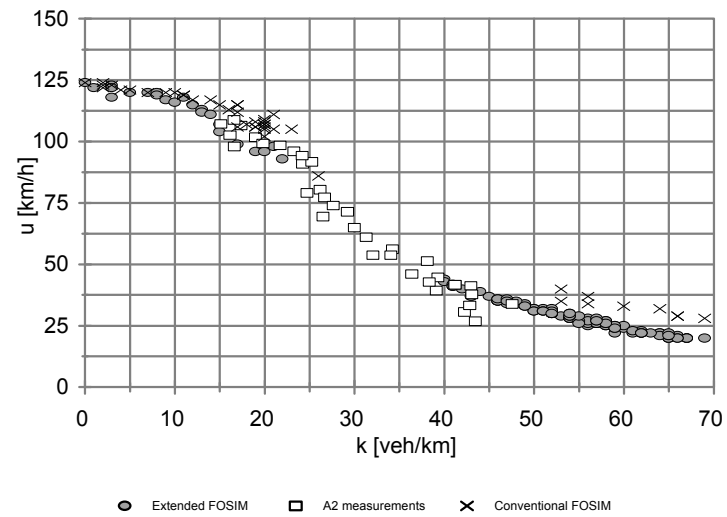
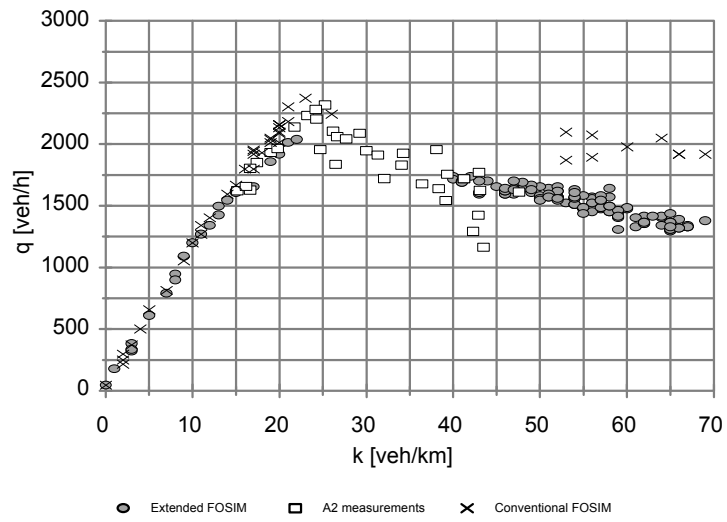


Figure 57: Comparison of the fundamental diagrams (5-minute values) from simulations of the A2 site with the extended and the conventional FOSIM models and from real-life values (A2 detector 1) for the middle lane

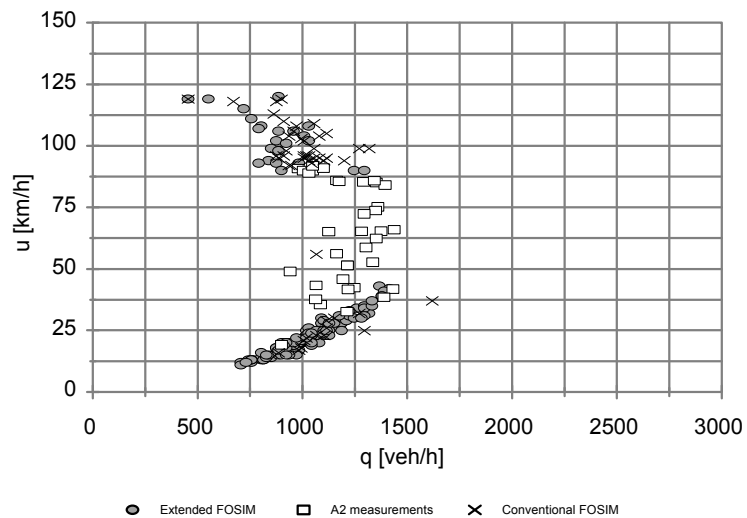
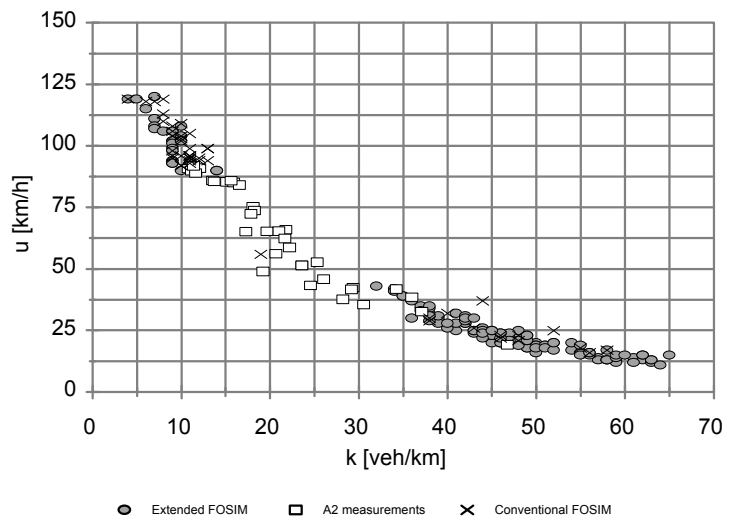
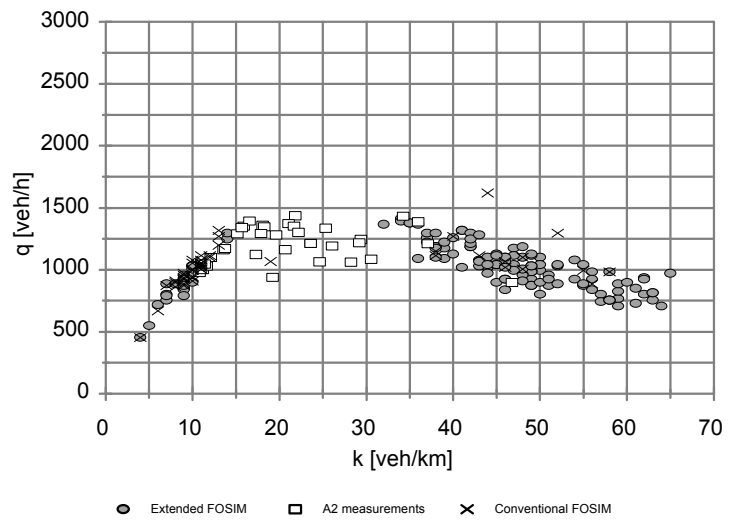


Figure 58: Comparison of the fundamental diagrams (5-minute values) from simulations of the A2 site with the extended and the conventional FOSIM models and from real-life values (A2, detector 1) for the shoulder lane

8.2 CONCLUSIONS DRAWN FROM THE SIMULATIONS WITH THE EXTENDED FOSIM MODEL

The fundamental diagrams presented in the previous section show that a simple model of different car-following for non-congested and congested flow performs much better (for the congested branch of the fundamental diagram) than the conventional model, which only represents the non-congested state well for the studied site.

The distance gap - speed relation is only one aspect of many of the FOSIM model. Changing this has consequences for other parts of the model. Also, probably not only the distance gap - speed relation differs by regime, but also other traffic characteristics.

The results of the presented model are therefore in no way final. Further research needs to be done. However, the consequences of different distance gap keeping appear to be important.

9 Conclusions

In this chapter, the performed research is briefly revisited (section 9.1), and the findings are summarized (section 9.2). Then conclusions are drawn from the findings (section 9.3), and recommendations (section 9.4) are given.

9.1 RESEARCH SUMMARY

This report focuses on differences in individual car-following behavior, that is distance gap keeping, for different flow regimes (congested, non-congested) on (Dutch) freeways. The main questions are whether differences between flow regimes exist, and whether they have a significant influence on traffic flow. If so, microscopic traffic flow models should incorporate these behavioral differences.

The questions are answered by analysis of data from sites at a 4 lane and a 6 lane freeway in the Netherlands. Measurements from cross sections at different locations relative to the bottleneck (upstream, downstream, and at the bottleneck) are used. The data are used to study both microscopic and macroscopic observations.

To study individual car-following behavior (i.e. microscopic), the relation between speed and distance gap of following drivers is developed for each lane and vehicle type. This is done separately for the non-congested and congested regimes. Macroscopic traffic characteristics are studied by plotting fundamental diagrams.

The findings are used for modeling purposes. Regime specific distance gap - speed functions data are established from the data. They are implemented in a micro simulation model (FOSIM), and the resulting macroscopic results are evaluated.

9.2 SUMMARY OF THE FINDINGS

The analysis of the distance gap - speed relation (of following drivers) shows that at both freeway sites the car-following behavior of *passenger car* drivers differs between the non-congested and congested regimes. No differences in car-following between the regimes were found for *trucks*.

At all analyzed cross sections, including those upstream, and downstream of a bottleneck, and at the bottleneck itself, the distance gaps of passenger cars are larger in congested flow than in non-congested flow for the same speed. The differences in distance gaps between the regimes are (relatively) largest in the median lanes and smallest in the shoulder lanes. The differences are somewhat larger at the 6 lane freeway site than at the 4 lane freeway site. In congested flow, at low speeds (<50 km/h) passenger cars follow with approximately the same distance gaps in all lanes. As speed increases, distance gaps of passenger cars in the shoulder lane increase faster than in the median and middle lanes.

Differences in individual driving behavior between regimes are reflected in the fundamental diagrams of the median and middle lanes. In congested flow, densities are smaller than expected according to the conventional (continuous) fundamental diagrams. This corresponds to the longer distance gaps that were found.

The congested parts of the fundamental diagrams for the median and middle lanes on the A2 freeway appear to be approximately equal. This corresponds to the similar distance gap - speed relations for passenger cars in the median and middle lanes for congested traffic.

The findings are suited for implementation in a (existing) microscopic traffic flow model. A first evaluation shows significant improvements of this model over the same model with equal car-following behavior for all regimes, and a good match with reality.

Further, with respect to the methods used in the research, it can be remarked that the identification of following and non-following drivers is not straightforward. In this research, the distinction is based on a critical gap as a boundary criterion. Determining reasonable values for this critical headway is a difficult task.

Distinguishing congested and non-congested traffic is easier. This is done by visual inspection of a plot of the flow rate - density data. However, a method for automatically separating the two regimes is not readily available.

9.3 CONCLUSIONS

From the findings, it can be concluded that the discovered differences in individual driving behavior between regimes are important for our insight in traffic processes. Anomalies in measured fundamental diagrams can plausibly be explained by differences in observed driving behavior at the microscopic level. Equally, differences in individual behavior by lane correspond with differences in macroscopic characteristics by lane. Further, differences found in following behavior are such that their incorporation into traffic flow models is necessary in order to improve their performance.

Finally, it is noted that there is no indication that the findings are an artefact of the measurement conditions.

9.4 RECOMMENDATIONS

This research project is aimed at studying traffic flow differences for the non-congested and congested regimes on freeways. Data from one 4 lane freeway site and one 6 lane freeway site are used. For both sites, differences in car-following between the regimes are found. It is strongly recommended to extend the research to additional sites in order to find out whether this behavior is of a more general nature. Measurements from other freeway sites, preferably of different types, should be compared with the findings reported in this report.

Different distance gap - speed relations by regime were found using cross section measurements. However, these measurements are not suited to explain *how* individual drivers change their behavior (e.g. instantaneously or gradually). To gain insight into this process, measurements of drivers over time should be analyzed in addition to cross section measurements. This will facilitate the development of theoretical explanations of the observed phenomenon.

One may speculate that regime dependent differences other than in distance gap keeping exist. Other aspects of driving behavior, such as lane changing, may differ as well. Again, individual drivers should be followed over time in addition to measuring at fixed cross sections. An extended measuring approach could be developed to analyze the car-following phenomenon more adequately.

Further, to improve the quality of analysis of car-following phenomena, more refined procedures to distinguish non-congested and congested traffic, and following and non-following drivers are needed.

All of these studies can be expected to further improve microscopic modeling of freeway travel.

References

- 1 May, A.D., *Traffic Flow Fundamentals*, Prentice Hall, Inc., Englewood Cliffs, New-Jersey, 1990
- 2 Hall, F.D., A. Pushkar & Y. Shi, 'Some Observations on Speed-Flow and Flow Occupancy Relationships under Congested Conditions', in *Transportation Research Record* 1398, TRB, National Research Council, Washington, D.C., 1993, pp. 24-30
- 3 Schuurman, H. & R.G.M.M. Vermijs, *Traffic Flow Operations at Freeway Discontinuities*, Delft University of Technology, Delft, 1993 (in Dutch)
- 4 Toorenburg, J.A.C. van, 'Applicability of Ramp Metering', in *Verkeerskunde*, Volume 40, 1988, Number 6, pp. 284-287 (in Dutch)
- 5 Special Report 209, *Highway Capacity Manual*, Transportation Research Board, National Research Council, Washington, D.C., 1994
- 6 Botma, H. & J.H. Papendrecht, *Traffic Flow Theory* (e26 course), Delft University of Technology, Delft, 1995 (in Dutch)
- 7 Hoogendoorn, S.P., H. Botma & P.H.L. Bovy, *Car Headway Distribution Modeling and Estimation*, Delft University of Technology, Delft, 1997
- 8 Wiedemann, R., *Traffic Flow Simulation*, Schriftenreihe des Instituts für Verkehrswesen der Universität Karlsruhe, Heft 8, Karlsruhe, 1974 (in German)
- 9 Herman, R., E.W. Montroll, R. Potts, R.W. Rothery, 'Traffic Dynamics: Analysis of Stability in Car-Following', in *Operations Research*, Volume 1, Number 7, 1959, pp. 86-106
- 10 Vermijs, R.G.M.M., 'The Use of Micro Simulation for the Design of Weaving Sections', in: Brannolte, U. (editor), *Highway Capacity and Level of Service*, Karlsruhe, 1991, pp. 419-427
- 11 Rijkswaterstaat, *Standards for Freeway Design (ROA)*, SDU Publishers, The Hague, 1993, (in Dutch)
- 12 Minderhoud, M.M., H. Botma & P.H.L. Bovy, *An Assessment of Roadway Capacity Estimation Methods*, Delft University of Technology, Delft, 1996
- 13 Minderhoud, M.M. & J.H. Papendrecht, *Capacity value Infrastructure Freeways (CIA-1), Phase 1 - Literature Survey*, Delft University of Technology, Delft, 1996 (in Dutch)
- 14 Road Research Laboratory, *Research on Road Traffic*, Department of Scientific and Industrial Research, London, 1965
- 15 Bennett, Chr.R. & R.C.M. Dunn, 'Critical Headways on two-lane Highways in New Zealand', in: Akçelik, R. (Editor), *Proceedings on the Second International Symposium on Highway Capacity*, Australian Road Research Board, Victoria, 1994

Appendices

Appendix A: Calculation of microscopic and macroscopic data

A scheme of the detector system, consisting of two induction loops for each lane, is shown in figure A.1. The system produces files containing:

- at the A2 site: activation moments of the detectors 1 and 2 (a_1 and a_2), and deactivation moments of detector 2 (d_2), in milliseconds;
- at the A9 site: vehicle passing moments (a_1), speed, and vehicle length.

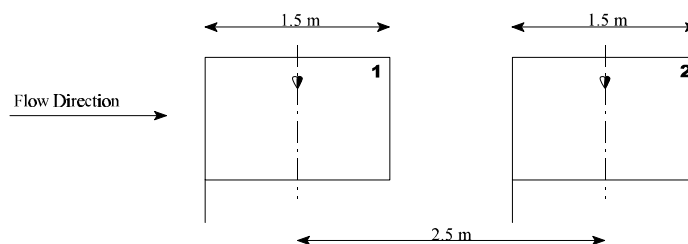


Figure A.1: Scheme of the detector system for each lane

Calculation of microscopic data

Microscopic quantities are calculated from the raw data:

i : leader

j : follower

- vehicle speed:

$$speed_j = \frac{2.5}{a_2/1000 - a_1/1000} \quad [m/s] \quad (A.1)$$

- vehicle length:

$$length_j = \left(\frac{d_2}{1000} - \frac{a_2}{1000} \right) \cdot speed_j - 1.5 \quad [m] \quad (A.2)$$

- relative speed (speed difference between leader and follower):

$$relative\ speed_j = speed_j - speed_i \quad [m/s] \quad (A.3)$$

- time headway:

$$time\ headway_j = \left(\frac{a_1}{1000} \right)_j - \left(\frac{a_1}{1000} \right)_i \quad [s] \quad (A.4)$$

- distance headway:

$$distance\ headway_j = time\ headway_j \cdot speed_j \quad [m] \quad (A.5)$$

- time gap:

$$time\ gap_j = time\ headway_j - \frac{length_i}{speed_i} \quad [s] \quad (A.6)$$

- distance gap:

$$distance\ gap_j = distance\ headway_j - length_i \quad [m] \quad (A.7)$$

Calculation of macroscopic data

Macroscopic quantities are obtained by aggregating the microscopic data for some period of time:

- the flow rate q is determined by simply counting the number of passing vehicles;
- the space mean speed u is determined by calculating the harmonic average of the speeds of the passing vehicles:

$$\bar{u}_{\text{harmonic}} = \frac{1}{\frac{1}{n} \sum_{i=1}^n \frac{1}{u_i}} \quad (\text{A.8})$$

- For the density at the A2 site, the occupation (amount of time a detector is activated) can be derived directly from the detector data (a_2 and d_2). This cannot be done for the data from the A9 site for which different detection output is available. Occupation is not equal to density. Moreover, there is only a simple (linear) relation between the two when the vehicle lengths are all (approximately) equal. Density is used best because of its fundamental relation with speed and flow. The density k is calculated from flow rate and speed: $k=q \cdot u$.

Aggregation intervals of 5 minutes are chosen in chapter 4.

Some criticism on the calculation method

The following can be noticed on the calculation of the microscopic quantities:

The calculation of the distance headway assumes that

- the vehicles drive with constant speed during the time between passage of the leader and follower;
- the follower's and leader's speed are equal. On average relative speeds are near zero which means that the assumption is permissible.

The activation/deactivation moments of the detections loops are not exactly equal to the moment the vehicle's front reaches/leaves the detection loop. Therefore the measured vehicle length ('electric length') is not exactly equal to the physical vehicle length. This error can be corrected but this has been omitted because of the relatively small error.

Appendix B: Determination of the critical gap value

Identification of followers is based on the measured microscopic data. Identification can be performed with time gaps. When time gaps are small, it is certain that drivers are following. When gaps are large, it is certain that drivers are not following. In between these extremes some drivers are following, some are not.

As a boundary criterion for identification of following drivers a critical time gap value can be selected. It is assumed that most drivers with smaller time gaps are following and with larger time gaps are non-following. Applying such a boundary criterion results in not selecting some drivers who are following, and selecting some who are not following (figure B.1, as described in chapter 2).

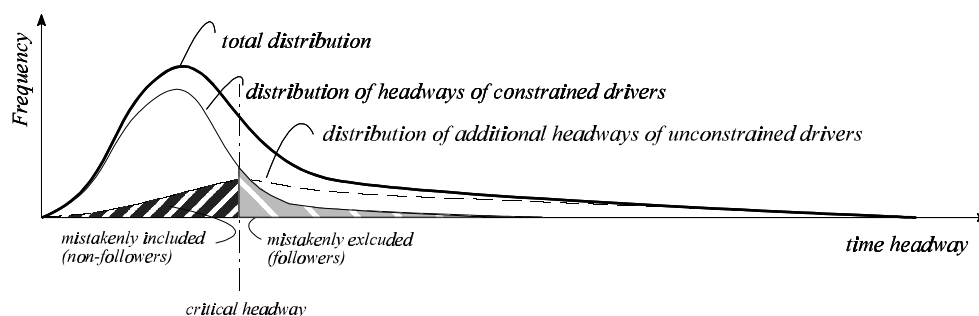


Figure B.1: Hypothetical distribution of time gaps of following and non-following drivers

Three ways to determine a critical time gap are used:

- 1 A reasonable value for the critical gap can be found by combining time gaps and relative speed (speed difference). Drivers with small gaps are following. Therefore relative speed is on average relatively small. More free drivers are included as gaps increase. Therefore, average relative speed will increase with increasing gap until it stays fairly constant for large gaps (all free drivers).

Plotting relative speed against time gaps can give a result like the example shown in figure B.2. The gap where relative speeds stabilize is chosen as the critical gap. Unfortunately this way the exact value only can be chosen somewhat arbitrarily.

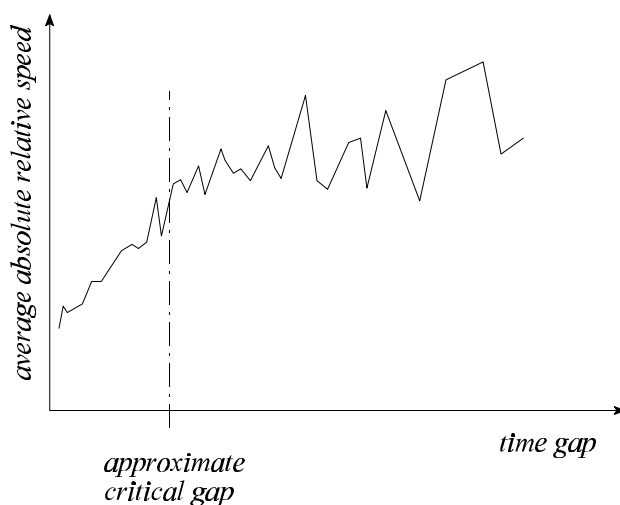


Figure B.2: An example of relative speed against time gaps to obtain critical time gap value (Botma and Papendrecht (6))

- 2 The critical gap value can also be chosen based on the independence of free drivers. A consequence of this independence is that the distribution of the time gaps can be described with a negative exponential distribution. The time gap where such a distribution is no longer valid is an estimate for the critical gap.

This principle can be shown graphically by plotting the natural logarithm of the probability that a time gap is exceeded against the time gap (figure B.3). The time gap where the plotted line is no longer straight is an estimate of the critical time gap. Again, the exact choice of the critical value is somewhat arbitrarily.

In a publication by Bennett and Dunn (15), which describes the application of methods 1 and 2, method 2 is recommended.

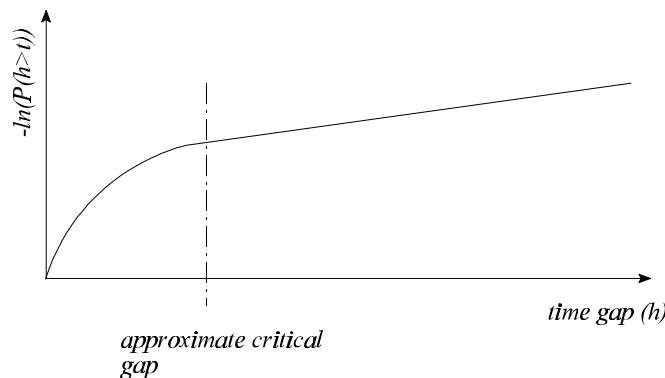


Figure B.3: Logarithm of the probability of exceeding a time gap (Botma and Papendrecht (6))

- 3 The method best suited to estimate an exact value for the critical time headway is the estimation of the complete distribution of time headways, e.g. as proposed by Branston (described by Botma and Papendrecht (6)). Then the critical headway value can be chosen which minimizes the number of selected non-followers and not selected followers (the shaded areas in figure B.1) for the estimated distribution. With this critical headway, a critical gap can be calculated.

The parameters of the composite distribution by lane and vehicle type are estimated for the data of *non-congested flow* with a method developed by Hoogendoorn, Botma, and Bovy (7). Very good resemblance of the measured distributions and the estimated distributions is found for all lanes and vehicle types. With the estimated composite distribution a value for the critical time gap is determined. It turns out to be unrealistically small. Apparently the estimated total distributions are good but the underlying distributions of gaps of free and constrained drivers do not give realistic results for the determination of the critical gap for this case.

Because the exact method using estimated distributions cannot be used, the other two methods are applied. In figure B.4 the relative speed against the time gap (in other words: clearance time excluded) is shown for all valid vehicle type/lane combinations (see chapter 4) of the A2 site. In figure B.5 the logarithm of the probability of exceeding a time gap is plotted against the time gap for passenger cars in the median lane of the A2 in non-congested traffic. Figure B.6 shows the same for light trucks and heavy trucks (in the shoulder lane).

The amount of measurement data for longer time gaps is fairly small. Therefore figure B.4 can only show data for time gaps smaller than 5 seconds. But even then, averages for vehicles in the shoulder lane for somewhat longer time gaps are not as reliable. This lack of data has somewhat smaller effects on method 2, which is also recommended by Bennett and Dunn (15).

The latter method shows useable results for passenger cars in the median and middle lanes, but less for the shoulder lane, which carries only a limited amount of passenger cars. Based on the available data, a critical time gap of 3.5 seconds is chosen for all passenger cars.

For trucks the methods do not show a very useable result. Therefore a critical gap cannot be determined directly and, unfortunately, assumptions cannot be avoided. To understand the consequences of different critical gap values, two values are used which are representative for the range of possible critical gap values. As the lower bound for this range, the critical gap value of passenger cars (3.5 seconds) is used, as the higher bound a critical time gap value of 5 seconds is used. This value of 5 seconds is often found in other, somewhat older studies, but now generally it is agreed that this value is too high for passenger cars on freeways.

The results of calculations with two critical gaps were compared, and the results were both used for calibration of a micro simulation model. Based on experience and micro simulation results, it is concluded that the 5 seconds value is most suited for trucks.

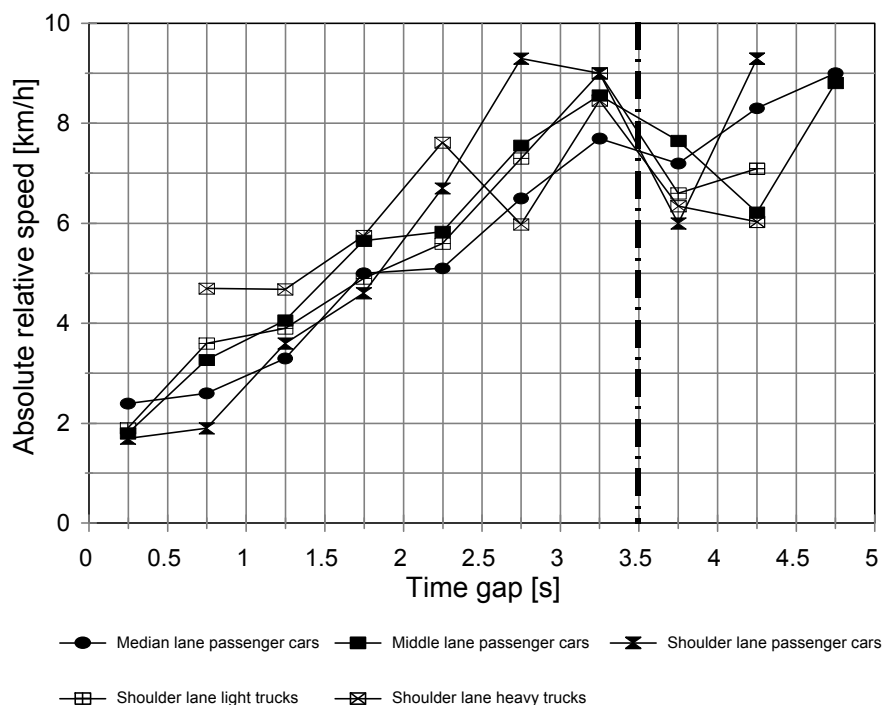


Figure B.4: Absolute relative speed - time gap for at the A2 site (detector 1) in non-congested traffic

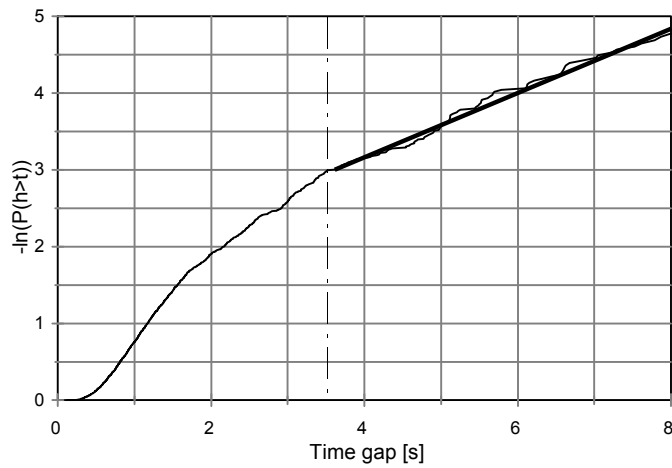


Figure B.5: Natural logarithm of the probability that a time gap is exceeded - time gap for passenger cars in the median lane of the A2 site (detector 1) in non-congested traffic

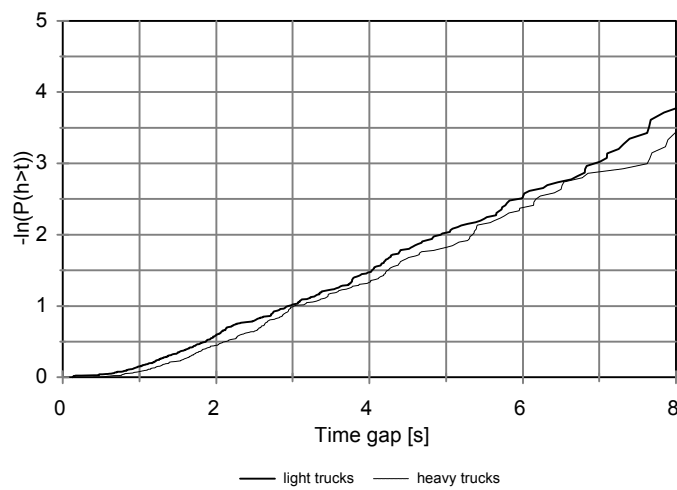


Figure B.6: Natural logarithm of the probability that a time gap is exceeded - time gap for light and heavy trucks at the A2 site (detector 1) in non-congested traffic

Appendix C: Distance gap data per 5 km/h speed interval

(average distance gap in meters)

A2 Detector 1	Median lane		Passenger cars		
Non-congested					
20-25 km/h	25-30 km/h		30-35 km/h		
sample size	0	sample size	0	sample size	0
average	0.00	average	0.00	average	0.00
35-40 km/h	40-45 km/h		45-50 km/h		
sample size	0	sample size	0	sample size	1
average	0.00	average	0.00	average	7.84
50-55 km/h	55-60 km/h		60-65 km/h		
sample size	3	sample size	0	sample size	3
average	12.66	average	0.00	average	20.98
standard deviation	8.06			standard deviation	8.95
65-70 km/h	70-75 km/h		75-80 km/h		
sample size	14	sample size	41	sample size	70
average	17.65	average	17.70	average	23.77
standard deviation	4.87	standard deviation	8.51	standard deviation	13.30
80-85 km/h	85-90 km/h		90-95 km/h		
sample size	97	sample size	138	sample size	232
average	20.73	average	24.61	average	23.55
standard deviation	12.18	standard deviation	12.67	standard deviation	12.76
95-100 km/h	100-105 km/h		105-110 km/h		
sample size	238	sample size	366	sample size	326
average	27.42	average	28.37	average	31.92
standard deviation	14.89	standard deviation	15.56	standard deviation	20.20
110-115 km/h	115-120 km/h		120-125 km/h		
sample size	268	sample size	274	sample size	186
average	34.08	average	40.57	average	47.91
standard deviation	20.93	standard deviation	22.07	standard deviation	27.71
125-130 km/h	130-135 km/h		135-140 km/h		
sample size	72	sample size	34	sample size	9
average	56.84	average	64.22	average	56.11
standard deviation	32.64	standard deviation	37.26	standard deviation	20.81
Congested					
20-25 km/h	25-30 km/h		30-35 km/h		
sample size	84	sample size	84	sample size	86
average	12.73	average	14.46	average	18.05

standard deviation	6.34	standard deviation	6.86	standard deviation	9.07
35-40 km/h		40-45 km/h		45-50 km/h	
sample size	109	sample size	127	sample size	160
average	18.86	average	21.30	average	21.80
standard deviation	9.03	standard deviation	10.08	standard deviation	9.36
50-55 km/h		55-60 km/h		60-65 km/h	
sample size	166	sample size	219	sample size	307
average	24.91	average	27.78	average	28.53
standard deviation	13.73	standard deviation	13.98	standard deviation	14.50
65-70 km/h		70-75 km/h		75-80 km/h	
sample size	310	sample size	302	sample size	335
average	31.13	average	31.13	average	33.94
standard deviation	17.26	standard deviation	19.25	standard deviation	18.83
80-85 km/h		85-90 km/h		90-95 km/h	
sample size	400	sample size	259	sample size	202
average	36.46	average	37.57	average	43.28
standard deviation	20.99	standard deviation	20.42	standard deviation	27.94
95-100 km/h		100-105 km/h		105-110 km/h	
sample size	95	sample size	19	sample size	7
average	45.37	average	50.62	average	89.34
standard deviation	25.50	standard deviation	39.21	standard deviation	25.87
110-115 km/h		115-120 km/h		120-125 km/h	
sample size	0	sample size	1	sample size	0
average	0.00	average	57.82	average	0.00
125-130 km/h		130-135 km/h		135-140 km/h	
sample size	0	sample size	0	sample size	0
average	0.00	average	0.00	average	0.00

A2 Detector 1	Middle lane	Passenger cars			
Non-congested					
20-25 km/h		25-30 km/h		30-35 km/h	
sample size	0	sample size	0	sample size	0
average	0.00	average	0.00	average	0.00
35-40 km/h		40-45 km/h		45-50 km/h	
sample size	0	sample size	0	sample size	1
average	0.00	average	0.00	average	14.38

50-55 km/h		55-60 km/h		60-65 km/h	
sample size	0	sample size	0	sample size	3
average	0.00	average	0.00	average	19.96
				standard deviation	9.88
65-70 km/h		70-75 km/h		75-80 km/h	
sample size	2	sample size	15	sample size	38
average	30.24	average	19.31	average	22.30
standard deviation	3.14	standard deviation	8.90	standard deviation	8.18
80-85 km/h		85-90 km/h		90-95 km/h	
sample size	96	sample size	200	sample size	259
average	27.36	average	27.52	average	31.06
standard deviation	15.15	standard deviation	15.08	standard deviation	17.52
95-100 km/h		100-105 km/h		105-110 km/h	
sample size	231	sample size	301	sample size	233
average	36.20	average	39.55	average	45.92
standard deviation	19.39	standard deviation	21.06	standard deviation	22.96
110-115 km/h		115-120 km/h		120-125 km/h	
sample size	132	sample size	91	sample size	41
average	50.94	average	58.24	average	57.61
standard deviation	24.49	standard deviation	27.27	standard deviation	26.76
125-130 km/h		130-135 km/h		135-140 km/h	
sample size	14	sample size	6	sample size	1
average	65.76	average	82.76	average	22.81
standard deviation	27.06	standard deviation	37.19		
Congested					
20-25 km/h		25-30 km/h		30-35 km/h	
sample size	75	sample size	66	sample size	73
average	13.85	average	15.93	average	18.18
standard deviation	7.16	standard deviation	8.35	standard deviation	7.47
35-40 km/h		40-45 km/h		45-50 km/h	
sample size	106	sample size	134	sample size	219
average	19.04	average	21.18	average	23.52
standard deviation	7.73	standard deviation	10.32	standard deviation	10.61
50-55 km/h		55-60 km/h		60-65 km/h	
sample size	249	sample size	280	sample size	304
average	24.47	average	25.90	average	28.29
standard deviation	11.73	standard deviation	13.22	standard deviation	16.46

65-70 km/h		70-75 km/h		75-80 km/h	
sample size	333	sample size	364	sample size	412
average	30.11	average	30.39	average	33.30
standard deviation	20.04	standard deviation	16.76	standard deviation	19.40
80-85 km/h		85-90 km/h		90-95 km/h	
sample size	308	sample size	153	sample size	78
average	39.62	average	41.17	average	45.80
standard deviation	25.53	standard deviation	23.12	standard deviation	25.21
95-100 km/h		100-105 km/h		105-110 km/h	
sample size	29	sample size	5	sample size	2
average	60.56	average	66.75	average	93.05
standard deviation	32.99	standard deviation	40.93	standard deviation	70.03
110-115 km/h		115-120 km/h		120-125 km/h	
sample size	1	sample size	0	sample size	0
average	72.05	average	0.00	average	0.00
125-130 km/h		130-135 km/h		135-140 km/h	
sample size	0	sample size	0	sample size	0
average	0.00	average	0.00	average	0.00

A2 Detector 1	Shoulder lane	passenger cars			
Non-congested					
20-25 km/h		25-30 km/h		30-35 km/h	
sample size	0	sample size	0	sample size	0
average	0.00	average	0.00	average	0.00
35-40 km/h		40-45 km/h		45-50 km/h	
sample size	0	sample size	0	sample size	1
average	0.00	average	0.00	average	29.37
50-55 km/h		55-60 km/h		60-65 km/h	
sample size	2	sample size	1	sample size	0
average	31.17	average	17.85	average	0.00
standard deviation	12.15				
65-70 km/h		70-75 km/h		75-80 km/h	
sample size	3	sample size	8	sample size	60
average	26.09	average	35.47	average	30.96
standard deviation	14.30	standard deviation	17.45	standard deviation	14.09
80-85 km/h		85-90 km/h		90-95 km/h	
sample size	112	sample size	84	sample size	70
average	31.73	average	42.77	average	44.62

standard deviation	17.74	standard deviation	20.36	standard deviation	19.29
95-100 km/h		100-105 km/h		105-110 km/h	
sample size	35	sample size	27	sample size	10
average	52.38	average	57.05	average	64.98
standard deviation	19.15	standard deviation	22.62	standard deviation	18.73
110-115 km/h		115-120 km/h		120-125 km/h	
sample size	12	sample size	4	sample size	3
average	55.76	average	89.06	average	48.72
standard deviation	34.15	standard deviation	23.56	standard deviation	44.56
125-130 km/h		130-135 km/h		135-140 km/h	
sample size	0	sample size	0	sample size	0
average	0.00	average	0.00	average	0.00
Congested					
20-25 km/h		25-30 km/h		30-35 km/h	
sample size	37	sample size	55	sample size	51
average	15.58	average	19.42	average	18.34
standard deviation	8.36	standard deviation	9.59	standard deviation	9.52
35-40 km/h		40-45 km/h		45-50 km/h	
sample size	66	sample size	103	sample size	107
average	20.82	average	21.97	average	25.58
standard deviation	11.42	standard deviation	12.42	standard deviation	14.92
50-55 km/h		55-60 km/h		60-65 km/h	
sample size	171	sample size	164	sample size	184
average	29.99	average	29.83	average	34.27
standard deviation	16.98	standard deviation	16.09	standard deviation	20.68
65-70 km/h		70-75 km/h		75-80 km/h	
sample size	200	sample size	204	sample size	150
average	36.45	average	41.45	average	49.52
standard deviation	23.05	standard deviation	23.92	standard deviation	35.70
80-85 km/h		85-90 km/h		90-95 km/h	
sample size	63	sample size	26	sample size	9
average	56.81	average	71.17	average	96.02
standard deviation	35.47	standard deviation	49.09	standard deviation	55.89
95-100 km/h		100-105 km/h		105-110 km/h	
sample size	5	sample size	1	sample size	1
average	97.00	average	114.60	average	72.58
standard deviation	65.37				

110-115 km/h		115-120 km/h		120-125 km/h	
sample size	0	sample size	0	sample size	0
average	0.00	average	0.00	average	0.00
125-130 km/h		130-135 km/h		135-140 km/h	
sample size	0	sample size	0	sample size	0
average	0.00	average	0.00	average	0.00

A2 Detector 1	Shoulder lane	Light trucks			
Non-congested					
20-25 km/h		25-30 km/h		30-35 km/h	
sample size	0	sample size	0	sample size	0
average	0.00	average	0.00	average	0.00
35-40 km/h		40-45 km/h		45-50 km/h	
sample size	0	sample size	0	sample size	0
average	0.00	average	0.00	average	0.00
50-55 km/h		55-60 km/h		60-65 km/h	
sample size	1	sample size	0	sample size	0
average	17.55	average	0.00	average	0.00
65-70 km/h		70-75 km/h		75-80 km/h	
sample size	3	sample size	8	sample size	53
average	51.05	average	52.45	average	45.16
standard deviation	17.76	standard deviation	27.53	standard deviation	26.48
80-85 km/h		85-90 km/h		90-95 km/h	
sample size	109	sample size	102	sample size	34
average	47.29	average	52.92	average	69.90
standard deviation	26.82	standard deviation	28.15	standard deviation	33.25
95-100 km/h		100-105 km/h		105-110 km/h	
sample size	4	sample size	6	sample size	1
average	79.92	average	58.32	average	75.82
standard deviation	39.42	standard deviation	47.96		
110-115 km/h		115-120 km/h		120-125 km/h	
sample size	0	sample size	0	sample size	0
average	0.00	average	0.00	average	0.00
125-130 km/h		130-135 km/h		135-140 km/h	
sample size	0	sample size	0	sample size	0
average	0.00	average	0.00	average	0.00

Congested

20-25 km/h		25-30 km/h		30-35 km/h	
sample size	6	sample size	14	sample size	8
average	15.02	average	19.02	average	22.87
standard deviation	8.10	standard deviation	7.79	standard deviation	9.26
35-40 km/h		40-45 km/h		45-50 km/h	
sample size	13	sample size	24	sample size	27
average	21.53	average	27.37	average	33.31
standard deviation	7.94	standard deviation	10.99	standard deviation	13.76
50-55 km/h		55-60 km/h		60-65 km/h	
sample size	44	sample size	38	sample size	36
average	31.20	average	32.34	average	35.82
standard deviation	15.73	standard deviation	16.87	standard deviation	18.05
65-70 km/h		70-75 km/h		75-80 km/h	
sample size	32	sample size	40	sample size	32
average	49.01	average	48.94	average	43.50
standard deviation	23.73	standard deviation	24.91	standard deviation	20.28
80-85 km/h		85-90 km/h		90-95 km/h	
sample size	15	sample size	3	sample size	0
average	51.80	average	53.35	average	0.00
standard deviation	25.93	standard deviation	19.88		
95-100 km/h		100-105 km/h		105-110 km/h	
sample size	0	sample size	0	sample size	0
average	0.00	average	0.00	average	0.00
110-115 km/h		115-120 km/h		120-125 km/h	
sample size	0	sample size	0	sample size	0
average	0.00	average	0.00	average	0.00
125-130 km/h		130-135 km/h		135-140 km/h	
sample size	0	sample size	0	sample size	0
average	0.00	average	0.00	average	0.00

A2 Detector 1**Shoulder lane****Heavy trucks****Non-congested**

20-25 km/h		25-30 km/h		30-35 km/h	
sample size	0	sample size	0	sample size	0
average	0.00	average	0.00	average	0.00

35-40 km/h		40-45 km/h		45-50 km/h	
sample size	0	sample size	0	sample size	0
average	0.00	average	0.00	average	0.00
50-55 km/h		55-60 km/h		60-65 km/h	
sample size	0	sample size	0	sample size	0
average	0.00	average	0.00	average	0.00
65-70 km/h		70-75 km/h		75-80 km/h	
sample size	0	sample size	3	sample size	32
average	0.00	average	28.80	average	52.11
		standard deviation	20.77	standard deviation	22.82
80-85 km/h		85-90 km/h		90-95 km/h	
sample size	94	sample size	75	sample size	27
average	54.20	average	55.88	average	64.94
standard deviation	24.57	standard deviation	28.05	standard deviation	30.91
95-100 km/h		100-105 km/h		105-110 km/h	
sample size	2	sample size	1	sample size	0
average	62.27	average	86.47	average	0.00
standard deviation	19.79				
110-115 km/h		115-120 km/h		120-125 km/h	
sample size	0	sample size	0	sample size	0
average	0.00	average	0.00	average	0.00
125-130 km/h		130-135 km/h		135-140 km/h	
sample size	0	sample size	0	sample size	0
average	0.00	average	0.00	average	0.00

Congested

20-25 km/h		25-30 km/h		30-35 km/h	
sample size	3	sample size	4	sample size	4
average	19.34	average	23.17	average	25.72
standard deviation	9.65	standard deviation	2.37	standard deviation	12.09
35-40 km/h		40-45 km/h		45-50 km/h	
sample size	12	sample size	12	sample size	15
average	29.85	average	25.69	average	35.01
standard deviation	14.16	standard deviation	10.54	standard deviation	15.43
50-55 km/h		55-60 km/h		60-65 km/h	
sample size	29	sample size	19	sample size	24
average	37.16	average	37.80	average	44.53
standard deviation	13.13	standard deviation	14.97	standard deviation	23.84

65-70 km/h		70-75 km/h		75-80 km/h	
sample size	44	sample size	25	sample size	22
average	43.54	average	52.40	average	56.56
standard deviation	17.92	standard deviation	27.18	standard deviation	24.66
80-85 km/h		85-90 km/h		90-95 km/h	
sample size	6	sample size	1	sample size	0
average	47.89	average	98.31	average	0.00
standard deviation	16.35				
95-100 km/h		100-105 km/h		105-110 km/h	
sample size	0	sample size	0	sample size	0
average	0.00	average	0.00	average	0.00
110-115 km/h		115-120 km/h		120-125 km/h	
sample size	0.00	sample size	0.00	sample size	0.00
average	0.00	average	0.00	average	0.00
125-130 km/h		130-135 km/h		135-140 km/h	
sample size	0.00	sample size	0.00	sample size	0.00
average	0.00	average	0.00	average	0.00

A9	Median lane		Passenger cars		
Non-congested					
20-25 km/h		25-30 km/h		30-35 km/h	
sample size	0	sample size	0	sample size	0
average	0.00	average	0.00	average	0.00
35-40 km/h		40-45 km/h		45-50 km/h	
sample size	0	sample size	0	sample size	0
average	0.00	average	0.00	average	0.00
50-55 km/h		55-60 km/h		60-65 km/h	
sample size	6	sample size	7	sample size	6
average	19.37	average	19.65	average	19.22
standard deviation	13.23	standard deviation	11.38	standard deviation	6.03
65-70 km/h		70-75 km/h		75-80 km/h	
sample size	9	sample size	33	sample size	111
average	17.20	average	16.79	average	22.10
standard deviation	7.93	standard deviation	7.70	standard deviation	11.20
80-85 km/h		85-90 km/h		90-95 km/h	
sample size	241	sample size	476	sample size	499
average	23.83	average	27.25	average	29.80
standard deviation	10.53	standard deviation	13.87	standard deviation	14.99

95-100 km/h		100-105 km/h		105-110 km/h	
sample size	316	sample size	170	sample size	87
average	34.94	average	34.11	average	42.36
standard deviation	17.64	standard deviation	17.17	standard deviation	22.02
110-115 km/h		115-120 km/h		120-125 km/h	
sample size	49	sample size	28	sample size	11
average	45.48	average	57.03	average	48.20
standard deviation	25.21	standard deviation	25.98	standard deviation	27.55
125-130 km/h		130-135 km/h		135-140 km/h	
sample size	3	sample size	0	sample size	1
average	66.09	average	0.00	average	102.00
standard deviation	47.35				

Congested

20-25 km/h		25-30 km/h		30-35 km/h	
sample size	25	sample size	29	sample size	11
average	10.43	average	11.914176	average	13.04
standard deviation	4.38	standard deviation	4.0229466	standard deviation	5.41
35-40 km/h		40-45 km/h		45-50 km/h	
sample size	15	sample size	18	sample size	26
average	18.87	average	18.99	average	17.96
standard deviation	8.88	standard deviation	7.29	standard deviation	6.78
50-55 km/h		55-60 km/h		60-65 km/h	
sample size	42	sample size	78	sample size	99
average	20.82	average	24.24	average	23.71
standard deviation	8.24	standard deviation	10.65	standard deviation	11.17
65-70 km/h		70-75 km/h		75-80 km/h	
sample size	174	sample size	343	sample size	469
average	24.99	average	28.52	average	30.34
standard deviation	11.93	standard deviation	14.10	standard deviation	15.00
80-85 km/h		85-90 km/h		90-95 km/h	
sample size	365	sample size	251	sample size	135
average	33.16	average	32.58	average	37.55
standard deviation	17.26	standard deviation	16.42	standard deviation	22.14
95-100 km/h		100-105 km/h		105-110 km/h	
sample size	64	sample size	30	sample size	8
average	41.27	average	47.84	average	40.43
standard deviation	29.85	standard deviation	30.64	standard deviation	15.41

110-115 km/h		115-120 km/h		120-125 km/h	
sample size	0	sample size	1	sample size	0
average	0.00	average	64.20	average	0.00
125-130 km/h		130-135 km/h		135-140 km/h	
sample size	2	sample size	0	sample size	0
average	73.81	average	0.00	average	0.00
standard deviation	34.35				

A9	Shoulder lane		passenger cars		
Non-congested					
20-25 km/h		25-30 km/h		30-35 km/h	
sample size	0	sample size	0	sample size	0
average	0.00	average	0.00	average	0.00
35-40 km/h		40-45 km/h		45-50 km/h	
sample size	0	sample size	1	sample size	0
average	0.00	average	28.58	average	0.00
50-55 km/h		55-60 km/h		60-65 km/h	
sample size	3	sample size	2	sample size	2
average	14.39	average	24.43	average	22.66
standard deviation	3.34	standard deviation	21.87	standard deviation	23.75
65-70 km/h		70-75 km/h		75-80 km/h	
sample size	19	sample size	64	sample size	192
average	28.50	average	24.39	average	28.00
standard deviation	12.38	standard deviation	13.80	standard deviation	14.57
80-85 km/h		85-90 km/h		90-95 km/h	
sample size	301	sample size	233	sample size	146
average	33.43	average	38.04	average	43.38
standard deviation	16.88	standard deviation	17.61	standard deviation	21.18
95-100 km/h		100-105 km/h		105-110 km/h	
sample size	62	sample size	29	sample size	13
average	51.19	average	53.87	average	66.25
standard deviation	23.19	standard deviation	22.27	standard deviation	20.44
110-115 km/h		115-120 km/h		120-125 km/h	
sample size	8	sample size	1	sample size	0
average	67.11	average	90.96	average	0.00
standard deviation	24.26				

125-130 km/h		130-135 km/h		135-140 km/h	
sample size	0	sample size	0	sample size	0
average	0.00	average	0.00	average	0.00
<hr/>					
Congested					
20-25 km/h		25-30 km/h		30-35 km/h	
sample size	2	sample size	19	sample size	17
average	12.77	average	10.29	average	17.30
standard deviation	0.66	standard deviation	4.79	standard deviation	11.17
35-40 km/h		40-45 km/h		45-50 km/h	
sample size	28	sample size	33	sample size	35
average	16.33	average	18.80	average	22.25
standard deviation	7.64	standard deviation	10.22	standard deviation	13.03
50-55 km/h		55-60 km/h		60-65 km/h	
sample size	58	sample size	73	sample size	125
average	24.72	average	23.55	average	26.62
standard deviation	16.16	standard deviation	11.40	standard deviation	14.91
65-70 km/h		70-75 km/h		75-80 km/h	
sample size	228	sample size	336	sample size	279
average	29.47	average	34.36	average	39.30
standard deviation	17.46	standard deviation	20.43	standard deviation	22.09
80-85 km/h		85-90 km/h		90-95 km/h	
sample size	125	sample size	77	sample size	25
average	44.94	average	48.83	average	52.51
standard deviation	27.06	standard deviation	26.95	standard deviation	32.86
95-100 km/h		100-105 km/h		105-110 km/h	
sample size	9	sample size	2	sample size	2
average	62.58	average	89.86	average	138.04
standard deviation	27.93	standard deviation	49.27	standard deviation	93.12
110-115 km/h		115-120 km/h		120-125 km/h	
sample size	0	sample size	0	sample size	0
average	0.00	average	0.00	average	0.00
125-130 km/h		130-135 km/h		135-140 km/h	
sample size	0	sample size	0	sample size	0
average	0.00	average	0.00	average	0.00

Appendix D: Standard error of the average distance gap - speed values

The figures of this appendix show the average distance gap - speed relation together with the standard error of the averages, calculated as:

$$\sigma_x = \frac{\sigma}{\sqrt{n}} \quad (\text{D.1})$$

with:

F_x = standard error of the calculated average X;

F = standard deviation of the sample;

n = the sample size.

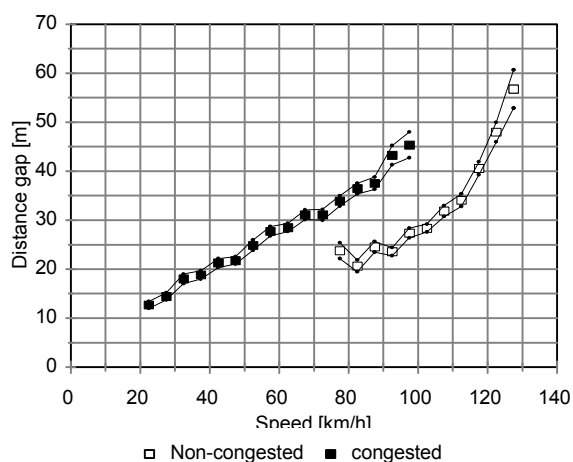


Figure D.1: Average distance gap per speed interval and standard error of the averages for passenger cars in the median lane at the A2 site

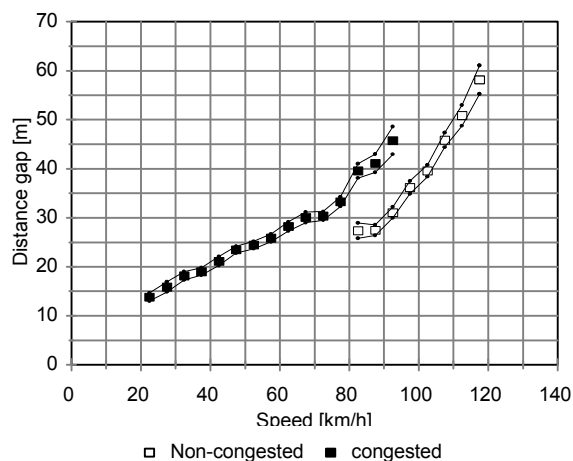


Figure D.2: Average distance gap per speed interval and standard error of the averages for passenger cars in the middle lane at the A2 site

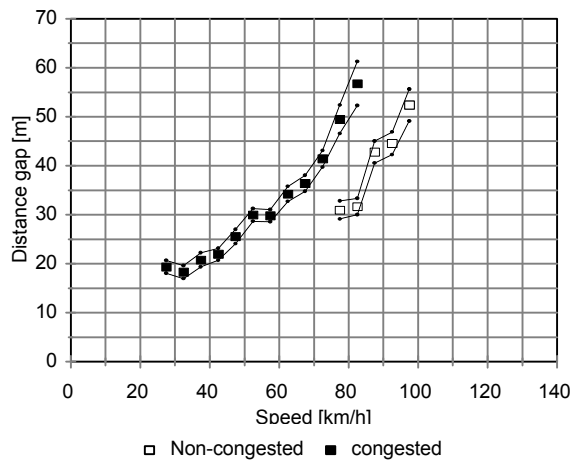


Figure D.3: Average distance gap per speed interval and standard error of the averages for passenger cars in the shoulder lane at the A2 site

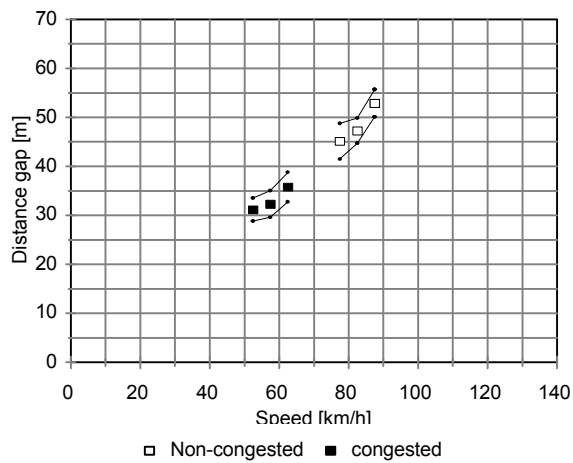


Figure D.4: Average distance gap per speed interval and standard error of the averages for light trucks in the shoulder lane at the A2 site

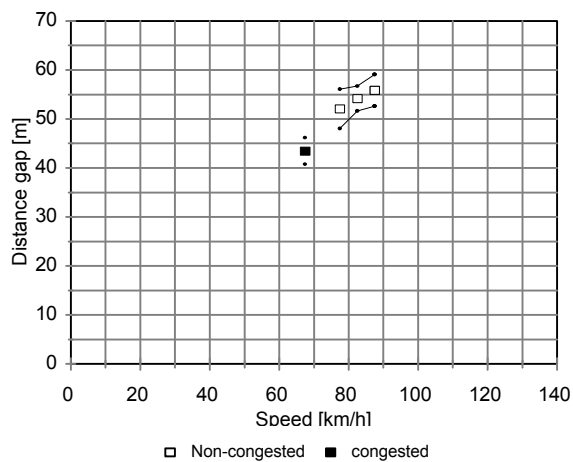


Figure D.5: Average distance gap per speed interval and standard error of the averages for heavy trucks in the shoulder lane at the A2 site

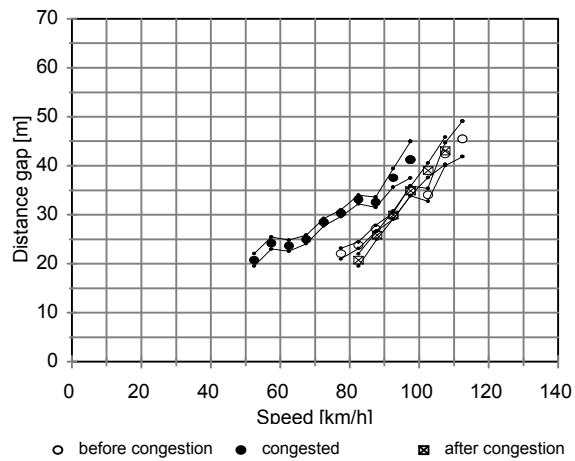


Figure D.6: Average distance gap per speed interval and standard error of the averages for passenger cars in the median lane at the A9 site

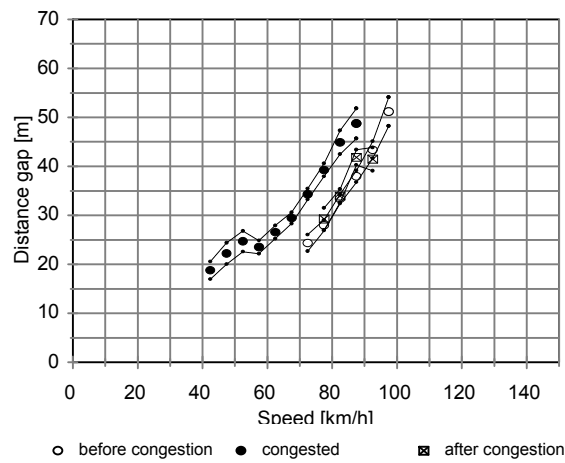


Figure D.7: Average distance gap per speed interval and standard error of the averages for passenger cars in the shoulder lane at the A9 site

Appendix E: Estimated parameter values for the distance gap - speed relationships

The estimated parameters of the distance gap - speed functions are shown in table E.1. Separate functions were estimated for the regimes and driver/vehicle types. Two functional forms were used:

$$g_d = a + b \cdot v \quad [m] \quad (\text{E.1})$$

$$g_d = a + b \cdot v + c \cdot v^2 \quad [m] \quad (\text{E.2})$$

Road	Lane and vehicle type	congested flow							non-congested flow						
		linear (eq. E.1)			quadratic (eq. E.2)				linear (eq. E.1)			quadratic (eq. E.2)			
		a	b	R ²	a	b	c	R ²	a	b	R ²	a	b	c	R ²
A2	median, passenger cars (type 1)	3	0.415	0.985	3	0.411	0.000058	0.985	no valid parameter estimates with the chosen parameter limitations			3	0	0.0028	0.88
	middle, passenger cars (type 2)	3	0.423	0.963	3	0.399	0.00034	0.965				3	0	0.0037	0.94
	shoulder, passenger cars (type 3)	3	0.539	0.891	3	0.321	0.0034	0.951				3	0	0.049	0.89
									non-congested and congested flow						
shoulder, light trucks (type 4)									3	0.54	0.973	3	0.454	0.00117	0.997
shoulder, heavy trucks (type 5)									3	0.62	0.954	3	0.611	0.0000485	0.954
A9	median, passenger cars (type 1)	3	0.359	0.932	3	0.277	0.001	0.961	no valid parameter estimates with the chosen parameter limitations			3	0	0.0032	0.96
	shoulder, passenger cars (type 2)	3	0.445	0.839	3	0.172	0.0038	0.963				3	0	0.0046	0.93

Table E.1: Estimated parameter values for the distance gap - speed functions with the A2(detector 1) and A9 data using the assumptions $a=3$, $b \geq 0$ and $c \geq 0$

The parameter estimation for congested flow for passenger cars shows equal or better results (highest R²) for equation E.2 compared to equation E.1. The c-parameters (quadratic part of the equations) for the median lanes on both the A2 and A9 are smallest, for the shoulder lanes largest.

When the assumptions for the parameter values are used, the parameters for non-congested flow for passenger cars can only be estimated reasonably with equation E.2.

Regression analysis is also executed without parameter limitations (table E.2) to improve the results for the non-congested distance gap - speed functions. Equation E.2 performs best. When these parameter values are used, some other function has to be used for lower speeds. A line tangent to the estimated function for higher speeds and with value 3 for zero speed is suitable.

The eventually used functional form depends on the R². When R² is equal for E.1 and E.2, the 'simpler' form, linear E.1, is used.

Road Lane and vehicle type		non-congested flow						
		linear (eq. E.1)			quadratic (eq. E.2)			
		a	b	R ²	a	b	c	R ²
A2	median, passenger cars	-32.1	0.632	0.847	155.4	-3.12	0.0183	0.985
	middle, passenger cars	-51	0.91	0.965	108	-2.31	0.0161	0.996
	shoulder, passenger cars	-57	1.11	0.936	49.5	-1.34	0.014	0.941
A9	shoulder, passenger cars	-31.4	0.67	0.961	36.3	-0.77	0.0076	0.974
	shoulder, passenger cars	-53.4	1.06	0.987	53.9	-1.49	0.015	0.998

Table E.2: Estimated parameter values for the distance gap - speed functions with the A2 (detector 1) and A9 data without limitations for the parameter values

Appendix F: Description of the microscopic traffic flow model FOSIM

(Extracted from a paper by Henk Schuurman and Raymond Vermijs (10))

Background

FOSIM (FOMIS), an INTRAS derivative, has been developed by Bullen (1982) to simulate traffic operations on basic motorway road sections, using a personal computer. FOSIM has been adjusted and further developed since 1987 for the Dutch situation by the TRL of the Delft University of Technology. Its field of application is the traffic operation on road sections of motorways with discontinuities. FOSIM has been applied successfully to Dutch capacity surveys near on-ramps and weaving sections.

Characteristics

FOSIM is a microscopic simulation model in which the traffic operation is simulated on the level of individual drivers and vehicles. The total simulation period is divided in time steps of 1 second. After each time step the position of all vehicles present on the road section under consideration is calculated, starting at the downstream end of the road section. The new position of a vehicle depends on characteristics of the vehicle and the driver, the interaction with the other road users and the geometry of the road section. Also the expected position after some time periods, the so called anticipation time, influences the new position.

In FOSIM it is possible to define a variety of geometric configurations, such as weaving sections, on-ramps, road works etc. The traffic is defined by different vehicle/driver combinations. Characteristics of traffic operation (volumes, speeds and densities) are calculated on detector cross sections defined in the simulated road section.

The vehicle process

For each time step a decision process is completed for each individual driver-vehicle combination, based on the flow chart of figure F.1. The actual lane is compared with the destination lane (each vehicle has a destination lane, determined by an input OD-matrix from lane to lane). If both lanes are not the same then a lane change is decided depending on the position on the road and other vehicles. If the origin and destination lanes are the same the driver can still decide to change lane in order to overtake a slower vehicle in front. If overtaking is decided FOSIM checks the possibility to do so in the same time step.

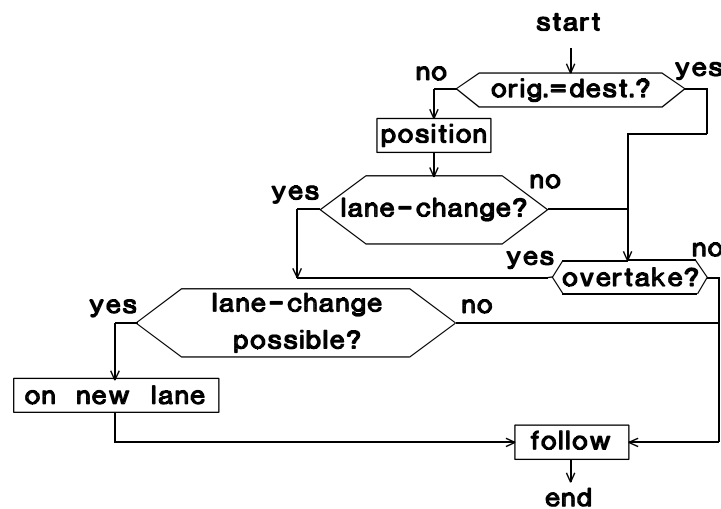


Figure F.1: Flow-chart vehicle process of the FOSIM model

Vehicle movement logic

In FOSIM every driver will always attempt to reach its (individual) desired speed. In case of the presence of a lead vehicle, the model computes the acceleration needed to maintain a sufficient headway. Positions of the vehicles are calculated some time in advance. This period of time is called 'anticipation time' and has a model value of 4 s. These positions are the basis for the determination of the acceleration needed.

The car-following vehicle will try to maintain a headway d_i equal to:

$$d_i = L_j + z_1 + z_2 v_i + z_3 v_i^2 \quad (\text{F.1})$$

where:

i, j	= index vehicle i , type j	
d_i	= space headway vehicle i	[m]
L_j	= vehicle length of leader	[m]
v_i	= actual speed of follower	[m/s]
z_{1-3}	= following parameters	

If a driver approaches the car in front in accordance with the line q-q' (see figure F.2) then he will decelerate if the combination of relative speed and space headway makes that necessary.

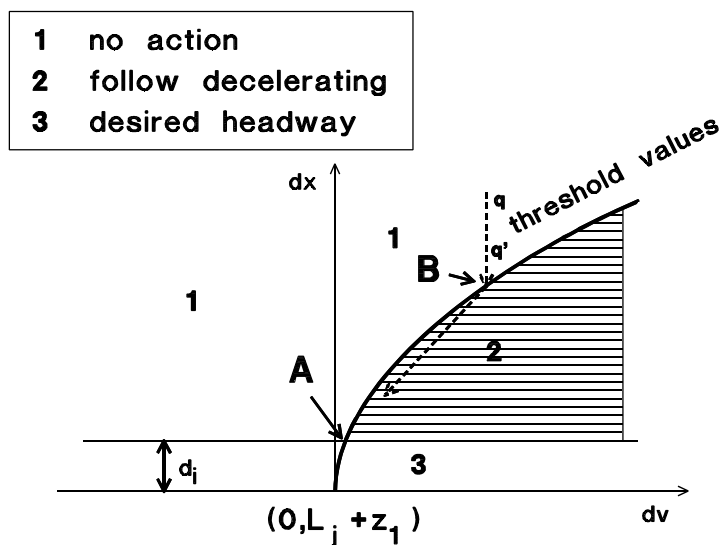


Figure F.2: Threshold values when approaching the vehicle in front

The threshold values that FOSIM uses for that purpose are related by:

$$dv = ((dx - L_j - z_1)/50)^2 \quad (\text{F.2})$$

where:

dv = speed follower - speed leader [m/s²]

dx = position leader - position follower [m]

After exceeding the threshold value in B an acceleration is calculated in order to reach situation A. To prevent collisions FOSIM has a built-in emergency routine. This routine computes the deceleration necessary to stop safely behind a leading vehicle.

Lane changing logic

The FOSIM model makes a distinction between desired lane change and mandatory lane change (figure F.3). A desired lane change in between cross section a and b is made in order to obtain a better starting-point for the mandatory lane change between cross section b and c. The risk a driver is willing to accept for a mandatory (obligatory) lane change is larger than the risk accepted for a desired lane change. This difference in risk acceptance is translated in FOSIM into a difference in the accepted deceleration to make a lane change possible. FOSIM also incidentally accepts extremely short headways, for instance during weaving operations.

If a parallel driving vehicle makes a lane change impossible, the driver can take some action to improve his possibilities in the next time step by accelerating or decelerating, depending on the driver type. In case of accelerating the impeding vehicle may decelerate to make space for the lane change.

Finally there are lane changes to overtake a slow vehicle ahead. There are two separate movements, to the left and to the right if speed advantage can be obtained. If the driver can continue to drive with his desired speed a lane change to the right may be possible too.

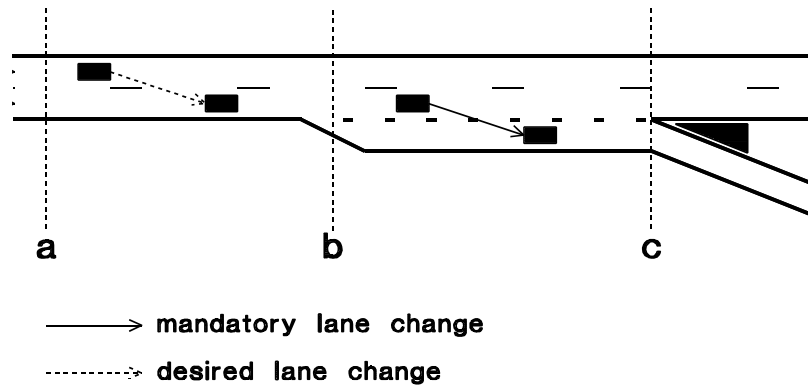


Figure F.3: Lane changing upstream an off-ramp